$$\sum_{i=1}^{n} i^2 = \frac{n(n+1)(2n+1)}{6}$$

$$x^2 + y^2 = R^2$$

$$f(x) = \int_a^b f(x)\,dx$$

RECENT TRENDS IN APPLIED MATHEMATICS

AND

COMPUTATIONAL TECHNIQUES FOR EMERGING TECHNOLOGIES

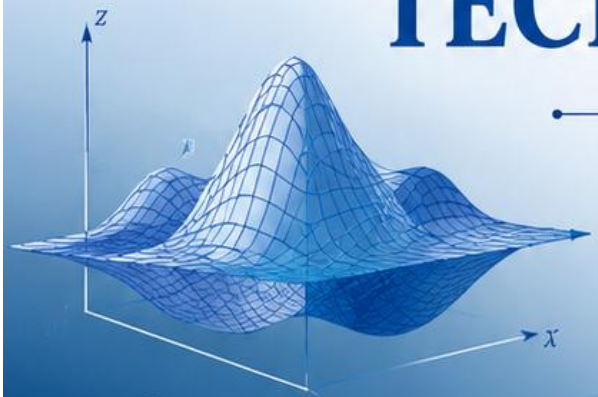

$$\frac{d^2y}{dx^2} + p\frac{dy}{dx} + qy = r(x)$$

EDITORIAL BOARD

CHIEF EDITORS

EDITORIAL BOARD

RESEARCH • INNOVATION • EDUCATION • LITERATURE

Book Subject : Mathematics
Book Category : Conference Proceedings
Copy Right : Editors
Volume : I
First Edition : June, 2026

Published by : **International Journal of Multidisciplinary Research (UIJMR)**
Vijayawada rural Vijayawada
Krishna district
Andhra Pradesh
Email: uijmreditor@gmail.com
Contact: 9121039899

ISSN Supported ISSN National Centre, India
National Science Library
CSIR-NIScPR, 14 Satsang Vihar Marg
New Delhi - 110067

First Edition June, 2026

Chief Editors' Message

It gives us immense pleasure and a deep sense of responsibility to present the proceedings of the Two-Day National Seminar on "Recent Trends in Applied Mathematics and Computational Techniques for Emerging Technologies" held on 19th and 20th February, 2026. The theme of this seminar is to explore the transformative role of Applied Mathematics and Computational Techniques in addressing contemporary scientific, engineering, industrial, and technological challenges, while fostering innovation for emerging technologies and sustainable development.

This seminar provided a dynamic academic platform for scholars, researchers, academicians, policymakers, development practitioners, industry experts, and students to exchange ideas, present cutting-edge research findings, discuss innovative methodologies, and explore interdisciplinary applications of mathematical and computational sciences in emerging technological domains. The deliberations highlighted the growing significance of mathematical modeling, data analytics, artificial intelligence, machine learning, optimization techniques, scientific computing, and computational intelligence in shaping the future of technology-driven societies.

As Editors-in-Chief, we extend our heartfelt gratitude to all the authors for their valuable scholarly contributions. We sincerely appreciate the efforts of the organizing committee, reviewers, session chairs, and volunteers whose dedication ensured the academic excellence of this seminar. Our special thanks are due to the keynote speakers and distinguished delegates whose insights enriched our discussions and inspired meaningful academic engagement.

The papers included in this volume reflect the diversity, depth, and relevance of contemporary research in Applied Mathematics and Computational Techniques. They offer significant theoretical perspectives, innovative computational approaches, and practical solutions to complex problems arising in emerging technologies and interdisciplinary fields.

We are confident that this publication will serve as a significant academic resource for researchers, policymakers, development agencies, industry professionals, educators, and students interested in Applied Mathematics, Computational Sciences, Artificial Intelligence, Data Science, Mathematical Modeling, Optimization, Scientific Computing, and emerging technology-driven research and innovation.

We hope that the knowledge shared through this seminar and its proceedings will stimulate further research, encourage interdisciplinary collaboration, and contribute to the advancement of science, technology, and society.

With best wishes for meaningful scholarship and impactful change

INDEX

INDEX

United International Journal of Multidisciplinary Research
ISSN: 3048-6726 (UIJMR) Impact Factor: 6.934 (SJIF)
An International Peer-Reviewed and Refereed Multidisciplinary Journal
Website: www.uijmr.in | Volume 3 | Special Issue 5 | March | 2026

Effects of chemical reaction and radiation absorption on MHD Free Convective Flow With Past An Inclined Plate

Dr. S. Sreelatha[*1], Dr B.Venkateswara Rao[2] and Prof. K.S. Balamurugan[3]

[1]Department of Mathematics, Government Degree College (A),Bhadrachalam,
Email:ssreelathamsc@gmail.com

[2]Department of Physics, Government DegreeCollege(A),Bhadrachalam,
Email:physicsgdcbcm@gmail.com

[3]Department of Mathematics, RVR&JC College of Engineering, Guntur, Andhra Pradesh, India
Email: muruganbalaks@gmail.com

Correspondingauthor:ssreelathamsc@gmail.com

ABSTRACT
The objective of this paper is to study the chemical reaction and radiation absorption effects on MHD free convective flow past a inclined porous platewith pastan inclined plane. The governing equations arereduced to asystem of non-linearordinarydifferential equations by applying perturbation technique and are solved mathematically. The results of this study will be discussed for the effects of pertinent parameters and will be shown graphically.

KeyWords: MHD, chemicalreaction, radiationabsorption, hallcurrent,Inclined plane

Introduction

The applications of hydromagnetic viscous incompressible flow in science and engineering, involving heat and mass transfer under the influence of chemical reactions, are of great importance in many areas of research and technology. These applications frequently occur in the petrochemical industry, power and cooling systems, cooling of nuclear reactors, heat exchanger design, chemical vapour deposition on surfaces, forest fire dynamics, geophysics, as well as magnetohydrodynamic power generation systems.
Chambre and Young [1] presented a study on first-order chemical reactions in the neighbourhood of a horizontal plate. Das et al. [2] investigated the effect of first-order homogeneous chemical reactions on the process of unsteady flow past a vertical plate with constant heat and mass transfer. Muthucumarswamy and Ganesan [3] studied the effects of chemical reaction and injection on the flow characteristics in the unsteady upward motion of an isothermal plate. Chamkha [4] investigated unsteady convective heat and mass transfer past a semi-infinite porous moving plate with heat absorption.

Hady et al. [5] studied the problem of free convection flow along a vertical wavy surface embedded in an electrically conducting fluid-saturated porous medium in the presence of internal heat generation or absorption effects. Hossain et al. [6] investigated natural convection flow along a vertical wavy surface with uniform surface temperature in the presence of heat generation and absorption. Ibrahim and Makinde [7] presented a mathematical model for a two-dimensional, steady, incompressible, electrically conducting laminar free convection boundary layer flow of a continuously moving vertical porous plate in a chemically reactive medium under the influence of a transverse magnetic field.
Shankar et al. [8] presented a numerical solution for radiation and mass transfer effects on unsteady MHD free convective fluid flow embedded in a porous medium with heat generation or absorption, using the Galerkin finite element method. Makinde and Olanrewaju [9] investigated unsteady mixed convection with Soret and Dufour effects past a vertical porous plate moving through a binary mixture of a chemically reacting fluid. Prakash et al. [10] investigated fluid flow with chemical reaction effects on unsteady MHD mixed convective flow over a moving vertical porous plate.

The study of heat generation or absorption effects in moving fluids is important in view of several physical problems, such as fluids undergoing exothermic or endothermic chemical reaction. Due to the fast growth of electronic technology, effective cooling of electronic equipment hasbecome warranted and coolingof electronic equipment ranges from individualtransistors to main frame computers and from energysupplierstо telephone switch boards and thermal diffusion effect has been utilized for isotopes separation in the mixture between gases with very light molecular weight (hydrogen and helium) and medium molecular weight. Agarwal et al. [11] analyzed hall current effect on MHD free convection flow with heat and mass transfer past a vertical porous plate. Balamurugan et al. [12]analyzed the effects of chemical reaction, thermal radiation and radiation absorption on unsteady double diffusive free convection flow of Kuvshinski fluid past a moving porous plate with heat generation under the influence of a uniform transverse magnetic field. M. Obulesu and R. Siva Prasad et.al [13] discussed about Hall Current Effects on MHD Convective Flow Past A Porous Plate with Thermal Radiation, Chemical Reaction and Heat Generation /Absorption .The present analysis aims to study the effects of chemical reaction and radiation absorptiononMHDfree convection flowpast aninclinedplateundertheinfluenceofapplied transverse magnetic field normal to the flow. The problem is governed by the system of coupled partial differential equations and employing a perturbation technique the solutionsare obtained.

2.FormationoftheProblem:

Let us consider a problem of unsteady two-dimensional free convection and mass transfer flow of anincompressibleviscousfluidpastaninfiniteinclinedplate. Thesuction Velocity v1=--U0 is considered normal to the plate.The plate temperature is constant. A system of rectangular co-ordinates O (x1, y1, z1) is taken, such that y1 = 0 on the plate and z1 axis is along its leading edge. All the fluid properties considered constant except that the influenceof the densityvariation with temperature is considered. The

influenceof the density variation in other terms of the momentum and the energy equation and the variation of the expansion coefficient with temperature is considered negligible. Under the usualBoussinesq's approximation the flow is generated by the following set of equations.

〖∂v〗^'/〖∂y〗^' = 0 (1)

〖∂u〗^'/〖∂t〗^' + v^'. 〖∂u〗^'/〖∂y〗^' = g (cos ψ)β(T^'- 〖T_∞〗^') + g(cos ψ) β^('^1) (C^'- 〖C_∞〗^') + ν (∂^2 u^')/(∂y^('^2)) - [〖σB_0〗^2/(ρ(1+m^2)) + ν/K^(-1)] u^' (2)

〖∂T〗^'/〖∂t〗^' + v^' 〖∂T〗^'/〖∂y〗^' = α [(∂^2 T^')/(∂y^('^2))] + R^*/(ρc_p) [C^'- 〖C_∞〗^'] (3)

〖∂C〗^'/〖∂t〗^' + v^' 〖∂C〗^'/〖∂y〗^' = D [(∂^2 C^')/(∂y^(〖'1〗^2))] + k(C^'- 〖C_∞〗^') (4)

Where, $v1$ are the velocity components, $T1$,$C1$ are the temperature and concentration components and α is the thermal conductivity.D is the concentration diffusivity, m is thehall currents parameter, K is chemical reaction rate constant, R* is the coefficient of proportionality for the absorption radiation.

The corresponding boundary conditions are:

u^'=0, T^'= 〖T_w〗^' , C^'= 〖C_w〗^' , at y^'= 0

u^'=0, T^'= 〖T_∞〗^' , C^'= 〖C_∞〗^' , at y^'→∞ (5)

Let us introduce the non-dimensional variables

u = u^'/U_0 , t = (t^' U_0^2)/ν , y=(y^' U_0)/ν , T=(T^'- T_∞^')/(T_w^'-T_∞^') , C = (C^'- 〖C_∞〗^')/(C_w^'-C_∞^')

K=(K^' U_0^2)/ν^2 , P_r=ν/α , S_c=ν/D , M=(〖σB〗 _(0)^2 ν)/(〖ρU〗 _0^2), M_1=M/(1+m^2)

R=(νR^* (C_w^'-C_∞^'))/(ρc_p (T_w^'-T_∞^';)U_0^2) , N=(β^' (C_w^'-C_∞^'))/(β(T_w^'-T_∞^')) , K_r=kν/(U_0^2) , G_r=(νgβ(T_w^'-T_∞^'))/(U_0^3) (6)

Where Pr is the Prandtl number,Gris the Grashof number, N is the buoyancy ratio, Sc is the Schmidt number, M is the magnetic parameter, K is the permeability parameter, $\beta$is the thermal expansion coefficient, β1 the concentration expansion coefficient, m is the hallcurrent parameter, Kr is the chemical reaction parameter and R is the absorption of radiation parameter.

Hence, usingtheabovenon-dimensionalquantities, theequations (2)-(4) inthenon-dimensional form can be written as

$\partial u/\partial t - \partial u/\partial y = G_r(T+NC) + (\partial^2 u)/(\partial y^2) – [M_1+1/K] u$ (7)

$\partial T/\partial t - \partial T/\partial y = 1/Pr\ (\partial^2 T)/(\partial y^2) + RC$ (8)

$\partial C/\partial t - \partial C/\partial y = 1/Sc\ (\partial^2 C)/(\partial y^2) + KrC$ (9)

The corresponding boundary conditions are

$u=0,\ T=1,\ C=1,\ \text{at}\ \ y=0$
$u=0,\ T=0,\ C=0,\ \text{at}\ \ y\to \infty$ (10)

Solution of the Problem

In order to reduce the above system of partial differential equations to a system of ordinary differential equations, the velocity, temperature, and concentration in the neighbourhood of the porous plate are assumed in the following form:

u(y,t)=u0(y)e−nt,u(y,t)=u_0(y)e^{-nt},u(y,t)=u0(y)e−nt, T(y,t)=T0(y)e−nt,T(y,t)=T_0(y)e^{-nt},T(y,t)=T0(y)e−nt, C(y,t)=C0(y)e−nt.(11)C(y,t)=C_0(y)e^{-nt}. \tag{11}C(y,t)=C0(y)e−nt.(11)

Substituting equation (11) into equations (7) to (9), we obtain

u0′′+u0′+[n−(M1+1K)]u0=−GrT0−GrNC0,(12)u_0" + u_0' + \left[n - \left(M_1 + \frac{1}{K}\right)\right]u_0 = -G_r T_0 - G_r N C_0, \tag{12}u0′′+u0′+[n−(M1+K1)]u0=−GrT0−Gr NC0,(12) T0′′+Pr T0′+Pr n T0=−Pr R C0,(13)T_0" + Pr\,T_0' + Pr\,n\,T_0 = -Pr\,R\,C_0, \tag{13}T0′′ +PrT0′+PrnT0=−PrRC0,(13) C0′′+Sc C0′+(n+Kr) Sc C0=0.(14)C_0" + Sc\,C_0' + (n + Kr)\,Sc\,C_0 = 0. \tag{14}C0′′+ScC0′+(n+Kr)ScC0=0.(14)

The corresponding boundary conditions are

u0=0,T0=1,C0=1at y=0,u_0 = 0,\quad T_0 = 1,\quad C_0 = 1 \qquad \text{at } y = 0,u0=0,T0=1,C0 =1at y=0, u0→0,T0→0,C0→0as y→∞.(15)u_0 \to 0,\quad T_0 \to 0,\quad C_0 \to 0 \qquad \text{as } y \to \infty. \tag{15}u0→0,T0→0,C0→0as y→∞.(15)

Solving equations (12) to (14) subject to the boundary conditions (15), the solutions are obtained as u0=(S2+S3)e−a6y−S2e−a4y−S3e−a2y,(16)u_0 = (S_2 + S_3)e^{-a_6 y} - S_2 e^{-a_4 y} - S_3 e^{-a_2 y}, \tag{16}u0=(S2+S3)e−a6y−S2e−a4y−S3e−a2y,(16) T0=e−a4y+S1(e−a2y−e−a4y),(17)T_0 = e^{-a_4

y} + S_1 \left(e^{-a_2 y} - e^{-a_4 y}\right), \tag{17}T0=e−a4y+S1(e−a2y−e−a4y),(17)
C0=e−a2y.(18)C_0 = e^{-a_2 y}. \tag{18}C0=e−a2y.(18)

3.Result and Discussion:

In order to get a physical insight into the problem, some numerical computations are carried out for the non-dimensional velocity *u*, temperature T and Concentration C in termsof the physical parameters Pr, Sc, M, k, R, Kr and m respectively. We have chosen Pr = 0.71 (air), Sc =.6, n = 0.1, t = 0.1 while the othernon-dimensional parameterstake various values. Figure 1 presents the effect of magnetic parameter M on velocity profiles. It is noticed that increasing the magnetic parameter slows down flow velocity.This is because, as M increases, it induces a damping effect on the velocity profile by creating a drag force that opposes the fluid motion, causing the velocity to decrease. Figure 2.shows that a rise in the value of the inclination angle means the flow needs to do more work to flow uphill, hence leading to a decline in the flow velocity. The effect of Prandtl number Pr on the temperature distribution is shown in figure 3. This figure shows that the temperature decreases with the increase of Prandtl number Pr. The reason is that smaller values of Pr are equivalent to increasingthe thermal conductivitiesand therefore heat is able to differ awayfrom theheated surfacemorerapidlythanforhighervaluesofPr. Hence, boundarylayer isthicker and rate of heat transfer is reduced.The effect of absorption radiation parameter R on the temperature distribution is shown in figure 4. It is noticed that the temperature decreases with an increase in absorption radiation parameter. Figure 5 displays the effect of chemical reaction parameter Krontheconcentrationdistri bution. It is seen that there is an over shoot in the concentration distribution for higher values of chemical reaction parameter.The influence of Schmidt number Sc on concentration distribution is plotted in figure 6. The concentration boundary layer thickness is drastically reduced as Sc values are increased.

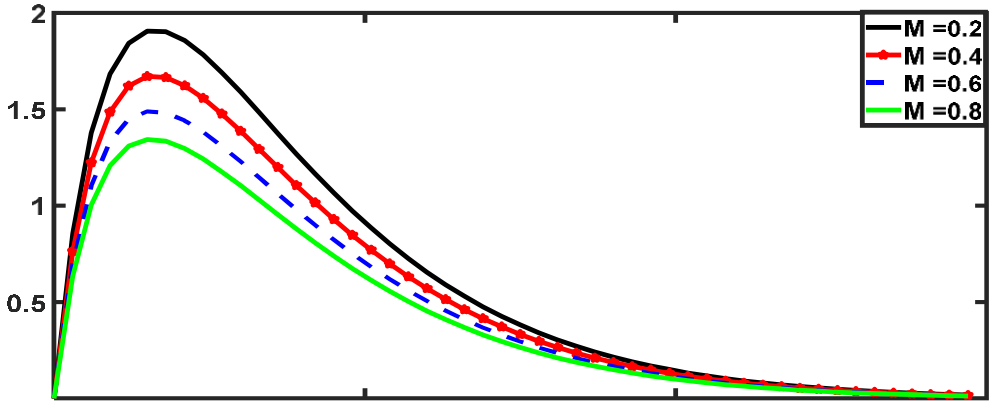

Figure1:**Velocity versus yundereffectofM**

igure2.**Velocity versus yundereffectof ψ**

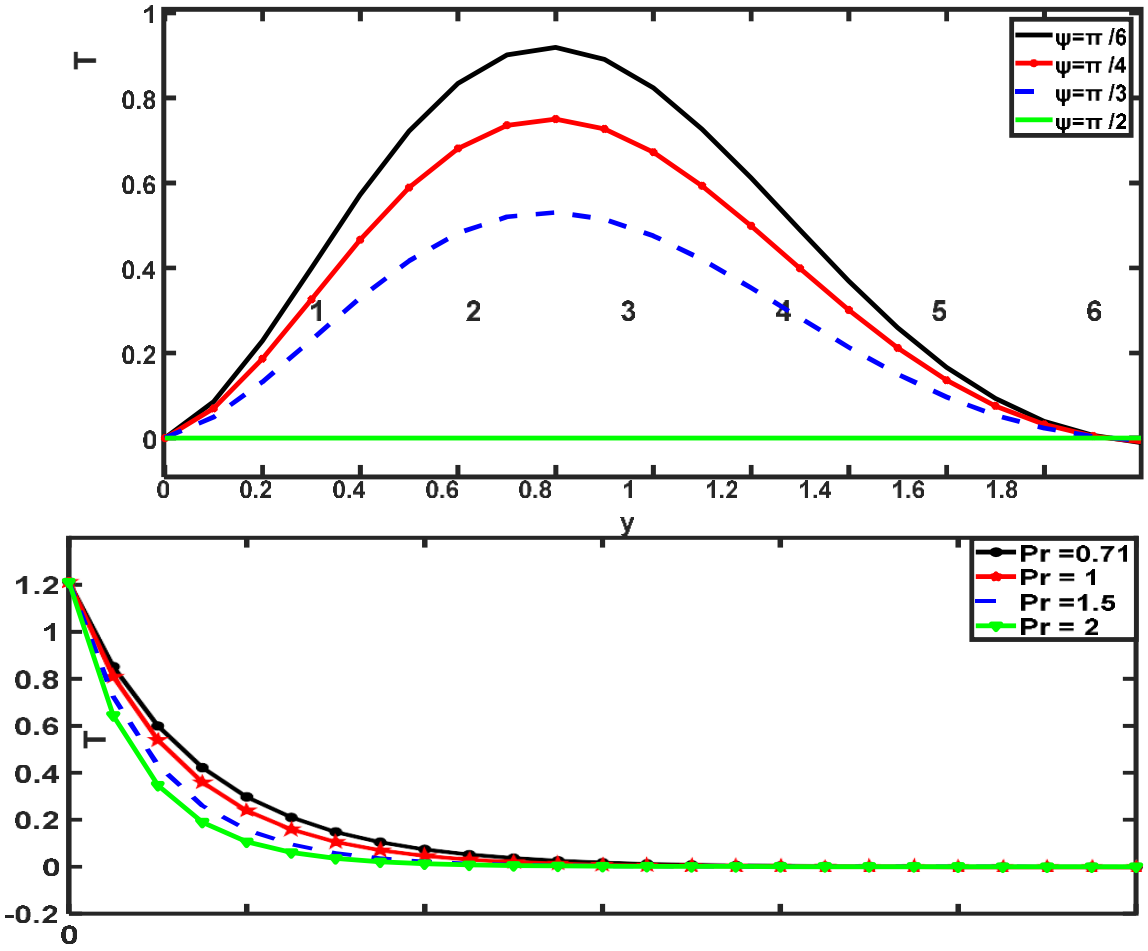

y

Figure3.**Temperature verses yundereffectofPr** Figure4 **Temperature verses y undereffectof**

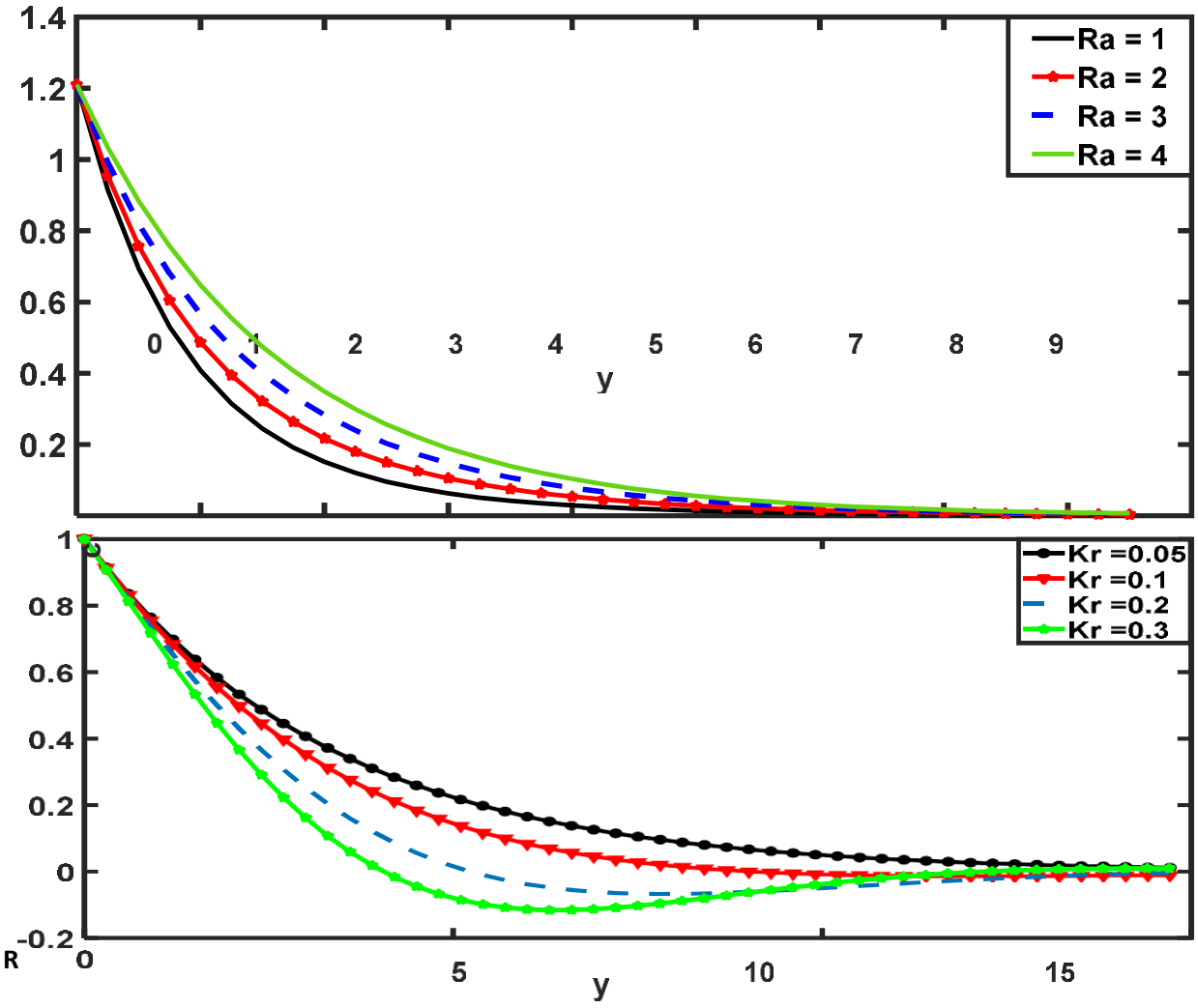

Figure5.**Concentrationversesyundereffectof Kr**

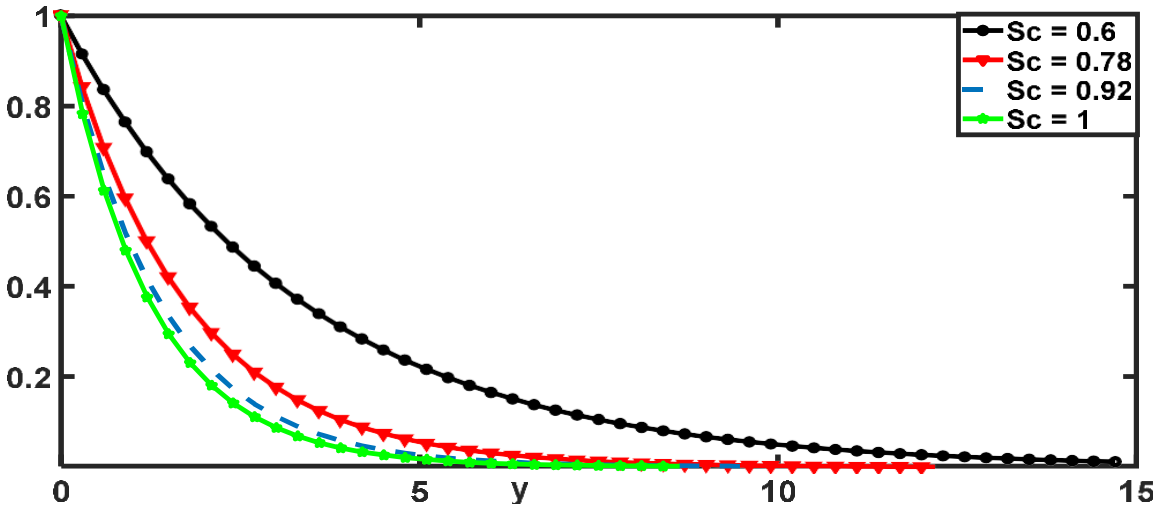

Figure6.**Concentrationversesyundereffectof Sc**

Conclusions:

In this paper we have studied chemical reaction and radiation absorption effects on MHD free convective flow past an inclined plate. A perturbation technique is employed to solve the resulting coupled partial differential equations. When angle of inclinationradiation absorption R and chemical reaction parameter Kr are equal to zero, this problem reduces to the problem of Agarwal et al. [12]. It is found that the velocitydecreases due to the effects of magnetic field parameter and radiation absorption parameter.The temperature of the plate decreases while increasing the values of the Prandtl number and radiation absorption parameter. The concentration increased due to increase in chemical reaction parameter while it decreased due to increase in Schmidt number.

References

1. Fluid Mechanics Chambre, P. L., and Young, J. D. “On the Diffusion of Chemically Reactive Species in a Laminar Boundary Layer Flow.” *Physics of Fluids*, vol. 1, 1958, pp. 48–54.

2. Das, U. N., Deka, R., and Soundalgekar, V. M. "Effects of Mass Transfer on Flow Past an Impulsively Started Infinite Vertical Plate with Constant Heat Flux and Chemical Reaction." *Forschung im Ingenieurwesen*, vol. 60, 1994, pp. 284–287.
3. Muthucumarswamy, R., and Ganesan, P. "Effect of the Chemical Reaction and Injection on the Flow Characteristics in an Unsteady Upward Motion of an Isothermal Plate." *Journal of Applied Mechanics and Technical Physics*, vol. 42, 2001, pp. 665–671.
4. Ali J. Chamkha "Unsteady MHD Convective Heat and Mass Transfer Past a Semi-Infinite Vertical Permeable Moving Plate with Heat Absorption." *International Journal of Engineering Science*, vol. 42, 2004, pp. 217–230.
5. Hossain, M. A., Molla, M. M., and Yaa, L. S. "Natural Convection Flow Along a Vertical Wavy Surface Temperature in the Presence of Heat Generation/Absorption." *International Journal of Thermal Sciences*, vol. 43, 2004, pp. 157–163.
6. Hady, F. M., Mohamed, R. A., and Mahdy, A. "MHD Free Convection Flows Along a Vertical Wavy Surface with Heat Generation or Absorption Effect." *International Communications in Heat and Mass Transfer*, vol. 33, 2006, pp. 1253–1263.
7. Ibrahim, S. Y., and Makinde, O. D. "Chemically Reacting MHD Boundary Layer Flow of Heat and Mass Transfer over a Moving Vertical Plate with Suction." *Scientific Research and Essays*, vol. 5, 2010, pp. 2875–2882.
8. Shankar, B., Prabhakar Reddy, B., and Ananda Rao, J. "Radiation and Mass Transfer Effects on Unsteady MHD Free Convection Fluid Flow Embedded in a Porous Medium with Heat Generation/Absorption." *Indian Journal of Pure and Applied Physics*, vol. 48, 2010, pp. 157–167.
9. Prakash, J., Sivaraj, R., and Kumar, B. R. "Influence of Chemical Reaction on Unsteady MHD Mixed Convective Flow over a Moving Vertical Plate." *International Journal of Fluid Mechanics*, vol. 3, 2011, pp. 1–14.
10. O. D. Makinde and Olenrewaju, P. O. "Unsteady Mixed Convection with Soret and Dufour Effects Past a Porous Plate Moving through a Binary Mixture of Chemically Reacting Fluid." *Chemical Engineering Communications*, vol. 198, no. 7, 2011, pp. 920–938.
11. Agarwal, V. P., Agarwal, Navin Kumar, Singh, Janemejay, and Varshney, N. K. "Effect of Hall Current on MHD Free Convection Flow with Heat and Mass Transfer Past a Vertical Porous Plate." *International Journal of Advanced Scientific and Technical Research*, vol. 1, no. 1, 2011, pp. 20–30.

12. Balamurugan, K. S., Ramaiah, P., Varma, S. V. K., and Ramaprasad, J. L. "Thermal Radiation and Radiation Absorption Effects on Unsteady MHD Double Diffusive Free Convection Flow of Kuvshinski Fluid Past a Moving Porous Plate Embedded in a Porous Medium with Chemical Reaction and Heat Generation." *Far East Journal of Mathematical Sciences*, vol. 91, no. 2, 2014, pp. 211–231.
13. Obulesu, M., and Siva Prasad, R. "Hall Current Effects on MHD Convective Flow Past a Porous Plate with Thermal Radiation, Chemical Reaction and Heat Generation/Absorption." *To Physics Journal*, vol. 2, 2019. ISSN: 2581-7396.

United International Journal of Multidisciplinary Research
ISSN: 3048-6726 (UIJMR) Impact Factor: 6.934 (SJIF)
An International Peer-Reviewed and Refereed Multidisciplinary Journal
Website: www.uijmr.in | Volume 3 | Special Issue 5 | March | 2026

Numerical Simulation of Unsteady MHD Bio-Convective Flow with Heat Flux Over a Stretching Surface

Dr.Abbaraju.Manjusree[1]
Department of Mathematics,Hindu College,Guntur-522002,Andhra Pradesh,India, CELL: 9885198640,
Email.ID: abbarajumanjusree@gmail.com

Dr.Srinivas Sai Panuganti[2]
Department of Mathematics,Narasaraopet,Palnadu district,Andhra Pradesh, India, CELL: 9985048923,
Email.ID: srinivasasaip28@gmail.com

Abstract

The model of current flow is set up to investigate the properties of mass and transmission of heat via a viscous fluid traveling over a permeableradiatativeexpanded exterior model in a time-dependent bio-convection slip pour. Along with emission and speed slip, the beginning of bio-thermal convection within a suspended matter of nanoparticles and gyrotactic bacteria is considered. In this investigation R-K fourth order shooting technique is utilised. Additionally, the combined impacts of the mass suction, heat source, and aligned magnetic field on the boundary are included in the current model. The local concentration of mobile microorganisms decreases as the stretching parameter and bio-convection Schmidt both improve.The concentration φ(η) gets stronger, and when Sc values increase, it decreases.The concentration of microorganism $h(\eta)$ is strengthened by increasing angle β, but it is diminished by increasing Pe, Sb and Sc, respectively.Even if the rate of temperature transmission (Nu) is maximal for positive values of A relative to negative values, the friction drags (C_f) are more powerful for negative values of A than for positive values of A.

Keywords: Brownian motion , thermo phoresis.

(1) Introduction

Due to the microorganism's stratification of varying densities, bio-convection occurs once they have assembled in the liquid's highest portion. In this manner, microorganisms are produced by bioconvection feathers and are transported from the fluid's uppermost region to its lowermost portion due to a difference in density. Turbines, geophysical fluid dynamics, nuclear power plants, computer disc drives, and gasses, MHD power plants, flow metersand other equipment all utilizing rotating flow disc

magnetohydrodynamic liquidflow. Surfaces utilized in electrochemistry are coated with optical and electrical materials using reactors for chemical vapour deposition featuring a revolving disc flow. These effective reactors require laminar gas pour near the top for further deposition. The breakdown of the laminar border linesheet, absolute instability, and straight spatial and chronologicaltimbre are all investigated in this work. Mahmood et al.[1] deliberates the entropy creation phenomenon for a This paper will provide a complete examination of 3-dimensional way of MHD stagnation point pour across a stretched surface with nonlinear thermal radiation. The present study examines the Anisotropic slip properties of carbon nanotubes in suspension will be investigated using a nanofluid. Hamza et al.[2] illustrated the-time-dependent mixed convection flow in a vertical duct involving an heat releasing liquidas influenced by MHD. Navier's slip conditions and convective heating arecarring into account. Syed Tauseef et al.[3] deliberates the Buongiorno's model is employ to demonstrate the mass and heat transport of a nanofluid waving in excess of a quickly moving flat shield. Since the results of thermophoresis and Brownian motion on the volume fraction of nanoparticles are passively rather than actively regulated at the boundary, this study differs from some of the earlier investigations. TousifIqra et al. [4] illustrates the ensuing temperary rotating gardget in boundarylevel layer flow caused by thelinear convective instability for a forced axial flow in isotropic and anisotropic surface roughness with nanofluid MHD. Saquib Ul Zaman et al. [5] described MHD and radiation attacts in the Williamson nanofluid wave flow through a thin cylinder. Various assumptions about density,viscosity, , and thermal conductivity are used to analyse the mass and heat transport. Xiyan Tian et al.[6] deliberates the unique qualities of magnetohydrodynamic (MHD) micropolar fluid include lightness, heat, magnetic characteristics, and more. It has a great deal of application. A micropolar fluid is used to explore the properties of mass, heatand flow convert in an MHD micropolar nanofluid border linesheet beyond a exordinarye xpandingshield. MunirahAali Alotaibi and Shreen El-Sapa [7] illustrated, the steady state pour of an Constant density flow pairpressure liquid inside of analytically studying two spheres that are inside each other. analysed un this paper. Translation proceeds at a constant speed outside the solid sphere and at a uniform speed inside. Esraaet al.[8] deliberates the Industrial perspectives on the pour behaviour of non-Newtonian liquids. Non-Newtonian liquids are necessary for a variety of Industrial along with technical procedures along with making polymer pages producing paper and making photographic films.

Salahuddin [9] illustrated the incompressible, two-dimensional Williamson fluid magnetohydrodynamic flow across a stretched sheet. Double Stratification and thickening due to friction are considered account while analysing the Cattaneo-Christovwarmth and attentivenesspour. Chen et al.[10] discussed the manipulate of the induced attractivemeadow (IMF) and Cattaneo-Christov duel diffusion on a Maxwell ternary flow nanofluid flow at its stagnation point. Superior massand heat transport of Maxwell ternary nanofluid mixed with duel dispersal and IMF is studied using aoriginalborder line constitution throughthe obnormalattractive reactance. Felipe Angeles[11] illustrated the heat flux's objective Cattaneo-type extension coupled to the space time equations of motion of a viscous compressible fluid. The quasilinear

version of these equations is used to determine which of the provided heat flux formulations permits the hyperbolicity of the system. For the Cauchy issue of such a framework of equations to be considered physically acceptable, this property is required .Hussain et al. [12] deliberates the There are numerous industrial and technological applications for bioconvection utilising nanomaterials. Modern nanofluids provide a dynamic means of shedding light on industrial and engineering issues pertaining to heat transport systems. Because mass remodelling and collaboration are becoming more commonplace in various microsystems, bioconvection finds several uses in bio-micro-systems.The astonishing and fascinating trend known as bioconvection is caused by the hydrodynamic instability of the microbes in the medium, which causes the microorganisms to rotate and increase the fluid's density [13], [14], [15], [16], [17].Nisar et al.[18] deliberates the MHD Considering gyrotactic bacteria, the bioconvection peristaltic activity of Siskonanofluid is examined. Flexible conduitis subjected to partial slip characteristics.In their discussion of the crown cavity's modified nanoliquid flow mediated by bioconvection (Cu–Al2O3–TiO2) and H2O.Rashid et al. [19] take into account the influence of gyrotactic microorganisms. A modified nonliquid, oxytactic bacteria, and a square obstruction are present in the crown cavity where the bioconvection flow is studied.Riaz Khan et al.[20] deliberates the A model of a porous radiative stretched surface is used to study the concentration and temperature transmission via a viscous nanofluid in a Time-dependent slip flow of bioconvection. The beginning of a suspension's bio-thermal convection include radiation and velocity slip, as well as gyrotactic bacteria and nanoparticles. Rao et al. [21] deliberates the Fluid velocity is deprecated by the porosity coefficient and Forchheimer numbers, while fluid temperature is improved by the Eckert number and concentration decreases with increasing chemical reaction coefficient. Faisal Shahet al. [22] Peristaltic transport of nanofluid with temperature dependent thermal conductivity: a numerical study. Faisal Shahet al. [23] illustratesNon-similar analysis of the Cattaneo-Christov model in MHD second-grade nanofluid flow with Soret and Dufour effects. Faisal Shahet al. [24] illustrates Nonclassical Transport Laws in Third-Grade Nanoliquid Flow on a Stretchable Surface: A Novel Approach Incorporating Soret and Dufour Effects. Faisal Shah et al. [25] describes Entropy optimization in a fourth grade nanofluid flow over a stretchable Riga wall with thermal radiation and viscous dissipation, International Communications in Heat and Mass Transfer.Faisal Shah et al. [26] illustrates Modeling and computational analysis of 3D radiative stagnation point flow of Darcy-Forchheimer subject to suction/injection, Computer Methods and Programs in Biomedicine.Faisal Shah et al. [27] illustratesHeat transfer analysis on MHD flow over a stretchable Riga wall considering Entropy generation rate: A numerical study.Faisal Shah et al. [28] describesAnalytical investigation on the combined impacts of the Soret and Dufour phenomenon in the forced convective flow of a non-Newtonian nanofluid by the movable Riga device**.** Faisal Shah et al. [29] illustratesNon-similar analysis of two-phase hybrid nanofluid flow with Cattaneo-Christov heat flux model: a computational study**.**M. Ijaz Khan et al. [30] describes First order chemical reaction response in mixed convective Falkner-SkanSutterby fluid with Cattaneo-Christov heat and mass flux model.The surface friction drag is

found to be deprecated by the Weissenberg and Forchheimer values. The mass transfer rate is significantly positively correlated with the Schmidt coefficent and chemical reaction.

Considering the aforementioned fascinating uses of microorganisms and Cattaneo-Chrystov heat flux, this reviseobserves the mass and temperaturetransport analysis of a viscous liquid in an uneven state MHD bio-convection trip sequence flow over a porous radiative stretching surface that is affected by both the heat and mass suction.The study's primary goal, improving the thermal profile, is achieved by the use of nanoparticles, while gyrotactic microorganisms produce bio-convection to enhance mass transfer. Using MATLAB's bvp4c approach, the following nonlinear ODEs have been numerically solved. The current unstable flow issue caused by radiation, porosity effects, convective mass and heat transfer, and velocity slip is entirely new and has not been treated previously, according to the authors' literature survey. Also taken into consideration is the possibility of aattractive behaviour meadow around the temperatureresource, which improves the literature's accuracy. This fascinating breakthrough could be applied to better heat transmission and the production of electro-conductive machinery. Graphic representations of the results are provided for temperature, velocity, concentration of nanoparticles, friction drag, rate of temperaturetransportation, local Sherwood coefficient, and thickness of motile microbes.Engineering thermal processes and industrial settings involving heat transfer can benefit from the theoretical understandings gathered from this study. The results that have been presented have possible nodes in the fields of solar systems, temperature machines, energy generation, mechanized procedure, and heating and cooling processes.

1. Mathematical Formulation

We study the time-dependent, viscous two-dimensional bio-convection slip flow across a absorbent radiative extendedexterior at the origin (x = 0, y = 0), as exposed graphically in Figure 1.Theexordinary sheet is positioned close to the horizontal-axis, and the verticle-axis capturedat right angles to the sheet. An intensity-dependent time-aligned attractive flux is $B(t) = \frac{B_0}{(1-\in t)^{1/2}}$ about an acute angle β governs the electrically conductive nanofluid. Additionallythe surface and stream free velocities are thought to be shifting from a stagnation point, which is described as $U_w(x,t) = \frac{ax}{1-\in t}$ and $U_e(x,t) = \frac{bx}{1-\in t}$, where $\in$, a and b are positive constants with the proportion of t^{-1}. The term $\frac{a}{1-\in t}$ illustrates the initial stretching and the stretching's effective rate. The term $\frac{\partial u}{\partial y}$ and $V_w(x,t) = \frac{-V_0}{\sqrt{1-\in t}}$ are independently altered to show the suction and slide velocities. The sheet's

radiative heat flux q_r is taken into accountandcoefficient of internal heat generation $Q_t = \frac{Q_0}{1 - \in t}$, where Q_0 symbolises the heat source's initial value (heat generation coefficient). The governing constitutions of the boundary layer flow have been determined as [20] after taking into account the previously described circumstances.

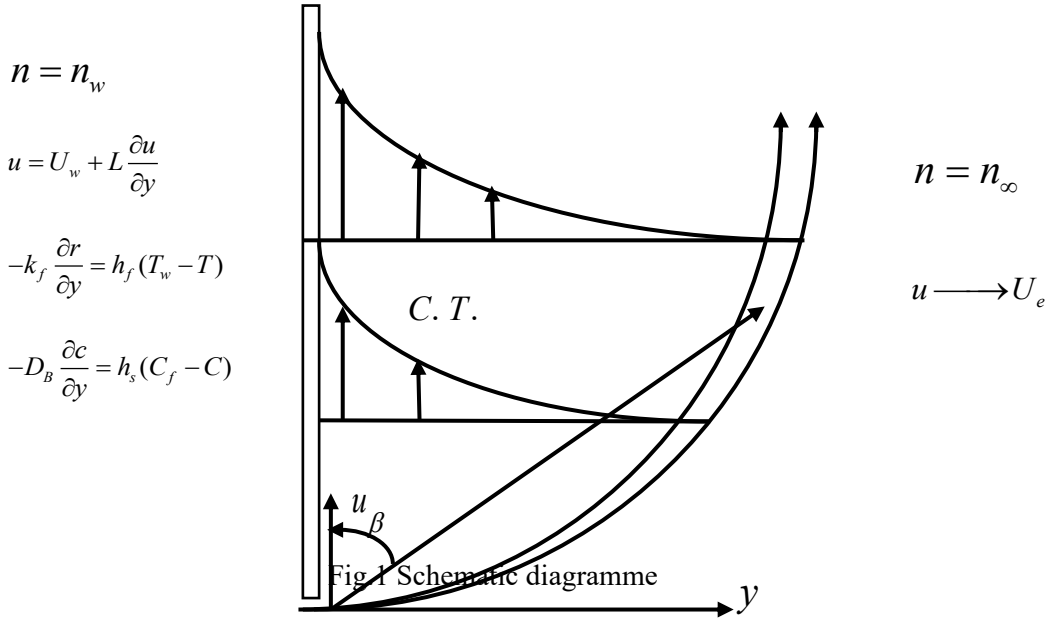

Fig.1 Schematic diagramme

$$\frac{\partial u}{\partial x} + \frac{\partial v}{\partial y} = 0, \quad (1)$$

$$\frac{\partial u}{\partial t} + u\frac{\partial u}{\partial x} + v\frac{\partial u}{\partial y} = \frac{\mu}{\rho_f}\frac{\partial^2 u}{\partial y^2} - \frac{\mu}{\rho_f}\frac{u}{K} - \frac{\sigma B^2(t)}{\rho_f}\sin^2\beta u, \quad (2)$$

$$\frac{\partial T}{\partial t} + u\frac{\partial T}{\partial x} + v\frac{\partial T}{\partial y} = \frac{k}{(\rho Cp)_f}\frac{\partial^2 T}{\partial y^2} - \frac{1}{(\rho Cp)_f}\frac{\partial q_r}{\partial y} + \frac{Q_t}{(\rho Cp)_f}(T - T_\infty) \quad (3)$$

$$\frac{\partial C}{\partial t} + u\frac{\partial C}{\partial x} + v\frac{\partial C}{\partial y} = D_M\frac{\partial^2 C}{\partial y^2} + D_T\frac{\partial^2 T}{\partial y^2} - K_c\left(C - C_\infty\right) \quad (4)$$

$$\frac{\partial n}{\partial t}+u\frac{\partial n}{\partial x}+v\frac{\partial n}{\partial y}=-\frac{cW_c}{C_f-C_\infty}\frac{\partial}{\partial y}\left(n\frac{\partial C}{\partial y}\right)+D_m\frac{\partial^2 n}{\partial y^2} \quad (5)$$

The plannedborder line constitutions for the above prototype are explained as [20].

$$u=U_w(x,t)+L\frac{\partial u}{\partial y},v=V_w(x,t),-\kappa\frac{\partial T}{\partial y}=h_f(T_w-T),-D_B\frac{\partial C}{\partial y}=h_s(C_f-C),n=n_w aty=0$$

$$u\to U_e(x,t),T\to T_\infty,C\to C_\infty,n\to n_\infty asy\to\infty \quad (6)$$

Equations (2)–(6) above, $K=k_1(1-\in t)$ defines the permeability of a porous media, where k_1 denotes the permeability The terms $\mu,\rho_f,\sigma,k,C_p,(\rho C_p)_p,(\rho C_p)_f,D_T,D_b,D_m,W_c,c$ accordingly refers to the maximum swimming cell speed, the ability of bacteria to diffuse, the viscosity of the fluid in which the nanoparticles and microorganisms are suspended, density, detailedtemperature, temperaturecapability of the nanoparticles,, thermal conductivity , electrical conductivity coefficient, and fluid heat capacity.furthermore, T,C with n symbolized the warmth, the attentiveness, with the density of microorganisms, respectively.These T,C, and n are illustrated away from the wall, they are $T_\infty,C_\infty,n_\infty$ respectively.The velocity's slip factor is shown by $L=\lambda\sqrt{1-\in t}$ The surface has a temperature of T_w because the third border linecircumstance, which as well specifies the temperaturetransport coefficient h_f, causes hot fluid to convectIf one ignores viscous dissipation, then the term $q_r=\frac{-16\sigma^* T_\infty^3}{3k^*}\frac{\partial T}{\partial y}$. is produced when the Rosseland approximation is taken into account, where σ^* and k^* stand for the Stefan-Boltzmann stableas well as the mean amalgamation coefficient, correspondingly.It is necessary to take into account the warmth differential in the pourinner in a way that T^4 allows Taylor's series to be expanded T_∞.

;

Leaving out the higher order words, we are attainment $T^4\approx 4T_\infty^3T-3\sigma^*T_\infty^4$,Accordingly, we can get $q_r=\frac{-16\sigma^* T_\infty^3}{3k^*}\frac{\partial T}{\partial y}$. Thus Eqn. (3) becomes

$$\frac{\partial T}{\partial t}+u\frac{\partial T}{\partial x}+v\frac{\partial T}{\partial y}=\frac{k}{(\rho Cp)_f}\frac{\partial^2 T}{\partial y^2}+\frac{1}{(\rho Cp)_f}\frac{16\sigma^* T_\infty^3}{3k^*}\frac{\partial^2 T}{\partial y^2}+\frac{Q_t}{(\rho Cp)_f}(T-T_\infty)\,(7)$$

The kindred for u,v,T,C,n are knownthrough

$$u=U_w=\frac{ax}{(1-\in t)},v=V_w=\frac{-V_0}{\sqrt{1-\in t}},T_w=T_\infty+T_0\frac{bx}{2v_f(1-\in t)^2},C_w=C_\infty+C_0\frac{bx}{2v_f(1-\in t)^2},$$

$$n_w=n_\infty+n_0\frac{bx}{2v_f(1-\in t)^2},u=U_e=\frac{bx}{(1-\in t)}$$

(8)

Where $a,b,\in,T_0,C_0,n_0$ are constants

We know the introduce different similarity variables are:

$$\psi=\sqrt{\frac{bv_f}{(1-\in t)}}xf(\eta),\eta=\sqrt{\frac{b}{v(1-\in t)}}y,T=T_\infty+T_0\frac{bx}{2v_f(1-\in t)^2}\theta(\eta),C=C_\infty+C_0\frac{bx}{2v_f(1-\in t)^2}\varphi(\eta),$$

$$n=n_\infty+n_0\frac{bx}{2v_f(1-\in t)^2}h(\eta)$$

(9)

The velocity constitutions are given by

$$u=\frac{bx}{(1-\in t)}f'(\eta),v=-\sqrt{\frac{bv_f}{(1-\in t)}}f(\eta) \qquad (10)$$

Considering the relationships between equations (9) and (10), (1)–(7) becomes

$$f'''-(f')^2+ff''-A\left(\frac{\eta}{2}f''+f'\right)-\frac{1}{D}f'-M^2\sin^2\beta f'=0 \quad (11)$$

$$\left(1+\frac{4}{3}Rd\right)\theta''+\Pr\left\{f\theta'-f'\theta-\frac{A}{2}(\eta\theta'+4\theta)+Q\theta\right\} \qquad (12)$$

$$\varphi''+ScSr\theta''+Sc(f\varphi'-\varphi f')-\frac{A}{2}(\eta\varphi'+4\varphi)=0 \quad (13)$$

$$h''+Sb(fh'-hf')-\frac{A}{2}Sb(\eta h'+4h)-Pe(\varphi' h'+h\varphi'')=0 \quad (14)$$

The following dimensionless boundary conditions can be created by transforming the boundary conditions (6):

$$f'(0)=\lambda_1+\lambda_2 f''(0), f(0)=S, \theta'(0)=-Bi(1-\theta(0)), \varphi'(0)=-Nd(1-\varphi(0)), \quad (15)$$
$$h(0)=1, f'(\eta)=1, \theta(\eta)=0, \varphi(\eta)=0, h(\eta)=0 as \eta\to\infty$$

In the formulas above $M^2=\frac{\sigma_f B_0^2}{b\rho_f}$ identifies the hatmann number, $D=Da_x \operatorname{Re}_x=\frac{bk_1}{\nu_f}, Da_x=\frac{\kappa}{x^2}=\frac{k_1(1-\in t)}{x^2}$ illustrates darcy coefficient, $A=\frac{\in}{b}$ deliberates unsteadiness coefficient, $Rd=\frac{4\sigma^* T_\infty^3}{kk^*}$ deliberates the radiation coefficient, $\Pr=\frac{\nu_f}{\alpha}$ signifies prandtl number, , $Q=\frac{Q_0}{b(\rho c_p)}$ signifies heat source parameter, $Sc=\frac{\nu_f}{D_B}$ similarly represents Schmidt number, $Sb=\frac{\nu_f}{D_m}$ represent bio convection schmidt coefficient, $Pe=\frac{bW_c D_m}{\nu_f^2}$ represents the Peclet coeffient, $S=\left(\frac{V_0}{\sqrt{b\nu_f}}\right)\succ 0$ symbolized the suction coefficient, $\lambda_1=\frac{b}{a}$ symbolized the expanding coefficient, $\lambda_2=L\sqrt{\frac{b}{\nu_f}}$ signifies speedslide parameter, $Bi=\frac{h_f}{k}\sqrt{\frac{\nu_f}{b}}$ symbolized Biot component, $N_d=\frac{h_s}{D_B}\sqrt{\frac{\nu_f}{b}}$ symbolized convection dispersalconstraint,

The researchers have defined the skin friction coefficient local Nusselt number Sherwood number and local density number of moving microorganisms.

$$C_{fx}=\frac{\tau_w}{\frac{1}{2}\rho_f U_w^2}, Nu_x=\frac{xq_w}{k_f(T_f-T_\infty)}, Sh_x=Sh=-\frac{x}{(C_w-C_\infty)}\left(\frac{\partial C}{\partial y}\right)_{y=0}$$
$$Nn_x=-\frac{x}{(C_w-C_\infty)}\left(\frac{\partial n}{\partial y}\right)_{y=0} \quad (16)$$

where τ_w deliberates local wall shear stress, q_w is illustrate local temperature flux, q_m is the mass flux coefficient and q_n is the microorganism coefficient flux, This can be shown as.

$$\tau_w=\mu\frac{\partial u}{\partial y}|_{y=0}, q_w=-k\frac{\partial T}{\partial y}|_{y=0}+(q_r)_w, Sh=-\frac{x}{(C_w-C_\infty)}\left(\frac{\partial C}{\partial y}\right)_{y=0}$$
$$Nn_x=-\frac{x}{(C_w-C_\infty)}\left(\frac{\partial n}{\partial y}\right)_{y=0} \quad (17)$$

Utilising the unpredictable listed in Equations 9 as well as 10, system (16) as well as (17) together yield system (18), as shown below.

$$C_{fx}=\sqrt{\mathrm{Re}_x}C_f=f''(0),$$
$$Nu_x=\frac{Nu}{\sqrt{\mathrm{Re}_x}}=-(1+\frac{4}{3}Rd)\theta'(0),$$
$$Sh_x=\frac{Sh}{\sqrt{\mathrm{Re}_x}}=-\phi'(0), \quad (18)$$
$$Nn_x=\frac{Nn}{\sqrt{\mathrm{Re}_x}}=-h'(0)$$

In (18) $\mathrm{Re}_x=\frac{U_w^2}{a\nu_f}$ represents the local Reynolds number

2. Numerical Solution

In this partthe non-linear ordinary differential equations (11) to (14) with respectto the border linecircumstances (15) is The problem was solved by using the R-K method with MATLAB software. This process engages changing a border line value problem into anpreliminary value problem.

$$f = y_1, f' = y_2, f'' = y_3$$

$$f''' = (y_2)^2 - y_1 y_3 + A\left(\frac{n}{2} y_3 + y_2\right) + \frac{1}{D} y_2 + M^2 \operatorname{Sin}^2 \beta y_2$$

(19)

$$\theta = y_4, \theta' = y_5$$

$$\theta'' = \frac{1}{(1+\frac{4}{3}Rd)}\left[-\Pr\left\{f y_5 - y_2 y_4 - \frac{A}{2}\right\}(\eta y_5 + 4y_4) + Q y_4\right]$$

(20)

$$\phi = y_6, \phi' = y_7$$

$$\phi'' = -ScSr\,\theta'' - Sc(y_1 y_7 - y_6 y_2) + \frac{A}{2}(\eta y_7 + 4y_6)$$

(21)

$$h = y_8, h' = y_9$$

$$h'' = -Sb(y_1 y_9 - y_8 y_2) + \frac{A}{2} Sb(\eta y_9 + 4y_8) + Pe(y_7 y_9 + y_8 \phi)$$

The suitable boundary conditions are:

$$y_2 = \lambda_1 + \lambda_2 y_3, y_1 = s, y_5 = -Bi(1 - y_4), y_7 = -Nd(1 - y_6)\ at\ \eta \to 0$$

(23)

$$y_8 \Rightarrow 1, y_2 \Rightarrow 1, y_4 \Rightarrow 0, y_6 \to 0\ at\ \eta \to \infty$$

To solve the equations (19)-(22) we have used the values of y_3, y_5 and y_7 which are not given at the initial conditions. So later finding the initial conditions are integrated by using R-K method with the successive iterative step length is 0.01.

Validation of results

To ensure the quality and dependability of the results, it is crucial to verify them in contrast to established remedies or experimental findings once the bvp4c solver has converged. In order to increase trust within the numerical solution and make sure it correctly depicts the physical system that is being investigated, this validation step is essential. In Table 1, which compares the current work to Rao et al. [21], the validation is displayed.

3. Results and Discussion

In this part, we've used the MATLAB built-in package bvp4c to provide the graphical outcomes of constitutions 11–14 along with the boundary circumstances (15). The results obtained were verified by contrasting them with the published findings of other publications in the books; the validation is displayed in Table 1. Fig. 2 shows the result in response to the velocity profile's increase. The result is two graphs, one showing the existence of the slip condition and the other not. An rise in λ1 indicates greater stretching along the x axis, which causes a rise in. Because the enlarge lessens the thick effect on the pour, the momentum boundary layer's thickness diminishes and increases as a result. Fig. 3 discusses the effect of the magnetic field's angle of inclination on demonstrating a diminishing effect. This is because a higher angle of inclination results in a greater at right anglespower acting on the nanofluid pour, which in turn lowers the swiftness. As seen in Fig. 4, an raises in the magnetic field constraint also results in a reduces in fluid flow. It occurs as a result of developing Lorentz forces, which createconfrontation to the fluid's speed. The injecting effect is indicated by the suction parameter's positive values. As seen in Fig. 5, the nanofluid pours quicker and through an enhanced speed as a result of this inserting power in the way of the pour. Furthermore, we can observe that the border thickness is lower for Figs. 2 and 5, but larger for Figs. 3 and 4. In contrast, it is more in the lack of a slip situationas well as less in the occurrence of one. As a result, when the velocity slip parameter rises, the flow resistance falls and increases, lowering the skin friction coefficient The Biot number (Bi_1),This is intimatelyconnected to the coefficient of temperaturetransport,is the result of convective heat transfer. Therefore, as appears in Fig6, a go upin also results in an uplifted in the coefficient of temperature transmission, which raises the warmth.Fig. 7 deliberates the collision of the Prandtl number on the activation. We recognised in the portrait that the portraits are enhanced with the enhancing values of the Prandtl number. It is also recognised in this plot that the portraits diminished with diminishing values of extending parameter. Figure 8 shows that when the number of Peclets increases, the cells begin to move more quickly, increasing the density of the material. As demonstrated in Fig. 9, the density of the microorganisms decreases dramatically when the diffusivity is inversely related to the Schmidt coefficient.It has been discovered that when slip effects are present, microbe concentrations are produced at greater levels but when they are absent, microorganism concentrations are minimised. Results were obtained for values of both the same and opposite .The pattern of for the optimistic outcomes of $A = 2.5$ is shown by the Red row, while the outline for the

negative values of $A = 2.5$ is shown by the green line. It is evident from the two scenarios that is more potent for negative values of .Furthermore, as can be observed in Figs. 10 loses power as improves . Similarly, *Nu* correspondinglydecreases as well asgrows through the enhancement of as seen in Fig. 11. The reason for this is that it lessens the gradient in surface temperature diminished and respectively, improve, as seen in Fig 12. It is evident from the two scenarios that has greater power for A's negative values than for its positive values. Additionally, when A is present, Nn is greater for the insignificant slip effect and less for the strong slip effects ,negative, even if the positive values of A show the opposite behaviour.

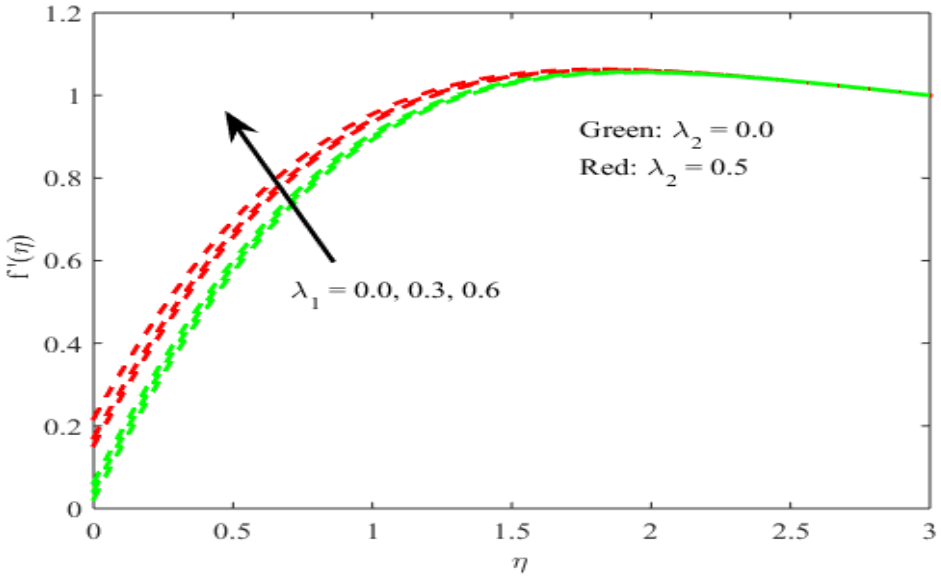

Fig.2performance of λ_1 on velocity profile

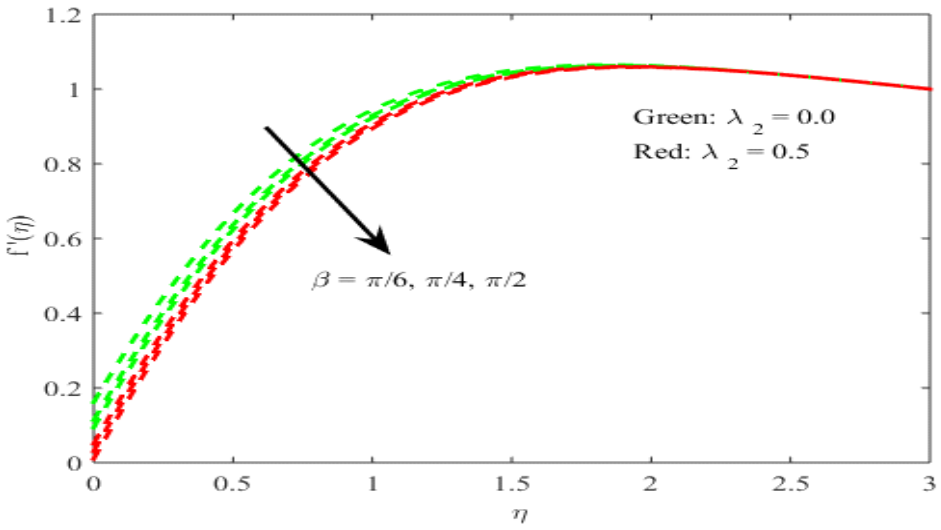

Fig.3 performance of β on velocity profile

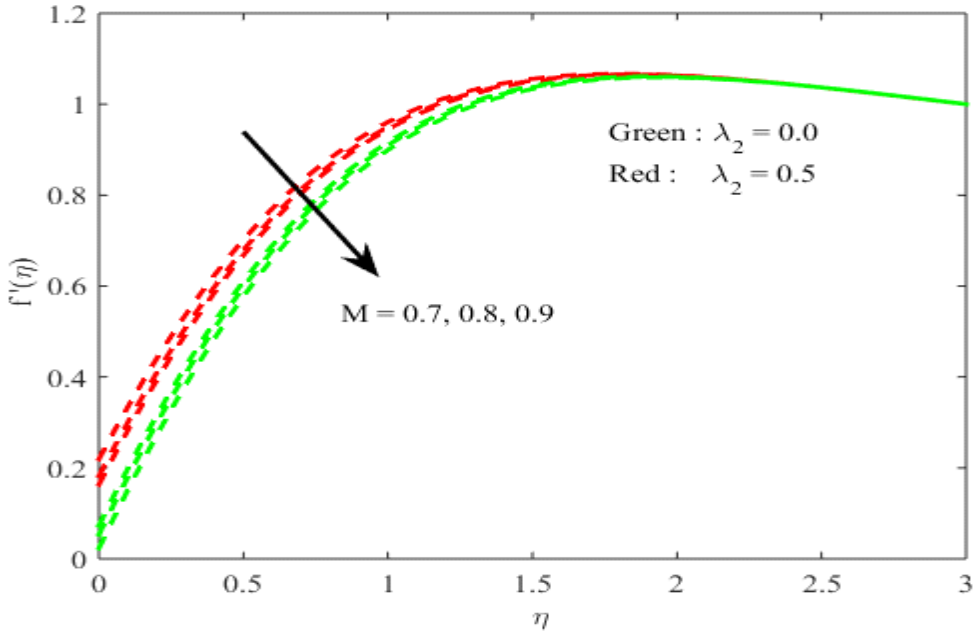

Fig.4 performance of M on velocity profile

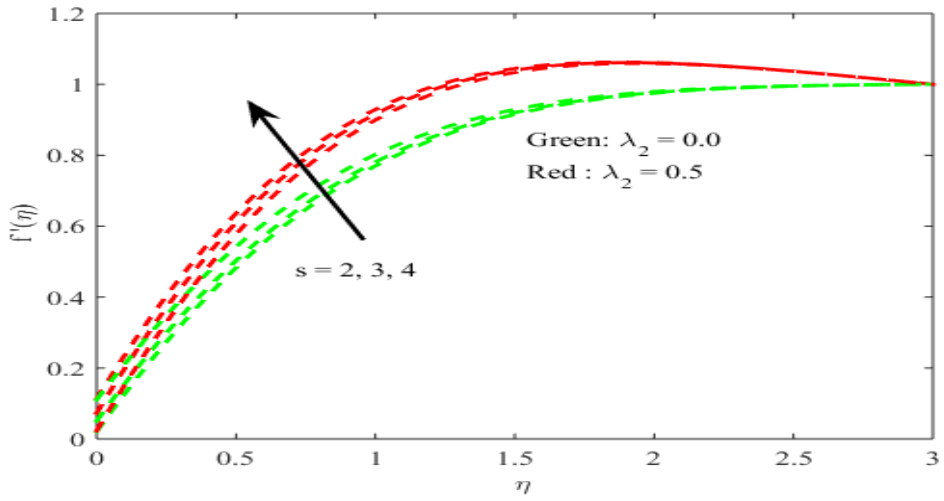

Fig.5 performance of son velocity profile

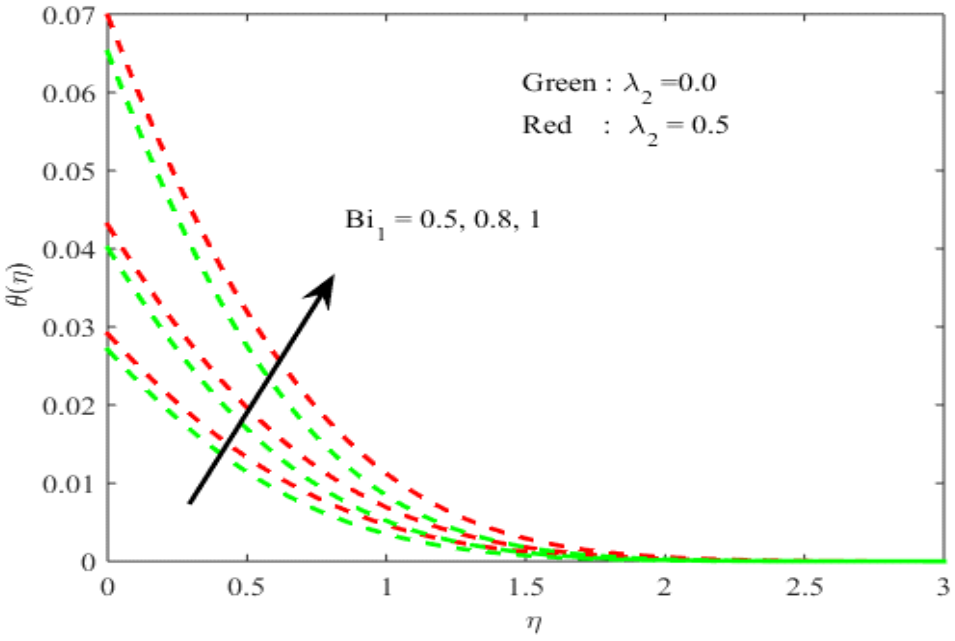

Fig.6 Performance of Bi_1 on temperature profile

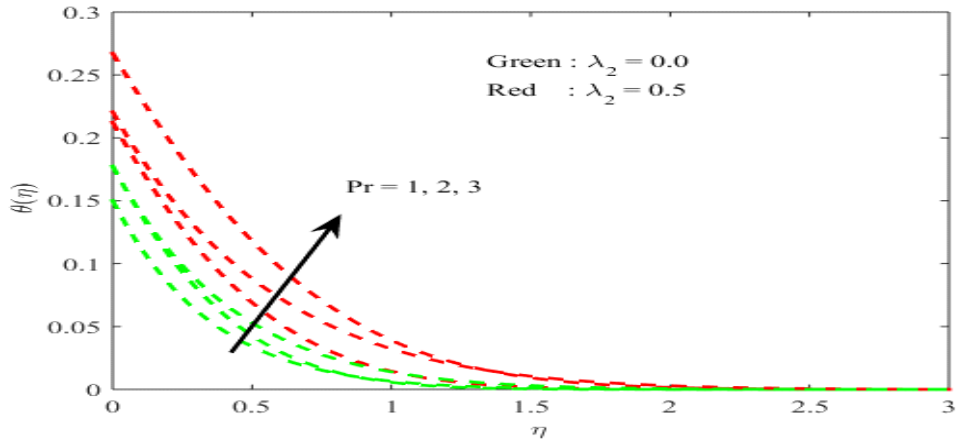

Fig.7 Performance of Pr on temperature profile

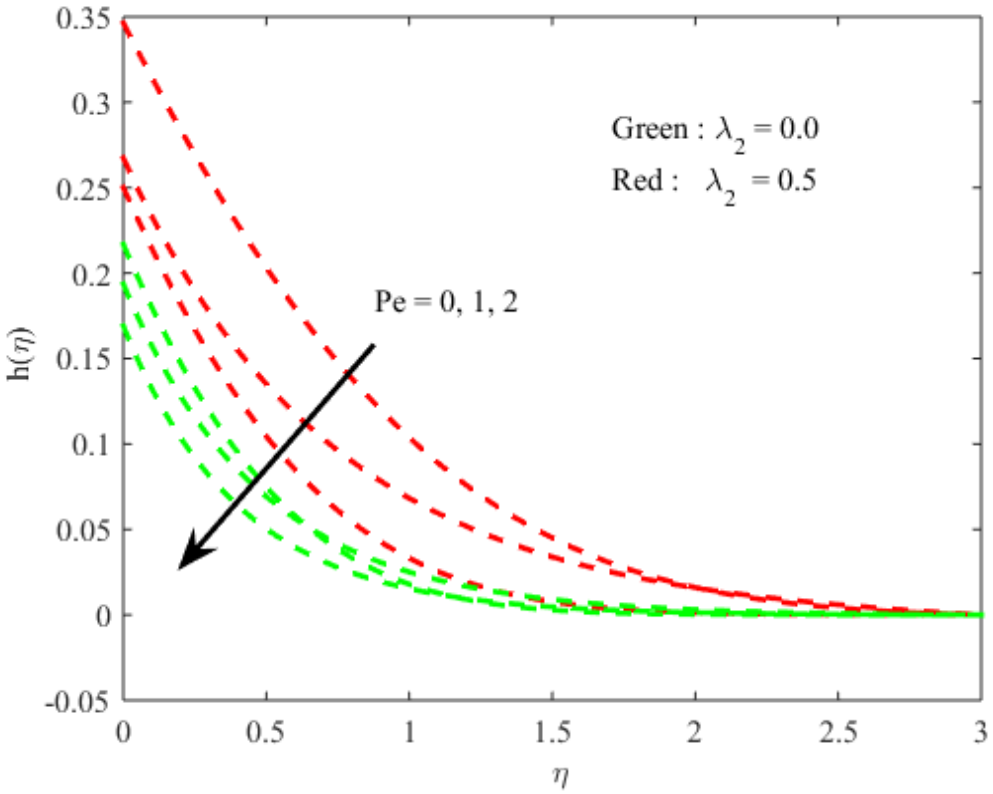

Fig.8 Performance of $\mathrm{P}e$ on $h(\eta)$

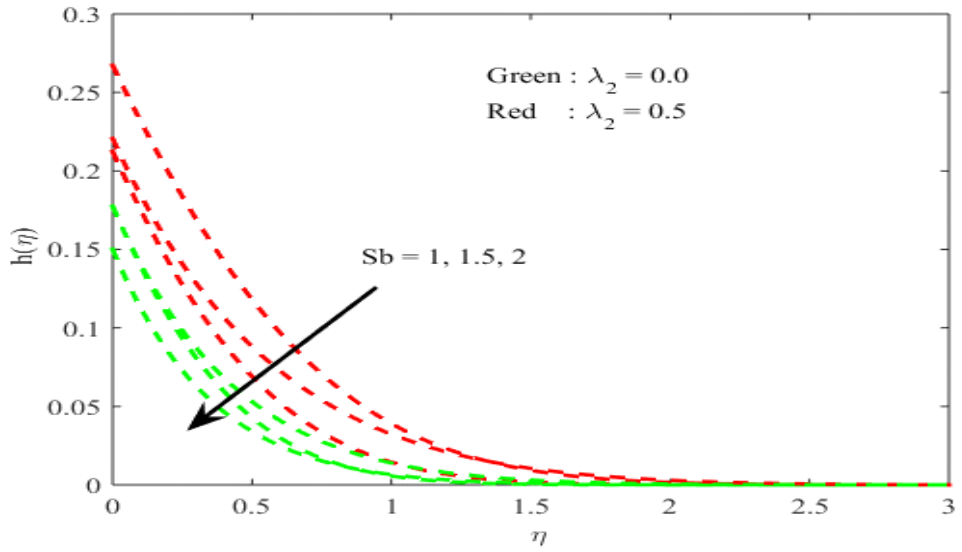

Fig.9 Performance of Sb on $h(\eta)$

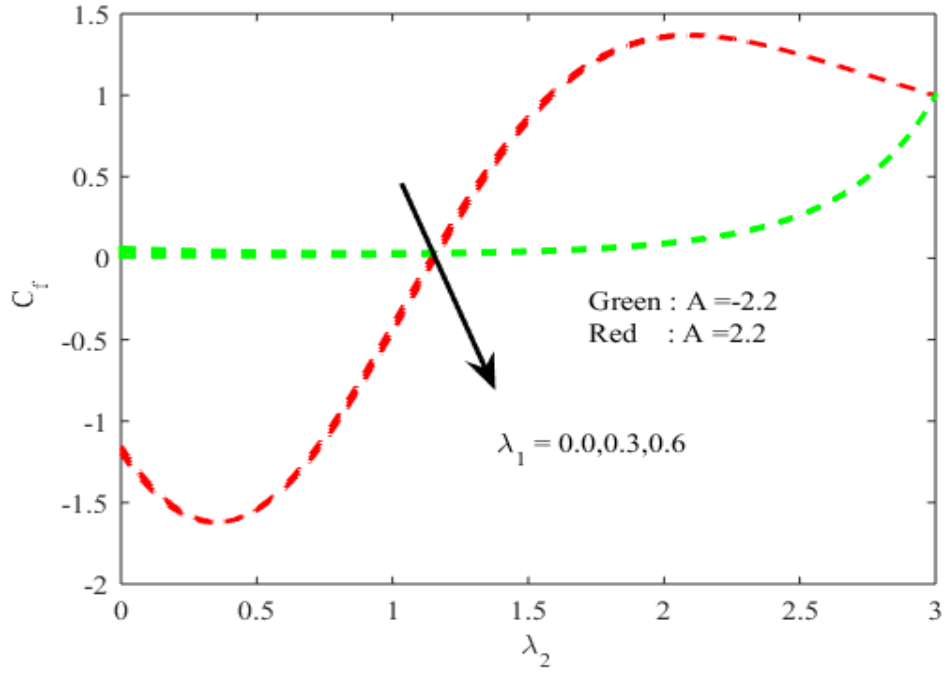

Fig.10Skin friction coefficient *Cf* match up to various values of $\lambda 1$ and Aagainst$\lambda 2$.

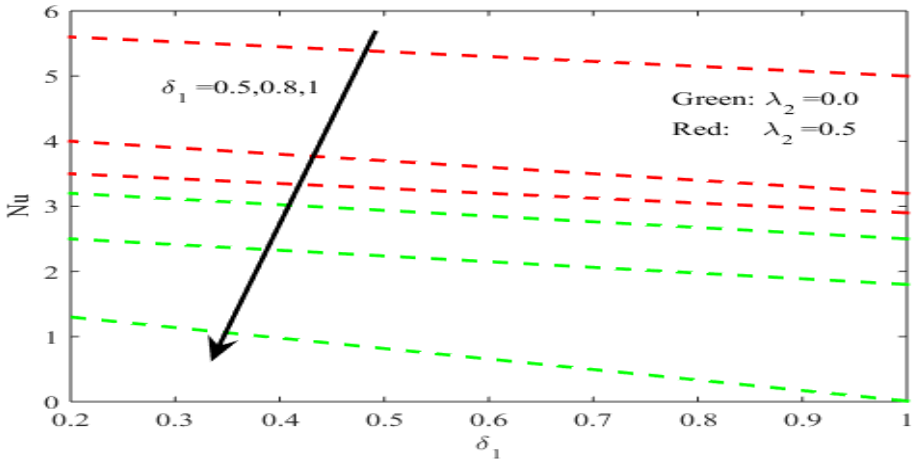

Fig.11 Nusselt number compared to various values

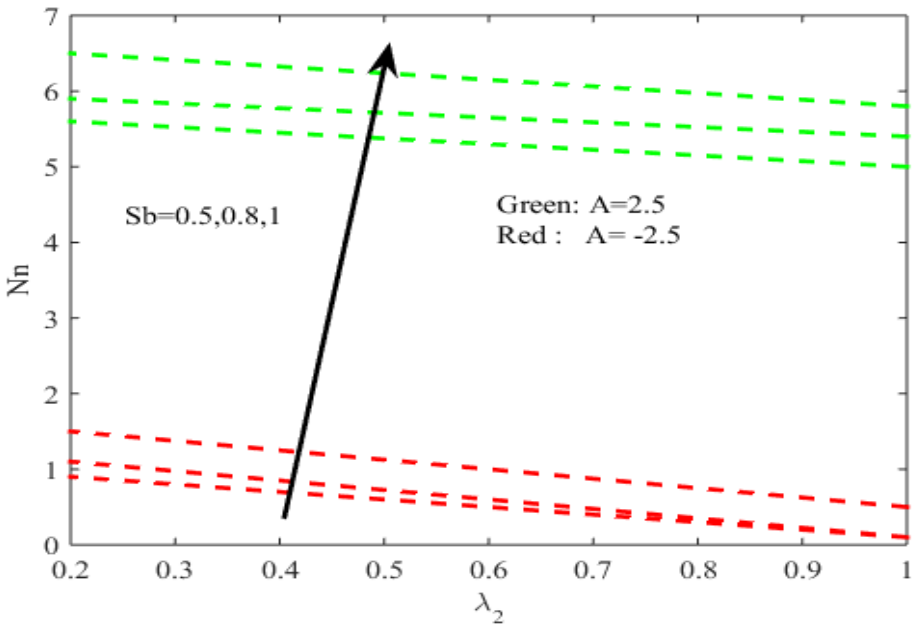

Fig.12Nn compared to various values

Table:1Comparison of skin friction coefficient values $-f''(0)$ with previous results :

	Riaz Khan et al. [20]	Rao et al.[21]	Present
1	1.000102	1.000000	1.000554
2	1.522235	1.522729	1.570098
3	1.923655	1.923612	1.981134
4	2.260669	2.260783	2.312245

Table:2 Computed values for skin friction coefficient, Nusselt number and Sherwood number for a variety of values of the important governing constraints

A	M	Rd	Pr	Q	Sc	Sr	Sb	Pe	λ	λ_2	Bi	Nd	$-f''(0)$	$-\theta'(0)$	$-\phi'(0)$	$-h'(0)$
0.5													0.28825	0.12003	0.18205	0.16578
1													0.29950	0.12838	0.18305	0.16627
1.5													0.30012	0.15986	0.18330	0.16659
	0.5												0.55478	0.11233	0.18386	0.16678
	0.8												0.60807	0.10125	0.18386	0.16739
	0.9												0.62814	0.09872	0.18386	0.16789
		0.8											0.32224	0.05098	0.20508	0.16834
		1.2											0.38148	0.10875	0.20508	0.16878
		1.5											0.40108	0.15605	0.20509	0.16945
			0.5										0.19375	0.10004	0.18365	0.16993
			0.8										0.19375	0.09874	0.18365	0.17152
			1.2										0.19375	0.08892	0.18366	0.17191
				0.6									0.27375	0.15783	0.20243	0.17256
				0.7									0.28375	0.16807	0.30156	0.17499
				0.8									0.30001	0.18880	0.35128	0.17450

					0.5								0.63255	0.19307	0.57137	0.17890
					1.0								0.63100	0.20001	0.57148	0.17999
					1.5								0.63000	0.21506	0.58100	0.18000
						0.09							0.28829	0.12138	0.18305	0.18123
						0.5							0.28830	0.11003	0.17306	0.18231
						1.0							0.28831	0.10004	0.15007	0.18351
							1.0						0.62953	0.20043	0.54792	0.18456
							1.5						0.61000	0.18894	0.55008	0.18798
							2.0						0.60001	0.16800	0.58001	0.18859
								0.5					0.64651	0.15792	0.59808	0.18899
								0.9					0.64651	0.16892	0.51234	0.19150
								1.5					0.64651	0.20081	0.50123	0.19289
									0.7				0.65001	0.12001	0.18101	0.19354
									0.9				0.65241	0.12003	0.18205	0.19547
									1.2				0.65291	0.12838	0.18305	0.19678
										1.5			0.30012	0.15986	0.18330	0.19764
										1.9			0.55478	0.11233	0.18386	0.19837
										2.0			0.60807	0.10125	0.18386	0.19894
											2.0		0.62814	0.09872	0.18386	0.20001
											2.3		0.32224	0.05098	0.20508	0.20453
											2.5		0.38148	0.10875	0.20508	0.22364
												0.2	0.40108	0.15605	0.20509	0.23462
												0.5	0.19375	0.10004	0.18365	0.27863

												1.1	0.19375	0.09874	0.18365	0.28743

4. Conclusion

- The velocity $f'(\eta)$ increases as λ_1 and S accumulate, but it decreases as β and M scale up, respectively.
- The$\theta(\eta)$ shoot ups with the collective values of , Q as well asβ respectively.
- The concentration φ(η) gets stronger, and when Sc values increase, it decreases.
- The concentration of microorganism $h(\eta)$is strengthened by increasing angle β, but it is diminished by increasing Pe, Sb and Sc, respectively.
- Even if the rate of temperature transmission (Nu) is maximal for positive values of A relative to negative values, the friction drags (C_f) are more powerful for negative values of A than for positive values of A .
- While Nn decreases with the development of $\lambda_1$and Sb, respectively, the Sherwood number Sh is magnified by the improvement of both Nd and Sc.

References

[1] Zafar Mahmood, Khadija Rafique , Umar Khan , TaseerMahamood and Ahmed m. Hasan, MHD unsteady flow of carbon nanotubes over nonlinear radiative surface with anisotropic slip conditions: computational analysis of irreversibility for Yamada-Ota model, Engineering Applications of Computational Fluid Mechanics , Vol 18, 2024 .https://doi.org/10.1080/19942060.2024.2309139.

[2] M. M. Hamza, S.Abdulsalam, and S.K. AhmadTime-Dependent Magnetohydrodynamic (MHD) Flow of an Exothermic Arrhenius Fluid in a Vertical Channel with Convective Boundary Condition, Advances in mathematical physics, Volume 2023, Article ID 7173925, 13 pages https://doi.org/10.1155/2023/7173925.

[3] Syed Tauseef Mohyud-Din , Umar Khan , Naveed Ahmed and Muhammad Mehdi Rashidi, A study of heat and mass transfer on magnetohydrodynamic (MHD) flow of nanoparticles, Propulsion and Power Research,Volume 7, Issue 1, March 2018, Pages 72-77.

[4] TousifIqra ,Sohail Nadeem , Hassan Ali Ghazwani, Faisal Z. Duraihem and Jehad Alzabut, Instability analysis for MHD boundary layer flow of nanofluid overa rotating disk with anisotropic and isotropic roughness, Haliyon, Volume 10, Issue 6, 30 March 2024, e26779.

[5] Saquib Ul Zaman, Muhammad Nauman Aslam , Muhammad Bilal Riaz , Ali Akgul , and Azad Hussan, Williamson MHD nanofluid flow with radiation effects through slender cylinder,Results in Engineering, Volume 14 , 2024, 101966.

[6] XiyanTian ,Bingbing Yang , Xin Na , Liankang Ba , and Yi Yuan, Cross-diffusive flow of MHD micropolar nanofluid past a slip stretching plate, Heliyon, Volume 10, Issue 5, 15 March ,2024, e26958.

[7] MunirahAali Alotaibi and Shreen El-Sapa , MHD Couple stress fluid between two concentric spheres with slip regime, Results in Engineering, Vol.21 ,2024, 101934.

[8] Esraa N. Thabet , A.M. Abd-All, H.A. Hosham , and S.M.M. El-Kabeir, Cattaneo-Christov heat and mass fluxes model of Casson fluid employing non-Fourier double diffusion theories with ion slip and Hall effects, Ain Shams Engineering Journal, 2024, 102618.

[9] T. Salahuddin , Muhammad Adil Iqbal , Ambreen Bano , Muhammad Awais , and Shah Muhammad, Cattaneo-Christov heat and mass transmission of dissipated Williamson fluid with double stratification, Alexandria Engineering Journal, Volume 80, 1 October 2023, Pages 553-558.

[10] Hui Chen ,Yiren Ma , Ming Shen , Panfeng He , and Hongmei Zhang, Significance of Cattaneo-Christov double diffusion and induced magnetic field on Maxwell ternary nanofluid flow with magnetic response boundary, Journal of Magnetism and Magnetic Materials, Volume 587, 1 December 2023, 171264.

[11] Felipe Angeles, Hyperbolic systems of quasilinear equations in compressible fluid dynamics with an objective Cattaneo-type extension for the heat flux, Mechanics Research Communications, Volume 130, July 2023, 104103.

[12] Zubair Hussain , Waqar Azeem Khan , M. Irfan , Taseer Muhammad , Sayed M. Eldin , M. Waqas , and P. V. Satya Narayana , Interaction of gyrotactic moment of microorganisms and nanoparticles for magnetized and chemically reactive shear-thinning fluid with stratification phenomenon, Royal Society of Chemistry, Volume 5, Issue 23, 21 November 2023, Pages 6560-6571.

[13] A.V. Kuznetsov, Nanofluid bioconvection: interaction of microorganisms oxytactic upswimming, nanoparticle distribution and heating/cooling from below,TheorComput Fluid Dyn, Vol.1 2012, pp. 291-310.

[14] S. Nadeem, M.N. Khan, N. Muhammad, S. Ahmad, Mathematical analysis of bio-convective micropolar nanofluid, J Comput Des Eng, Vol.3, 2019, pp. 233-242.

[15] M.K. Nayak, J. Prakash, D. Tripathi, V.S. Pandey, S. Shaw and O.D. Makinde,3D Bioconvective multiple slip flow of chemically reactive Casson nanofluid with gyrotactic micro-organisms, Heat Transf-Asian Res , Vol.1, 2020, pp. 135-153.

[16] N. Parveen, M. Awais, S.E. Awan, S.A. Shah, A. Yuan, M. Nawaz, R. Akhtar and M.Y. Malik,Thermophysical properties of chemotactic microorganisms in bio-convective peristaltic rheology of nano-liquid with slippage, Joule heating and viscous dissipation, Case Stud, ThermEng, Vol. 27 , 2021, Article 101285.

[17] H. Waqas, S.A. Khan, S.U. Khan, M.I. Khan, S. Kadry, Y.M. Chu, Falkner-Skan time-dependent bioconvrction flow of cross nanofluid with nonlinear thermal radiation, activation energy and melting process, Int Commun Heat Mass, Vol.120 , 2021, Article 105028.

[18] Zahid Nisar , Bilal Ahmed , Hassan Ali Ghazwani , Khursheed Muhammad , Mohamed Hussien ,and Arsalan Aziz , Numerical study for bioconvection peristaltic flow of Sisko nanofluid with Joule heating and thermal radiation, Heliyon, Vol 9, Issue 12, 2023, e2250.

[19] Umair Rashid , Naeem Ullah , Hamiden Abd El-Wahed Khalifa and Dianchen Lu , Bioconvection modified nanoliquid flow in crown cavity contained with the impact of gyrotactic microorganism, Case Studies in Thermal Engineering, Vol 47, July 2023, 103052.

[20] M. Riaz Khan , V. Puneeth , Mohammed KbiriAlaoui , and Alaa OmranAlmagrabi, Numerical simulation of unsteady MHD bio-convective flow of viscous nanofluid through a stretching surface, Case Studies in Thermal Engineering, Vol. 53 ,2024 ,103830.

[21] P.C.D. Rao, S. Thiagarajan, S.V. Kumar, Darcy–forchheimer flow of Ree–Eyring fluid over an inclined plate with chemical reaction: a statistical approach, Heat Transfer Vol. 50 (7), 2021, 7120–7138.

[22] Faisal Shah, Desheng Zhang ,Bilal Ahmed and Zahid Nisar, . Peristaltic transport of nanofluid with temperature dependent thermal conductivity: a numerical study, Numerical Heat Transfer, 2024, https://doi.org/10.1080/10407782.2024.2316845

[23] **Faisal** Shah, **Tasawar** Hayat and **Shaher** Momani, Non-similar analysis of the Cattaneo-Christov model in MHD second-grade nanofluid flow with Soret and Dufour effects, Alexandria Engineering Journal, Vol 70, 2023

[24] Faisal Shah,D. Zhang, Furqan Ahmad, M. Waqas and M. Ijaz Khan, Nonclassical Transport Laws in Third-Grade Nanoliquid Flow on a Stretchable Surface: A Novel Approach Incorporating Soret and Dufour Effectshttps://doi.org/10.1142/S0219876224410019

[25] **Faisal** Shah, **Tasawar** Hayat and **Ahmed** Alsaedi, Entropy optimization in a fourth grade nanofluid flow over a stretchable Riga wall with thermal radiation and viscous dissipation, International Communications in Heat and Mass TransferVol 127, 2021

[26] **Faisal** Shah, **M. Ijaz** Khan, **T.** Hayat, **M. Imran** Khan and **A.** Alsaedi, Modeling and computational analysis of 3D radiative stagnation point flow of Darcy-Forchheimer subject to suction/injection, Computer Methods and Programs in Biomedicine
Volume 184, February 2020

[27] Faisal Shah, Muhammad Ijaz Khan, Yu-Ming Chu, Seifedine Kadry, Heat transfer analysis on MHD flow over a stretchable Riga wall considering Entropy generation rate: A numerical study, November 2020, https://doi.org/10.1002/num.22694

[28] Faisal Shah and M. Ijaz Khan, Analytical investigation on the combined impacts of the Soret and Dufour phenomenon in the forced convective flow of a non-Newtonian nanofluid by the movable Riga device, Waves in Random and Complex Media, 2022, https://doi.org/10.1080/17455030.2022.2154407

[29] Faisal Shah,D. Zhang and G. Linlin, Non-similar analysis of two-phase hybrid nanofluid flow with Cattaneo-Christov heat flux model: a computational study, Engineering Applications of Computational Fluid Mechanics Vol 18, 2024.

[30] **M.** Ijaz Khan, **Faisal** Shah, **Farhan** Ali and **Faris** Alzahrani, First order chemical reaction response in mixed convective Falkner-SkanSutterby fluid with Cattaneo-Christov heat and mass flux model, Alexandria Engineering Journal, Vol 80, 2023.

Nomenclature

A Unsteadiness coefficient
$B(t)$ Time aligned attractive flux
Bi Biot Component
C Concentration
Cfx Skinfriction number
C_∞ Ambient concentration
C_p Specific heat
D, Dax Darcy Coefficient
h_f Heat transfer coefficient
K Permability of porous media
K_1 Permability
L Viscosity ship factor
Md Convection diffusion parameter
M^2 Hartmann number
Nnx Micro organism coefficient
Nux Nusselt number
Pe Peclet number
Pr Prandtl number
qm Mass flux
qn Micro organism coefficient

qw Local heat flux

qr Rosseland approximate

Q heat source parameter

Q_0 heat source initial value

Rd Radiation coefficient

S Suction coefficient

Sb Schmidt coefficient

Sc Schmidt number

Shx Shearwood number

t time

T Temperature

T_w Wall temperature

T_∞ Ambient temperature

u, v Velocity components

$U_w(x, y)$ Stagnation point

$V_w(x)$ Slide velocity

We Electric conductivity coefficient

Greek Symbols

β Acute angle

λ_1 Stretching coefficient

λ_2 Velocity ship parameter

σ Thermal conductivity

σ^* Stefan boltzman constant

K^* Mean absorption coefficient

δu Heat source parameter

United International Journal of Multidisciplinary Research
ISSN: 3048-6726 (UIJMR) Impact Factor: 6.934 (SJIF)
An International Peer-Reviewed and Refereed Multidisciplinary Journal
Website: www.uijmr.in | Volume 3 | Special Issue 5 | March | 2026

Optimization Techniques and Operations Research in Academic Administration and Institutional Planning

Dr.Sunitha Sanga
Assistant Professor of Hindi,SR Government Arts & Science College,Kothagudem, Bhadradri, Telangana
Contact: +91 9849029666
Email: 109sunee@gmail.com

Shainaj Khan (Babji),
Lecturer in Hindi,Government Degree College (A),PALONCHA-507115,
Bhadradri Kothagudem District,Telangana State,CELL: 7995509950, CELL: 8520909922,
E.MAIL: babjiyellandu@gmail.com

ABSTRACT

The increasing complexity of academic administration demands systematic and quantitative approaches for effective institutional planning and resource management. Problems such as faculty workload distribution, timetable scheduling, and optimal utilization of academic infrastructure can be formulated as constrained optimization problems within the framework of operations research. This paper presents a mathematical approach to academic administration using optimization techniques to support efficient and equitable decision-making.

The study models key administrative processes using linear programming, where decision variables represent academic resources and activities, objective functions are designed to minimize workload imbalance and resource inefficiency, and constraints reflect institutional policies, regulatory norms, and operational limitations. Emphasis is placed on incorporating fairness and balance as measurable parameters within the optimization framework, informed by long-term experience in academic leadership and gender-conscious educational research.

A conceptual case illustration is provided to demonstrate the formulation of objective functions and constraints for faculty workload allocation and timetable optimization. The results highlight how optimization models enable transparent, data-driven planning and reduce administrative conflicts. The paper further discusses the scope of integrating these mathematical models with emerging digital academic management systems and computational decision-support tools.

The study concludes that the application of optimization techniques and operations research offers a viable mathematical foundation for improving academic administration, promoting inclusive institutional planning, and supporting sustainable development in higher education.

Keywords: Linear Programming, Optimization Techniques, Operations Research, Academic Administration, Institutional Planning

1. Introduction

Higher education institutions today operate in an environment characterized by increasing student enrolment, limited resources, regulatory constraints, and rising expectations for quality and inclusivity. Academic administration plays a crucial role in balancing these competing demands through effective planning, coordination, and resource allocation. Traditional administrative practices often rely on experience-based decision-making, which, while valuable, may lead to inefficiencies, workload imbalances, and suboptimal utilization of resources.

Operations Research (OR) and optimization techniques provide a scientific and mathematical approach to decision-making by enabling administrators to model complex problems, evaluate alternatives, and arrive at optimal solutions under given constraints. Originally developed for industrial and military applications, OR techniques have gradually found relevance in service sectors, including education. The application of mathematical optimization in academic administration offers opportunities to enhance transparency, efficiency, and fairness in institutional planning.

This paper focuses on the application of optimization techniques and operations research to address key administrative challenges in academic institutions. Drawing from long-term experience in educational leadership and administration, the study emphasizes the importance of balancing efficiency with equity, particularly in faculty workload distribution and institutional planning. By framing administrative challenges as mathematical optimization problems, this work demonstrates how quantitative models can support informed and inclusive decision-making in higher education.

2. Operations Research and Optimization Techniques

Operations Research is a multidisciplinary field that uses mathematical models, statistical tools, and logical reasoning to support decision-making in complex situations. In simple terms, operations research helps decision-makers choose the best possible option from many alternatives when resources such as time, money, or manpower are limited.

Linear Programming: A Simple Definition

Linear Programming (LP) is one of the most basic and widely used techniques in operations research. It is a mathematical method used to optimize, that is, to either maximize or minimize a particular objective such as cost, time, or workload, while satisfying a set of limitations known as constraints.

In a linear programming problem:

- The objective function represents what we want to optimize, for example minimizing workload imbalance.
- The decision variables represent the choices available to the decision-maker, such as teaching hours assigned to faculty members.
- The constraints represent real-life restrictions including institutional rules, availability of resources, and regulatory limits.

The word linear means that the relationships between variables are proportional and expressed using first-degree terms only. Because many administrative decisions in educational institutions follow such proportional relationships, linear programming offers a simple, transparent, and practical framework for academic planning problems.

3. Mathematical Modelling of Academic Administration

Academic administration involves multiple interrelated activities that require careful planning and coordination. These activities can be mathematically modelled by identifying relevant decision variables, defining appropriate objective functions, and incorporating institutional constraints.

3.1 Decision Variables

Decision variables represent controllable elements of the system. In academic administration, decision variables may include:

- Number of teaching hours assigned to each faculty member
- Allocation of classrooms and laboratories
- Scheduling of courses and examinations
- Distribution of administrative responsibilities

3.2 Objective Functions

The objective function reflects the goal of the optimization process. In academic administration, common objectives include:

- Minimizing faculty workload imbalance
- Maximizing utilization of academic infrastructure
- Minimizing timetable conflicts
- Enhancing overall administrative efficiency

For example, an objective function may be formulated to minimize the deviation between actual and ideal faculty workload distribution.

3.3 Constraints

Constraints represent limitations and requirements that must be satisfied. Typical constraints in academic administration include:

- Maximum and minimum teaching load per faculty member
- Availability of classrooms and laboratories
- Institutional policies and regulatory norms
- Human and ethical considerations

By incorporating these constraints, the optimization model ensures that solutions are both feasible and acceptable within the institutional context.

4. Faculty Workload Optimization: A Conceptual Model

Faculty workload allocation is a critical administrative challenge in higher education institutions. Inequitable distribution of teaching and administrative responsibilities can lead to dissatisfaction, reduced productivity, and institutional inefficiencies. This problem can be effectively represented using a simple linear programming model.

Let us consider a simplified mathematical formulation for faculty workload optimization.

Let:

- x_i denote the number of teaching hours assigned to the i-th faculty member. This is the decision variable, as it represents the quantity we want to determine.
- W_i denote the ideal or recommended teaching workload for the i-th faculty member, based on experience, designation, or institutional norms.

Objective Function

The objective of the model is to minimize the total imbalance in workload among faculty members. This imbalance is measured as the difference between the assigned workload and the ideal workload.

Minimize: Z = sum from i = 1 to n of |x_i − W_i|

Here, Z represents the total deviation from the ideal workload. By minimizing Z, the model attempts to distribute teaching hours as evenly and fairly as possible across all faculty members.

Constraints

The model is subject to the following constraints:

- L_i ≤ x_i ≤ U_i, which ensures that each faculty member is assigned teaching hours within permissible minimum and maximum limits.
- The sum of x_i for all faculty members equals T, where T represents the total teaching requirement of the institution.

These constraints ensure that the solution is practical, feasible, and compliant with institutional policies. The model can be solved using standard linear programming techniques after appropriate linearization.

Objective Function

$$\text{Minimize } Z = \sum_{i=1}^{n} |x_i - W_i|$$

Constraints

$$L_i \leq x_i \leq U_i, \quad i = 1, 2, \ldots, n$$

$$\sum_{i=1}^{n} x_i = T$$

Where

- x_i = teaching hours assigned to the i^{th} faculty member
- W_i = ideal teaching workload of the i^{th} faculty member
- L_i, U_i = minimum and maximum permissible workload limits
- T = total teaching requirement of the institution

5. Timetable and Resource Optimization

Timetable scheduling and resource allocation are complex problems involving multiple constraints and competing objectives. Optimization techniques enable administrators to generate conflict-free schedules that maximize resource utilization.

A timetable optimization model may include decision variables representing course-room-time assignments, with constraints ensuring that:

- No two courses are scheduled in the same room at the same time
- Faculty availability is respected
- Classroom capacity meets course enrolment requirements

The objective function may aim to minimize scheduling conflicts or maximize utilization efficiency. Such models can significantly reduce manual effort and improve scheduling accuracy.

6. Equity and Inclusive Planning in Optimization Models

Beyond efficiency, academic administration must address issues of equity and inclusiveness. Optimization models can incorporate fairness by assigning weights to objective functions or introducing additional constraints that ensure balanced outcomes.

Gender-conscious and inclusive planning principles can be reflected by:

- Limiting excessive workload concentration
- Ensuring equitable access to institutional resources
- Supporting transparent and unbiased decision-making

By embedding such considerations into mathematical models, optimization techniques can align administrative efficiency with social responsibility.

7. Integration with Emerging Technologies

Artificial intelligence and machine learning techniques can be integrated with traditional operations research models to handle large datasets and dynamic environments. Such integration allows optimization models to move beyond static assumptions and adapt continuously to changing academic demands, faculty availability, and student enrollment patterns. Predictive analytics can forecast workload requirements, resource utilization, and scheduling conflicts, while optimization algorithms can generate near-optimal solutions in real time. This synergy between emerging technologies and classical optimization techniques enhances the accuracy, scalability, and responsiveness of academic decision-making systems, thereby supporting more informed, equitable, and sustainable institutional governance.

References

- Sharma, S. D., Operations Research. Galgotia Publishers.
- Rao, S. S., Optimization Theory and Applications. New Age International.
- Joshi, M. C., & More, K. M., Optimization Techniques: Theory and Practice. Narosa Publication

United International Journal of Multidisciplinary Research
ISSN: 3048-6726 (UIJMR) Impact Factor: 6.934 (SJIF)
An International Peer-Reviewed and Refereed Multidisciplinary Journal
Website: www.uijmr.in | Volume 3 | Special Issue 5 | March | 2026

CATTANIO CHRYSTOV ANALYSIS ON 3D MAGNETO-CARREAU NANOFLUID FLOW IN A VERTICAL STRETCHING SHEET

[1.] J. Manjula
Department of Mathematics,TGSWRDCW, KHAMMAM, Telangana, India-507170
Mail Id:manjulajonnadula73@gmail.com

[2]. Pothapragada Himabindu
Department of Mathematics,SBIT, Khammam,Mail Id:bindu68287@gmail.com

[3.] .Ch.Neeraja
Department of Mathematics,CMR Institute of Science &Technology, kandlakoya
Hyderabad, Telangana, India.
Mail Id:neeraja.maths@gmail.com

ABSTRACT

In this frame work, the three dimensional (3D) flow of hydromagneticCarreauNanofluidtransport over a stretching sheet has been adressed by considering the impacts of nonlinear thermal radiation and convective conditions. Infinite Shear rate viscosity impacts are invoiced in themodeling. In this investigation the Cattaneo-Christov model is illustrated to analyse the features of thermal relaxation time. Suitable similar variables are exercised to transmute the governing partial differential equations in to regular differential equations. The outcomes of different sundry variables on velocity, temperature, and concentration are discussed. The heat transport charectaristics are explored by employing the effects of magnetic field, thermal nonlinear radiation and buoyancy effects. Rudimentary governing PDEs are represented and are altered to ordinary differential equations by the similarity transformation. The non-linear ODEs along with the boundary restrictions are resolved with the aid of Runge-Kutta-Fehlberg scheme (RKFS) based on Shooting technique. Further moreImpacts of important variables on skin friction, Nusselt have been scrutinized through tables and graphical plots. Velocity distribution is suppressed by greater values of Hartmann number. The velocity components in x & y directions of fluid are raised with viscosity ratio parameter and tangential slip parameter, but these components are reduced with N^*, α^*.

Key words: Non-linear Radiation; MHD; CarreauNanofluid; Stretching sheet; Convection Conditions;

United International Journal of Multidisciplinary Research
ISSN: 3048-6726 (UIJMR) Impact Factor: 6.934 (SJIF)
An International Peer-Reviewed and Refereed Multidisciplinary Journal
Website: www.uijmr.in | Volume 3 | Special Issue 5 | March | 2026

1. INTRODUCTION

The aspect of heat transfer analysis under the impact of radiation has significant role in engineering and industrial processes. Heat transfer arises in petroleum reservoirs, space technology, nuclear waste disposal, gas turbines etc.The linear radiation is not valid at high temperature difference process. Viscosity, density and thermal conductivity of ordinary materials represent the heat transfer efficiency. Hayat et al. [1] have investigated the heat transfer and mass flow properties with heat generation/absorption and chemical reaction. HongtaoXu et al. [2] have established the lattice Boltzmann model to the heat transfer between fluid and solid. Mamatha et al. [3] have investigated the behaviour of active parameters and MHD parameters with dusty fluid flow. Anjalidevi et al.[4] have reported the effect of radiation on a viscous boundary layer forced convective flow over a non-linear stretching surface with variable wall temperature and non-uniform heatsource/sink. Das et al.[5] represented the spectral local linearization method to find the solution for the fluid velocity,fluid temperature and concentration.Vajravelu et al. [6] have reported an analysis of thermal and mass diffusion impacts on 2D boundary layer transport of Ostwald-de Waele viscous fluid.

Nanofluids contain nano sized particles. This word is proposed by Choi and Eastman [7] in 1995. Nanofluids are mostly visualized in biomedical engineering and medicine non-therapeutic devices.Gnaneswara Reddy [8] has observed the role of MHD , heat radiation upon boundary layer of the nanofluid flow due to a surface area in presence of slip conditions and Biot numbers.Habib-olahSayehvand and Amir Basiripasra [9] have investigated the nano particles effect in front of magnetic fluid by permeable medium.Rudraswamy and Gireesha [10] represented their report on the heat transport of nano-liquid in the existence of chemical reaction, heat radiation effects over an expanding stretching sheet.Rashidi et al. [11] have presented the entropy fluid model and utilized to replicate the phenomena of evaporation and condensation in solar still. This fluid model is used to represent the potential of nanofluid water and to develope productivity of a solar still. The simultaneous characteristics of thermal radiation and the bio effects of heat transfer melting are presented in the flow of carbon nanotubes in stagnation was investigated by Hayat et al. [12].Heat and mass transfer of thermophoretic flow has potential applications such as air cleaning,aerosol particles sampling, nuclear reactor safety and micro electronics manufacturing.Outline of the thermophoresis is transmigration of suspended small nanoparticles in a non-isothermal gas represents diminish a heat gradient and velocity obtained by this particle is known as thermophereticvelocity.This brief consideration is studied by Das et al.[13].Ibrahim and Makinde [14] investigated heat and mass flow effects on MHD of power law nanofluid. Gnaneswara Reddy et al. [15] have consideredthe velocity slip on hydromagnetic 3D Cassonnanofluid and obtained the numerical solution for that system. Abdul Hakeem et al. [16] have explained that slip has to be included in stretching sheet on nanofluid with MHD effect.

Now in days, the investigations have been mostly focused on the flow of non-Newtonian fluids due to extensive and prominent.The theory of non-Newtonian fluids phenomena has attrached more

attention when contrasted to Newtonian liquids.Recent analytical and numerical studies related to the flow and heat transfer non-Newtonian fluids.

Schowalter [17] was the first one,who formulated the boundary layer flow of non-Newtonian fluid and established the conditions for the existence of a similarity solution.The heat transfer aspects of non-Newtonian liquid motion engendered by a nonlinearly stretched surface with respect to viscous dissipation were examined by Kishan and Kavitha [18].The articles [19],[20] deal with the peristaltic transport of distinct non-Newtonian fluids in a rectangular channel. Raju and Sandeep [21] analyzed the influence of Soret and Dufour numbers on non-Newtonian bio-convective flow past two different geometries with magnetic field. Ramana Reddy et al.[22] represent the heat and mass transport effect on the flow of two different non-Newtonian fluids.The flow is generated by stretching of the surface. Khan et al. [23] have investigated flow of magnetohydrodynamicCarreaufluid in the presence of non-linearradiation thermal with heated surface. Gnaneswarareddy et al. [24] have represented the flow analysis on Carreau fluid over a convectively heated sheet. Khan and Azam [25] have been reported that species flow in effected by hydromagneticCarreau fluid across stretching sheet with numerically.

Cattaneo [26] and Christov [27] explained about thermal relaxation time in the presence of Fourier's law and to attain the numerical invariant. Cattaneo-Christov protocol in the movement of viscous liquid was encouraged by Straughan [28]. Hayat et al. [29] interrogated 3-D flows related toCattaneo-Christov model. They consummated that δ_e and δ_c uplifted Sherwood number and Nusselt number has boosted. Mamatha et al [30] was scrutinized by dual types of flows with dusty nano fluid. They are demonstrating plotting illustrates for duel values of Nano particle at $\phi = 0.0, 0.5$. Hydromagnetic performance on non-Newtonian liquid on cone/wedge was scrutinized by Reddy [31].

The idea of current research is to scrutinize the three dimensional Carreau Nano fluid flow over a stretching sheet with the impacts of nonlinear radiation and convective conditions. Non-zero infinite shear rate viscosity is considered in the mathematical formulation. Non linear radiation, buoyancy effects, and magnetic field are involved in the heat transport. R-K fourth order method and shooting techniques are used in current work for the finding the numerical result of modelled equations. The effects of all important variables, on velocity, concentration, temperature, skin friction ,Nusselt and Sherwood numbers are presented through graphs and tables. The current work is an extension study of Massod Khan et al. [31].

2. Description of physical model

We considered the steady-state, three dimensional, MHD Carreaunanofluid boundary layer anisotropic slip flow of the stretching sheet. The physical model of problem is illustrated in Fig.1.

United International Journal of Multidisciplinary Research
ISSN: 3048-6726 (UIJMR) Impact Factor: 6.934 (SJIF)
An International Peer-Reviewed and Refereed Multidisciplinary Journal
Website: www.uijmr.in | Volume 3 | Special Issue 5 | March | 2026

Temperature difference generates the buoyancy forces. The surface velocity is represented by $U_w = ax$, $V_w = by$. Brownian motion and Thermopheresis effects are included in this model.

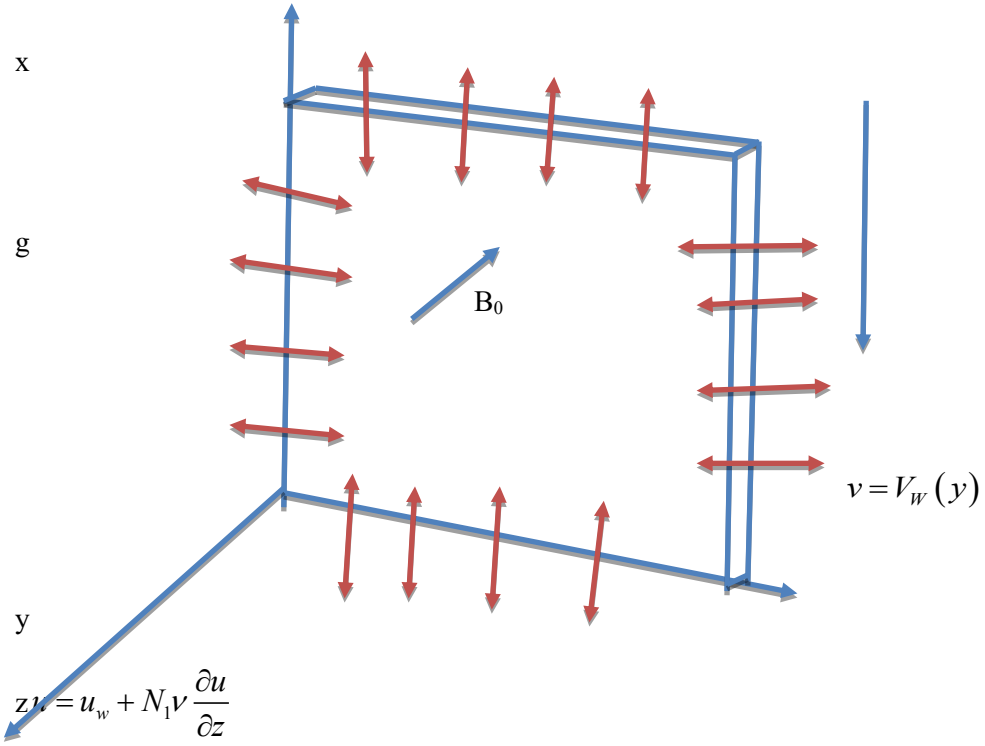

Fig.1 Physical model (Schematic diagram)

3. Flow equations

The three dimensional Boussinesq-Oberbeck equations are considered here:

$$\frac{\partial u}{\partial x} + \frac{\partial v}{\partial y} + \frac{\partial w}{\partial z} = 0 \qquad (1)$$

$$u\frac{\partial u}{\partial x}+v\frac{\partial u}{\partial y}+w\frac{\partial u}{\partial z}=\nu\frac{\partial^2 u}{\partial z^2}\left(\beta^*+(1-\beta^*)\left\{1+\Gamma^2\left(\frac{\partial u}{\partial z}\right)^2\right\}^{\frac{n-1}{2}}\right)$$

$$+\nu_f(n-1)\left(1-\beta^*\right)\Gamma^2\left(\frac{\partial^2 u}{\partial z^2}\right)\left(\frac{\partial u}{\partial z}\right)^2\left\{1+\Gamma^2\left(\frac{\partial u}{\partial z}\right)^2\right\}^{\frac{n-3}{2}} \quad (2)$$

$$+g\left(\lambda_0(T-T_\infty)+\lambda_1(T-T_\infty)^2+\lambda_2(C-C_\infty)+\lambda_3(C-C_\infty)^2\right)-\frac{\sigma B_0^2}{\rho_f}u$$

$$u\frac{\partial v}{\partial x}+v\frac{\partial v}{\partial y}+w\frac{\partial v}{\partial z}=\nu\frac{\partial^2 v}{\partial z^2}\left(\beta^*+(1-\beta^*)\left\{1+\Gamma^2\left(\frac{\partial v}{\partial z}\right)^2\right\}^{\frac{n-1}{2}}\right)+$$

$$\nu_f(n-1)\left(1-\beta^*\right)\Gamma^2\left(\frac{\partial^2 v}{\partial z^2}\right)\left(\frac{\partial v}{\partial z}\right)^2\left\{1+\Gamma^2\left(\frac{\partial v}{\partial z}\right)^2\right\}^{\frac{n-3}{2}}-\frac{\sigma B_0^2}{\rho_f}v \quad (3)$$

$$u\frac{\partial T}{\partial x}+v\frac{\partial T}{\partial y}+w\frac{\partial T}{\partial z}=\alpha_1\left(\frac{\partial^2 T}{\partial z^2}\right)-\frac{1}{\left(\rho c_p\right)_f}\frac{\partial}{\partial z}(q_r)+\tau\left[D_B\frac{\partial T}{\partial z}\frac{\partial C}{\partial z}+\frac{D_T}{T_\infty}\left(\frac{\partial T}{\partial z}\right)^2\right]$$

$$\lambda_1\left(\begin{array}{l}u_a\dfrac{\partial u}{\partial x}\dfrac{\partial T}{\partial x}+v\dfrac{\partial v}{\partial y}\dfrac{\partial T}{\partial y}\\ +u\dfrac{\partial v}{\partial x}\dfrac{\partial T}{\partial y}+v\dfrac{\partial u}{\partial y}\dfrac{\partial T}{\partial x}\\ +2uv\dfrac{\partial^2 T}{\partial x\partial y}+u^2\dfrac{\partial^2 T}{\partial x^2}+v^2\dfrac{\partial^2 T}{\partial y^2}\end{array}\right) \quad (4)$$

Here thermal diffusivity is $\alpha_1 = \frac{k}{\rho C_p}$, specific heat is C_p, kinematic viscosity is $\nu_f = \frac{\mu_0}{\rho_f}$, the ratio of non-zero infinite shear rate viscosity to the zero shear rate viscosity is $\beta^* = \frac{\mu_\infty}{\mu_0}$, the electric charge density is σ, magnetic induction is B_0, surface temperature parameter is T, power law index is n, the ratio of heat capacity of the nanoparticle material and base fluid heat capacity is $\tau = \frac{\rho C_p}{(\rho C_p)_f}$, Brownian motion coefficient is D_B, coefficient of thermophoretic diffusion is D_T, ratio of thermal expansion coefficients λ_0, λ_1, ratio of concentration expansion coefficients λ_2, λ_3.

Adapting to Roseland approximation , heat radiation flux q_r is recorded as :

$$q_r = -\left(\frac{4\sigma^*}{3k^*}\frac{\partial T^4}{\partial z}\right) \tag{6}$$

σ^* is Stefan-Boltzmann constant , k^* mean absorption coefficient respectively. Equation (4) is the nonlinear power equation is high and it is difficult to find a solution. Researchers have found a solution to this problem in the past, indicating the small temperature differences within the flow.

The nonlinear thermal radiation of energy equation is given by:

$$u\frac{\partial T}{\partial x} + v\frac{\partial T}{\partial y} + w\frac{\partial T}{\partial z} = \frac{1}{\left(\rho c_p\right)_f}\frac{\partial}{\partial z}\left[\left(\alpha_1 + \frac{16\sigma^*}{3k^*}\frac{T^3}{\rho c_p}\right)\frac{\partial T}{\partial z}\right] + \tau\left[D_B\frac{\partial T}{\partial z}\frac{\partial C}{\partial z} + \frac{D_T}{T_\infty}\left(\frac{\partial T}{\partial z}\right)^2\right] \tag{7}$$

The following boundary conditions are precribed

$$u = u_W + N_1\nu\frac{\partial u}{\partial z},\ v = V_W(y),\ w = 0,\ -k\frac{\partial T}{\partial z} = h_1\left(T_f - T\right),\quad -k\frac{\partial C}{\partial z} = h_2\left(C_f - C\right) \text{ at z=0} \tag{8}$$

$$`u = v = 0\ ,\ T \to T_\infty,\ \ C \to C_\infty \text{ as } z \to \infty \tag{9}$$

To create a flow model without dimension, let us use the dimensionless quantities of the following:

United International Journal of Multidisciplinary Research
ISSN: 3048-6726 (UIJMR) Impact Factor: 6.934 (SJIF)
An International Peer-Reviewed and Refereed Multidisciplinary Journal
Website: www.uijmr.in | Volume 3 | Special Issue 5 | March | 2026

$$\eta = z\sqrt{\frac{a}{\nu_f}},\ u = axf'(\eta),\ v = ayg'(\eta),\ w = -\sqrt{a\nu_f}\left[f(\eta)+g(\eta)\right],\quad \theta(\eta) = \frac{T-T_\infty}{T_f-T_\infty}, \tag{10}$$

$$\phi(\eta) = \frac{C-C_\infty}{C_f-C_\infty}$$

The continuity equation is automatically inspected by realizing a stream function $\psi(x,y)$ such that:

$$u = \frac{\partial\psi}{\partial y}\ ,\ v = -\frac{\partial\psi}{\partial x}\ ,\ T = T_\infty + \left[1+\left(\theta_w - 1\right)\theta\right]$$

ambient fluid temperature is T_∞, ambient fluid concentration is C_∞ ,temperature ratio parameter is $\theta_w = \frac{T_f}{T_\infty}$. Using non dimensional parameters in equation (11), the equations (2), (3), (5) and (8) reduced to:

$$f'''\left[\beta^* + (1-\beta^*)\left\{1+We^2\left(f''\right)^2\right\}^{\frac{n-3}{2}}\left\{1+nWe^2\left(f''\right)^2\right\}\right] \tag{11}$$
$$+\left(f+g\right)f''-\left(f'\right)^2+\alpha\theta+\beta_T\theta^2+\alpha N^*\left(\phi+\beta_C\phi^2\right)-M^2f'=0$$

$$g'''\left[\beta^* + (1-\beta^*)\left\{1+We^2\left(g''\right)^2\right\}^{\frac{n-3}{2}}\left\{1+nWe^2\left(g''\right)^2\right\}\right]$$
$$+\left(f+g\right)g''-\left(g'\right)^2-M^2g'=0$$

(12)

$$\frac{1}{\Pr}\left[\frac{4}{3N_R}\left(\left(\left(1+\left(\theta_w-1\right)\theta\right)^3\theta''+3\left(\theta_w-1\right)\theta'^2\left(1+\left(\theta_w-1\right)\theta\right)^2\right)\right)\right]+ \tag{13}$$
$$\left(f+g\right)\theta'+Nt\theta'^2+Nb\theta'\phi'+\delta_1\left(ff'\theta'+f\theta''\right)=0$$

We are getting following associated boundary conditions

$$f(0)=g(0)=0,\quad f'(0)=1+\delta_u f''(0),\quad g'(0)=\alpha^*,$$
$$\theta'(0)=-\gamma_1\left[1-\theta(0)\right], \qquad (15)$$
$$f'(\infty)\to 0,\quad g'(\infty)\to 0,\ \theta(\infty)\to 0,$$

Here the differentiation is with respect to η in the above equations.

$M^2=\dfrac{\sigma B_0^{\,2}}{\rho_f a}$ is Hartmann number, $\alpha^*=\dfrac{b}{a}$ is ratio of stretching sheet, $We=\sqrt{\dfrac{a^3\Gamma^2x^2}{\nu_f}}$ is Weissenberg number, $\Pr=\dfrac{\mu C_p}{k}$ is the Prandtl number, $N_R=\dfrac{kk^*}{4\sigma^* T_\infty^{\,3}}$ is nonlinear radiation parameter, local Biot numbers $\gamma_1=\dfrac{h_1}{k}\sqrt{\dfrac{\nu_f}{a}}$, $\delta_1=\lambda_1 a$ is non-dimensional thermal relaxation time,

α is mixed convection parameter, β_T is nonlinear convection parameter, N^* is concentration to thermal buoyancy forces ratio, β_C is nonlinear convection parameter due to concentration which are given by:

$$\alpha=\frac{g\lambda_0\left(T-T_\infty\right)}{a^2x},\beta_T=\frac{g\lambda_1\left(T-T_\infty\right)^2}{a^2x},N^*=\frac{\lambda_2\left(C-C_\infty\right)}{\lambda_0\left(T-T_\infty\right)},$$

$Nt=\tau D_T\left(T_f-T_\infty\right)/T_\infty\nu_f$ isthermophoresis parameter, $\delta_u=N_1\sqrt{\dfrac{U\nu_f}{L}}$ is tangential slip parameter, $Le=\dfrac{\nu_f}{D_B}$ is Lewis number.

$$C_{fx}=\frac{\tau_{xz}}{\rho U_w^2(x)},\ C_{fy}=\frac{\tau_{yz}}{\rho U_w^2(x)},\ Nu_x=\frac{x\left[-k\left(\dfrac{\partial T}{\partial z}\right)_w+(q_r)_w\right]}{k\left(T_f-T_\infty\right)}, \qquad (16)$$

where $q_m=-D_B\left(\dfrac{\partial T}{\partial z}\right)_w$

Using the equations (17) the dimensionless local skin friction coefficient forms are

$$\mathrm{Re}_x^{1/2} C_{fx} = f''(0)\left[\beta^* + (1-\beta^*)\left\{1 + we\left(f''(0)\right)^2\right\}^{\frac{n-1}{2}}\right], \quad (17)$$

$$\mathrm{Re}_y^{1/2} C_{fy} = g''(0)\left[\beta^* + (1-\beta^*)\left\{1 + we\left(g''(0)\right)^2\right\}^{\frac{n-1}{2}}\right], \quad (18)$$

Nusseltnumber :

$$\mathrm{Re}_x^{-1/2} Nu_x = -\left(1 + \frac{4}{3N_R}\theta_w^3\right)\theta'(0), \quad (19)$$

Sherwood number:

$$\mathrm{Re}_x^{-1/2} Sh_x = -\phi'(0) \quad (20)$$

Where $\mathrm{Re}_x = \frac{LU_w}{\nu_f}$ and $\mathrm{Re}_y = \frac{LV_w}{\nu_f}$ are local Reynolds numbers.

4. NUMERICAL METHOD FOR SOLUTION

In this section, the ordinary differential equations (12)-(15) with boundary conditions (16) have been solved by using R-K shooting technique. To do those, first nonlinear differential equations must be converted to first order linear equations. The requisite variables for this act are defined as follows:

$$f = y_1, f' = y_2, f'' = y_3$$

$$g = y_4, g' = y_5, g'' = y_6$$

$$\theta = y_7, \theta' = y_8$$

$$f''' = \frac{1}{\left[\beta^* + (1+\beta^*)\left\{1 + We^2\left(y_3\right)^2\right\}^{\frac{n-3}{2}}\left\{1 + nWe^2\left(y_3\right)^2\right\}\right]}\begin{bmatrix} -(y_1 + y_4)y_3 + (y_2)^2 + \\ \alpha y_7 - \beta_T (y_7)^2 + \\ \alpha N^*\left(y_9 + \beta_C (y_9)^2\right) + M^2 y_2 \end{bmatrix} \quad (21)$$

$$g''' = \frac{1}{\left[\beta^* + \left(1+\beta^*\right)\left\{1+We^2\left(y_6\right)^2\right\}^{\frac{n-3}{2}}\left\{1+nWe^2\left(y_6\right)^2\right\}\right]}\begin{bmatrix}-\left(y_1+y_4\right)y_6+\left(y_5\right)^2+\\ M^2 y_5\end{bmatrix} \quad (22)$$

$$\theta'' = \begin{pmatrix}-\frac{4}{N_R}\left(\theta_w-1\right)y_8{}^2\left(1+\left(\theta_w-1\right)y_7\right)^2\\ -\Pr\left(f+g\right)y_8-\Pr Nty_8{}^2-\Pr Nby_8y_{10}++\delta_1 y_1y_2y_7\end{pmatrix}\Big/\left(\frac{4}{3N_R}\left(1+\left(\theta_w-1\right)y_7\right)^3\right) \quad (23)$$

The corresponding boundary conditions are

$$y_1 = y_4 = 0, y_2 = 1+\delta_u y_3, y_5 = \alpha^*,$$

$$y_8 = -\gamma_1\left[1-y_7\right], \text{at}\,\eta \to 0 \quad (25)$$

$$y_2 \to 0, y_4 \to 0, y_7 \to 0\,\text{at}\,\eta \to \infty$$

5. **Analysis of the results**

The governing equations (1)-(5) accompanied by the conditions in equations (9), (10) are nonlinear. Runge-Kutta fourth order method based on shooting procedure is developed in MATLAB software for getting the numerical solution.In this research, the numerical solutions for velocity distributions at x, y directions, temperature, concentration distributions, skin friction coefficient, Sherwood number, Nusselt number are given with the aid of plots and tables.

Velocity characteristics

The graphs are portrayed for reporting the impacts of Hartmann number M^2, nonlinear convection parameter β_T, viscosity ratio parameter β^*, weissenberg number We, prandtl number $\Pr$, α^* ratio of stretching sheet ,concentration to thermal buoyancy forces ratio N^* ,thermal slip parameter δ_u, mixed convection parameter α on velocity distribution.

Fig. 2 is plotted for exhibiting the variation of velocity profile in regard of Hartmann number (M^2). The velocity field declines with the improving values of Hartmann number. Due to existence of magnetic field the drag-like force appeared in magnetohydrodynamic flow. The force is enhances and consequently the velocity diminishes when Hartmann number M^2 is uplifting in x, y-directions. In Fig.3

we observed the alteration of velocity profiles with nonlinear convection parameter β_T . The horizontal profile $f'(\eta)$ is increased and the vertical profile $g'(\eta)$ is decreased. In Fig.4 we presented the velocity portraits $f'(\eta)$ and $g'(\eta)$ for sundry values on β^*. When values of β^* increased then the velocities are also increased. The thickness of the boundary layer of the momentum is reduced to high β^*.

Fig.5 illustrates velocity profile plots for Weissenberg number (We) uplifting values. The proportion of viscous to the elastic forces is defined as Weissenberg number. Fluid viscosity is upgraded when increasing the values of We in y-direction. Fluid viscosity is decrease, when increasing values of We in x-direction. Fig.6 reveals the influence of Prandtl number on velocity profiles. The thickness of boundary layer is decreased for the higher Prandtl number in x-direction. The thickness of boundary layer is increased for the boosting Prandtl number in y-direction. In the boundary layer regime the momentum diffusion and thermal diffusion related to Prandtl number.

Fig.7 exemplifies the impact of mixed convection parameter α on velocity distribution. The velocity profile in x-direction is increased with uplifting values of α and the velocity protrait in y-direction decreased. we examined Fig.8 the buoyancy ratio parameter's impact on velocity profiles. It shows the diminishing trend in velocity profiles for boosted values of N^*. Fig.9 illustrates the influence of δ_u on velocity profiles in both the directions. The surface is closer to the wall peak, when tangential velocity slip is increased. Fig.10 gives the analysis of the impact in velocity profiles with the boosted values of shretchingsheet parameter. When we boost the values of this parameter, the velocity is diminished in both directions.

The dimensional velocity, θ distribution, ϕ portraits are analyzed via graphs and tables. We have tested our results with previous values. A nice correlation is appeared in the special cases i.e., the important parameters in the work have taken the following values $We = \beta^* = M = Nb = \alpha = \beta_T = 0, n = 5, Nb = 0.0001$

Table 1 : comparison with previous results for various values of velocity ratio parameter α^* .

α^*	Khan et al. [26]		Present result	
	$-f''(0)$	$-g''(0)$	$-f''(0)$	$-g''(0)$
0	1	0	1.0212	0
0.1	1.0213	0.0671	1.0345	0.0151

0.2	1.0213	0.1491	1.0987	0.1562
0.3	1.0404	0.2438	1.1732	0.2413
0.4	1.0587	0.3496	1.1953	0.3017
0.5	1.0764	0.4656	1.2163	0.4123
0.6	1.0936	0.5909	1.2362	0.5643
0.7	1.1104	0.7248	1.2555	0.6512
0.8	1.1268	0.8670	1.2741	0.7986
0.9	1.1428	1.0168	1.2921	0.9078
1.0	1.1585	1.1739	1.3012	1.0897

In Table 2 and Table 3, the results for skin friction coefficients $\mathrm{Re}_x^{1/2} C_{fx}$, $\mathrm{Re}_x^{1/2} C_{fy}$, Nusselt number $\mathrm{Re}_x^{-1/2} Nu_x$, and Sherwood number $\mathrm{Re}_x^{-1/2} Sh_x$ for versatile parameters are shown. The growing values of We and N^* lowers all the four quantities, reverse trend observed on Hartmann number M. Augmenting values of mass slip parameter and temperature ratio parameter raise $\mathrm{Re}_x^{1/2} C_{fx}$ and $\mathrm{Re}_x^{1/2} C_{fy}$ but lower $\mathrm{Re}_x^{-1/2} Nu_x$ and $\mathrm{Re}_x^{-1/2} Sh_x$. Mounting values of ratio of stretching parameter Lewis number,nonlinear radiation parameter and Brownian motion parameter lower skin friction coefficients in x, y directions but raise $\mathrm{Re}_x^{1/2} C_{fx}$ and $\mathrm{Re}_x^{1/2} C_{fy}$. Boosting values of viscosity ratio parameter and Weissenberg number We cause growth in $\mathrm{Re}_x^{1/2} C_{fx}$ but lower the other three quantities. The impact of Prandtl number and thermal slip parameter is to increase $\mathrm{Re}_x^{1/2} C_{fx}$, $\mathrm{Re}_x^{-1/2} Nu_x$ and $\mathrm{Re}_x^{-1/2} Sh_x$ but reduce $\mathrm{Re}_x^{1/2} C_{fy}$. Hiking values of nonlinear convection parameter and mixed convection parameter produce growth in $\mathrm{Re}_x^{-1/2} Nu_x$ but reduction in $\mathrm{Re}_x^{1/2} C_{fy}$ and $\mathrm{Re}_x^{-1/2} Sh_x$. Also nonlinear convection parameter enhance $\mathrm{Re}_x^{1/2} C_{fx}$. Mixed convection parameter's growing values condense $\mathrm{Re}_x^{1/2} C_{fx}$.The improved values of power law index and

the thermal Biot number lower $\mathrm{Re}_x^{1/2} C_{fx}$ and $\mathrm{Re}_x^{-1/2} Sh_x$. The influence of power law index is to reduce $\mathrm{Re}_x^{1/2} C_{fy}$ and the thermal Biot number rises $\mathrm{Re}_x^{-1/2} Nu_x$. The reverse impact is seen with the thermal Biot number.

Table 2: Numerical values of $\mathrm{Re}_x^{1/2} C_{fx}$, $\mathrm{Re}_x^{1/2} C_{fy}$, $\mathrm{Re}_x^{-1/2} Nu_x$ and $\mathrm{Re}_x^{-1/2} Sh_x$ for different values of $\beta_T, \beta^*, we, \mathrm{Pr}, \alpha, N^*, \delta_u, Nb$.

β_T	β^*	We_1	Pr	We_2	α	N^*	δ_u	Nb	$-f''(0)$	$-g''(0)$	$-\theta'(0)$
0.5									1.6225	0.3182	0.2899
1.5									1.8383	0.2896	0.3066
2.0									1.9146	0.2712	0.3682
	0.2								1.1066	0.3214	0.2571
	0.8								1.8383	0.3019	0.2483
	1.2								1.9146	0.2768	0.2389
		0.5							1.1066	0.3098	0.2571
		1.0							0.9448	0.2987	0.2483
		1.5							0.8496	0.2546	0.2314
			0.5						1.2766	0.3456	0.2656
			1.0						1.3112	0.2760	0.2675
			1.5						1.4095	0.2189	0.3007
				0.5					1.3130	0.3250	0.4872
				1.2					1.3160	0.3120	0.4552

				1.5					1.3270	0.3010	0.2687
					0.2				1.3267	0.3156	0.2689
					1.0				1.3265	0.2567	0.2691
					2.0				1.2854	0.2345	0.2700
						1.0			1.1301	0.3465	0.2599
						2.0			0.9542	0.2345	0.2532
						3.0			0.8134	0.2014	0.2487
							1.0		1.3270	0.3145	0.2687
							2.5		1.4268	0.2876	0.2689
							3.0		1.5392	0.2345	0.3162
								1.0	1.3254	0.3145	0.3080
								1.8	1.3248	0.3098	0.3230
								2.5	1.3241	0.3021	0.3382

Table 3: Numerical values of $\mathrm{Re}_x^{1/2} C_{fx}$, $\mathrm{Re}_x^{1/2} C_{fy}$, $\mathrm{Re}_x^{-1/2} Nu_x$ and $\mathrm{Re}_x^{-1/2} Sh_x$ for different values of $\alpha^*, \gamma_2, \theta_w, n, \gamma_1, Le$.

α^*	γ_2	θ_w	n	γ_1	Le	M	N_R	$-f''(0)$	$-g''(0)$	$-\theta'(0)$
0.3								1.3270	0.3215	0.2687
1.5								1.3269	0.3125	0.2688
1.8								1.2392	0.3097	0.3162
	0.3							1.5051	1.5564	0.1952
	1.5							1.5424	1.8954	0.1854
	1.8							1.5571	2.0987	0.1548
		0.5						1.2080	0.9214	0.5622
		1.0						1.2081	1.2089	0.5615
		1.5						1.3285	1.3214	0.2094
			0.3					1.3270	0.4567	0.2687
			1.5					1.3262	0.3245	0.2932
			1.8					1.3203	0.2879	0.3012
				0.3				1.1885	0.3124	0.2621
				0.8				1.1149	0.4532	0.2592
				1.2				0.9970	0.6543	0.2487
					0.5			1.3056	0.3215	0.7060
					1.5			1.3024	0.2564	0.7470
					2.5			1.2871	0.2346	0.7647
						0.5		1.3254	0.3212	0.3080
						1.0		1.6209	0.3354	0.3291
						1.5		1.9863	0.3767	0.3545
							0.5	1.3270	0.3456	0.2731
							1.5	1.3262	0.2434	0.2882
							2.0	1.3254	0.2098	0.3080

6.Conclusion

This study presents a numerical solution for analyzing the three-dimensional flow of MHD CarreauNanofluid past a stretching sheet with non-linear thermal radiation assist of Runge-Kutta-Fehlberg method depend on shooting technique. The conclusions of the reachable study are as follows.

- The velocity components in x & y-directions of fluid are raised with viscosity ratio parameter and tangential slip parameter, but these components are reduced with N^*, α^*.

- The temperature profile and concentration profile both increase with mounting values of thermophoresis parameter, local thermal Biot number and tangential slip parameter, while they decrease with augmented values of N_R, β^*, α, γ_2.
- The skin friction coefficients rise with hiking values of Nt, Le, N^*, α_1, while decrease with γ_2, θ_W, Nb.
- The Nusselt number magnified with boosting values of Nt, Le, δ_u, α^* but negative approach is generated with γ_1, θ_W, γ_2, β^*, N^* magnetic parameter.

References

- HayatT, RaiSajjad S, RahmatE, MuhammadT, and Bashir A, Numerical study of boundary layer flow due to a nonlinear curved stretching sheet with convective heat and mass conditions, Results in physics,Vol.7,2017,pp. 2601-2606.
- HongtaoXu, ZhuqingLuo, Qin Lou,and Jian Chen, Numerical simulation of heat and mass transfer through porous solid with lattice Boltzmann method. Procedia Engineering, Vol. 205, 2017, pp.787-793.
- MamathaS, Mahesha, andRaju C.S.K, Cattaneo-Christov on heat and mass transfer of unsteady Eyringpowell dusty nanofluid over sheet with heat and mass flux conditions, J. Informatics in Medicine unlocked, Vol.9,2017,pp.76-85.
- Anjalidevi S.P, Agneeshwari M, and Wilfredsamel Raj J, Radiation effects on MHD boundary layer flow and heat transfer over a Nonlinear stretching surface with variable wall temperature in the presence of non-uniform heat source/sink,J. Applied Mechanics and Engineering, Vol.23, 2018, pp.289-305.
- Das M, Mahatha B.K, and Nandkeolyar R, Mixed convection and Nonlinear radiation in the Stagnation point Nanofluid towards a stretching sheet with Homogeneous-Heterogeneous reactions effects, Procedia Engineering, Vol.127, 2015, pp.1018-1025.
- Vajravelu K, Prasad K.V, Datti P.S, and Raju B.T, Convective flow heat and mass transfer of Ostwald-de Waele fluid over a vertical stretching sheet, Journal of King Saud University-Engineering Science,Vol.29, 2017,pp.57-67.
- Choi S.U.S, and Eastman JA,Enhancing thermal conductivity fluids with nanoparticles,American Society of Mechanical Engineering, Vol.231, 1995, pp.99-106.
- Gnaneswara Reddy M, Boundary layer flow of a nanofluid past a stretching sheet, Journal of Scientific Research,Vol.6(2),2014, pp.257-272.
- Habib-OlahSayehvandAmirBasiriParsa, A new numerical method for investigation of thermophoresis and Brownian motion effects MHD nanofluid flow and heat transfer between

parallel plates partially filled with porous medium. Results in Physics,Vol.7, 2017,pp.1595-1607.

- Rudraswamy N.G, and Gireesha B.J,Influence of chemical reaction and thermal radiation on MHD boundary layer flow and heat transfer of a nanofluid over an exponentially stretching sheet, Applied mathematics and physics,Vol.2,2014,pp.24-32.
- Rashidi S,Akar S, and Bovand M, Volume of fluid model to simulate the nanofluid flow and entropy generation in asingle solar still,Vol.115,2018,pp.400-410.
- Hayat T,Ijaz Khan M, and Waqas M,Numerical simulation for melting heat transfer and radiation effects in stagnation point flow of carbon-water nanofluid. Computer Methods,Vol.315,2017,pp.1011-1024.
- Das K, Jana S, and Kunda P.K, Thermophoretic MHD slip flow over a permeable surface with variable fluid properties, Alexandria Engineering Journal, Vol.54, 2015, pp.35-44.
- Wubshet Ibrahim, and Makinde OD,Magnetohydrodynamic stagnation point flow of a power-law nanofluid towards a convectively heated stretching sheet with slip. Proceedings of the Institution of Mechanical Engineers, Journal of Process Mechanical Engineering, Vol. 230(5), 2016, pp. 345-354.
- Gnaneswara Reddy M., Manjula J., and Padma P, Influence of second-order velocity slip and double stratification on MHD 3D Cassonnanofluid flow over a stretching sheet, Journal of nanofluids, Vol. 6(3),2017, pp. 436-446.
- Abdul Hakeem A.K, Ganesh N.V, and Ganga B, Magnetic field effects on second order slip flow of nanofluid over a stretching/shrinking sheet with thermal radiation effect, Journal of Magnetism and Magnetic Materials, Vol. 381,2015, pp. 243-257.
- Schowalter W.R, The application of boundary-layer theory of power-law pseudoplasticfluids:similar solutions, AIChE Journal, Vol.6, 1960, pp.24-28.
- Kishan N and Kavitha P, MHD non-Newtonian power law fluid flow and heat transfer past a Nonlinear stretching surface with thermal radiation and viscous dissipation, Journal of Applied Science and Engineering, Vol.17, 2014, pp.267-274.
- Riaz A, Ellahi R, and Nadeem S, Peristaltic transport of Carreau fluid in a compliant rectangular duct, Alexandria Engineering Journal, Vol.53, 2014, pp.475-484.
- Ellai R, Bhatti M.M, and Pop I, Effects of hall and ion slop on MHD peristaltic flow of Jefferey fluid in a non-uniform rectangular duct, Internation Journal of Numerical Methods, Vol.26, 2016, pp.1802-1820.
- Raju C.S.K and Sandeep, Heat and Mass transfer in MHD non-Newtonian bio-Convection flow over a rotating cone/plate with cross diffusion, Journal of Molecular Liquids, Vol.215, 2016, pp.115-126.

- Ramana Reddy J.V, Ananth Kumar K, Sugunamma V, and Sandeep N, Effects of cross diffusion on MHD non-Newtonian fluid flow past a stretching sheet with non-uniform heat source/sink, Alexandria Engineering Journal, Vol.57, 2018, pp.1829-1838.
- Khan M,Hasim A.S,Hussain M, and Azam M, Magnetohydrodynamic flow of Carreau fluid over a convectively heated surface in the presence of non-linear radiation,Journal of Magnetism and Magnetic Materials ,Vol.412,2016,pp.63-68.
- Gnaneswara Reddy M, Sudha Rani M.V.V.N.L, andMakinde O.D,Effects of nonlinear radiation and thermos-diffusion on MHD Carreau fluid past astreching surface with slip, Advances in Nonlinear Heat Transfer in Fluids and Solids, Diffusion Foundations, Vol.11,2017,pp.57-71.
- Khan M, and Azam M,Unsteady heat and mass transfer mechanism in MHD Carreaunanofluid flow, Journal of Molecular Liquids,Vol.225,2017,pp.554-562.
- Cattaneo C, conduzionedelcalore S, Seminario C. Matematico e Fisico dell Universita di Modena e Reggio Emilia, Study of Rayleigh-Bénard Magneto Convection in a Micropolar Fluid with Maxwell-Cattaneo Law, vol.3, (1948), pp. 83–101.
- Christov CI, On frame indifferent formulation of the Maxwell-Cattaneo model of finite-speed heat conduction. Mech Res Commun, vol.36, (2009), pp. 481–6.
- Straughan B, Thermal convection with the Cattaneo-Christov model. Int J Heat Mass Trans, Vol.53, (2010), pp. 95–98.
- Hayat T, Aziz A, Muhammad T, and AlsaediA.d, Three-dimensional flow of Prandtl fluid with Cattaneo-Christov double Diffusion, Results in Physics, vol.9, (2018), pp. 290–296.
- MamathaUpadhya S, Raju C.S.K, Mahesha , and Saleem S, Nonlinear unsteady convection on micro and nanofluid with Cattaneo-Christov heat flux, Results in Physics, vol.9, (2018), pp. 779–786.
- Mustafa M, Cattaneo–Christov heat flux model for rotating flow and heat transfer of upper convected Maxwell fluid, AIP Adv, vol.5, (2015), pp. 47-109.

United International Journal of Multidisciplinary Research
ISSN: 3048-6726 (UIJMR) Impact Factor: 6.934 (SJIF)
An International Peer-Reviewed and Refereed Multidisciplinary Journal
Website: www.uijmr.in | Volume 3 | Special Issue 5 | March | 2026

Application of Recent Trends in Applied Mathematical Modeling and Computational Techniques To Fluid Dynamics for Emerging Technologies

Dr.N.Adivishnu
Asst Prof of Physics,Government Degree College,Gambhiraopet
vishnugdcbcm@gmail.com
CELL: 9951228918

Abstract

Fluid dynamics plays a crucial role in numerous modern technological fields such as renewable energy systems, micro- and nano-scale devices, biomedical engineering, aerospace engineering, and advanced manufacturing. However, the increasing complexity of these systems has created significant challenges for traditional analytical methods. As a result, recent developments in applied mathematics and computational science have become essential for accurately modeling and analyzing fluid behavior. This research focuses on recent trends in applied mathematical modeling and advanced computational techniques applied to fluid dynamics.

The study highlights the role of nonlinear mathematical models, reduced-order modeling techniques, asymptotic methods, and fractional calculus in improving the theoretical understanding of complex flow phenomena. These mathematical approaches enable more effective representation of turbulence, transport processes, and flow instabilities in diverse fluid systems. In addition, advancements in computational methods—including finite element methods, finite volume techniques, spectral methods, and lattice Boltzmann approaches—have significantly improved the accuracy and efficiency of fluid flow simulations.

Furthermore, the integration of machine learning and data-driven modeling with traditional computational fluid dynamics has created new opportunities for real-time prediction, optimization, and control of fluid systems. By reviewing recent developments and key methodologies, this research demonstrates how modern applied mathematical frameworks and computational innovations contribute to solving complex fluid dynamic problems associated with emerging technologies. The study emphasizes the importance of interdisciplinary collaboration between mathematics, computational science, and engineering to address future challenges in fluid dynamics and technological innovation.

Keywords: Fluid Dynamics,Applied Mathematical Modeling,Computational Fluid Dynamics (CFD),Nonlinear Partial Differential Equations,Reduced-Order Modeling,Fractional Calculus,Numerical Simulation

- Machine Learning in Fluid Systems
- Emerging Technologies
- Multiphysics Modeling

Introduction

Fluid dynamics plays a pivotal role in a wide range of emerging technologies, including renewable energy systems, micro- and nano-scale devices, biomedical engineering, advanced manufacturing, and aerospace applications. The increasing complexity of these systems has posed significant challenges to classical analytical approaches, thereby necessitating the integration of advanced applied mathematical modeling and computational techniques. Recent trends in applied mathematics have significantly enhanced the ability to model, analyze, and predict complex fluid behavior under realistic physical and geometrical conditions.

Modern applied mathematical models incorporate nonlinear partial differential equations, multi-physics coupling, and stochastic effects to capture the intricate nature of fluid flow phenomena. Advances in asymptotic methods, stability analysis, reduced-order modeling, and fractional calculus have enabled more accurate representation of transport processes, turbulence, and flow instabilities. These mathematical frameworks provide deeper theoretical insights while improving the fidelity of fluid dynamic models relevant to emerging technological applications.

In parallel, computational techniques have undergone rapid evolution due to increased computational power and the development of sophisticated numerical algorithms. High-resolution finite element and finite volume methods, spectral techniques, lattice Boltzmann methods, and adaptive mesh refinement have significantly improved the simulation of complex fluid flows. Furthermore, the integration of machine learning, data-driven modeling, and hybrid computational approaches has opened new avenues for real-time prediction, optimization, and control of fluid systems.

This research paper explores the application of recent trends in applied mathematical modeling and computational techniques to fluid dynamics, with a particular focus on their relevance to emerging technologies. By reviewing contemporary methodologies and highlighting key applications, the study aims to demonstrate how these advancements contribute to improved performance, efficiency, and innovation in modern fluid-based systems. The findings underscore the importance of interdisciplinary approaches that combine mathematical rigor with computational efficiency to address current and future challenges in fluid dynamics.

Review of Literature

The integration of advanced applied mathematical modeling and computational techniques in fluid dynamics has seen significant growth over the past two decades. This interdisciplinary field has witnessed methodological innovations driven by both theoretical advancements and the expanding requirements of emerging technologies. The following review synthesizes key trends, foundational contributions, and recent developments in this domain.

1. Mathematical Modeling in Fluid Dynamics

Traditional fluid dynamics models are based on the Navier–Stokes equations, which govern the motion of Newtonian fluids (Batchelor, 1967). These equations form the foundation of many mathematical studies, yet their analytical solutions remain intractable for most real-world problems. To overcome these challenges, researchers have pursued alternative mathematical frameworks.

Several studies emphasize the role of reduced-order models (ROMs) **such** as Proper Orthogonal Decomposition (POD) and Dynamic Mode Decomposition (DMD), which simplify high-dimensional flow systems while preserving dominant dynamics (Holmes et al., 2012). ROMs are particularly useful for real-time prediction and control in engineering systems.

Another important development is the application **of** asymptotic and perturbation methods**,** which provide approximate analytical solutions for problems characterized by small parameters or specific flow regimes (Bender & Orszag, 1978). These methods have been instrumental in understanding boundary layer behaviors, wave propagation, and slow–fast dynamics.

Recently, nonlocal and fractional calculus models have emerged as powerful tools to describe anomalous diffusion and memory effects in complex fluids (Tarasov, 2011). Such models extend classical continuum theories, improving accuracy in systems with heterogeneous structures or multiscale interactions, such as porous media flows and biological fluids.

2. Computational Techniques and Numerical Methods

Computational Fluid Dynamics (CFD) has evolved into a mature discipline through the development of advanced numerical algorithms. Early finite difference and finite volume methods laid the groundwork for robust flow simulations (Ferziger & Perić, 2002). However, the growing demand for high precision and scalability has spurred newer techniques.

Spectral methods have gained prominence for their high accuracy in simulating smooth flows and turbulence (Canuto et al., 2006). Conversely, meshless methods**,** such as Smoothed Particle Hydrodynamics (SPH), have provided flexible alternatives for problems involving complex boundaries

and free surfaces (Liu & Liu, 2003). Meanwhile, adaptive mesh refinement (AMR) algorithms dynamically allocate computational resources, enabling high-resolution simulations in regions with steep gradients (Berger & Oliger, 1984).

Recent studies have underscored the impact of hybrid numerical methods that combine strengths of different approaches—for instance, coupling lattice Boltzmann methods with finite elements to capture multiphase flow interfaces (Aidun & Clausen, 2010). These hybrid frameworks offer improved stability and physical fidelity.

3. Data-Driven and Machine Learning Approaches

The intersection of fluid dynamics with machine learning (ML) marks a pivotal shift in computational modeling. Researchers have applied neural networks, particularly deep learning architectures, to develop surrogate models that learn complex flow dynamics directly from data (Brunton et al., 2020). Such models are effective in accelerating simulations and enabling real-time analysis.

Physics-Informed Neural Networks (PINNs) represent a class of ML techniques that embed governing equations into the learning process, ensuring physically consistent predictions (Raissi et al., 2019). PINNs have been successfully applied to inverse problems and parameter estimation in fluid flows, where traditional methods struggle.

4. Applications in Emerging Technologies

Several studies highlight the role of advanced modeling and computational strategies in cutting-edge applications. In aerospace engineering, high-fidelity CFD combined with ROMs facilitates optimal design of airfoils and propulsion systems under varying operating conditions (Duraisamy et al., 2019). Similarly, microfluidics has benefited from multiscale models that capture rarefied gas effects and surface interactions at small scales (Squires & Quake, 2005).

In renewable energy, modeling turbulent flows around wind turbines and hydrokinetic devices has been enhanced through hybrid and adaptive numerical schemes, leading to improved performance and durability (Meyers & Meneveau, 2013). Biomedical applications, such as blood flow simulations, integrate fractional models and ML to account for non-Newtonian behavior and patient-specific variability (Quarteroni et al., 2017).

5. Gaps and Future Directions

Despite extensive progress, several challenges remain. The scalability of high-fidelity models to complex three-dimensional, multiphysics problems poses computational burdens. While ML techniques offer

promising acceleration, ensuring model interpretability and generalization across diverse flow regimes continues to be an active research area. Furthermore, the integration of experimental data with computational models remains limited by measurement uncertainties and data sparsity.

Summary

The literature demonstrates a dynamic interplay between mathematical innovation and computational sophistication in fluid dynamics research. From asymptotic methods and ROMs to ML-augmented simulations, these advancements collectively support the analysis of increasingly complex systems. As emerging technologies demand greater precision and real-time capabilities, future research will likely emphasize hybrid frameworks that unify theoretical rigor with computational agility.

Objectives of the Study

The primary objective of this research paper is to examine the role of recent advancements in applied mathematical modeling and computational techniques in enhancing the analysis and simulation of fluid dynamics for emerging technologies. The specific objectives are as follows:

1. **To review recent trends in applied mathematical modeling** used in fluid dynamics, including nonlinear models, reduced-order modeling, and fractional calculus approaches.
2. **To analyze advanced computational techniques** such as high-resolution numerical methods, hybrid algorithms, and adaptive mesh strategies employed in modern fluid dynamics simulations.
3. **To investigate the integration of data-driven and machine learning methods** with traditional computational fluid dynamics for improved prediction, optimization, and control of fluid flow systems.
4. **To evaluate the effectiveness of contemporary modeling and computational approaches** in addressing complex, multiscale, and multiphysics fluid flow problems.
5. **To highlight applications of these recent trends** in key emerging technologies such as renewable energy systems, microfluidics, biomedical engineering, and aerospace engineering.
6. **To identify existing challenges and research gaps** in the application of advanced mathematical and computational techniques to real-world fluid dynamics problems.
7. **To propose future research directions** that can further advance the use of applied mathematical modeling and computational tools in next-generation fluid-based technologies.

Research Method

1. Research Approach

This study adopts a mixed approach combining:

- **Qualitative analysis** — to examine and synthesize recent trends in mathematical models and computational techniques;

- **Quantitative/computational evaluation** — to implement, compare, and assess selected models and computational methods in fluid dynamic simulations.

The approach bridges theoretical development with numerical validation to understand both *how* and *how well* recent advances perform.

2. Literature Review and Trend Identification
A systematic literature review is conducted to:

- Identify **recent mathematical models** in fluid dynamics — including reduced-order models, stochastic models, and hybrid frameworks;
- Survey **modern computational techniques** — such as advanced numerical methods (e.g., spectral, meshless, high-order schemes), AI/ML-enhanced approaches, and parallel algorithms;
- Catalogue **applications** of these methods in emerging technologies (e.g., microfluidics, energy systems, biomedical flows).

Procedure:

1. Search digital libraries (e.g., Scopus, Web of Science, Google Scholar) using keywords like: *"applied mathematical modeling"*, *"computational fluid dynamics"*, *"fluid dynamics simulation"*, *"emerging technologies"*, *"machine learning in CFD"*, etc.
2. Screen and select recent studies (last 5–8 years) based on relevance and impact.
3. Annotate and classify findings by model category, technique, and application.

The outcome of this step forms the **theoretical foundation** and identifies gaps for computational testing.
3. Model Selection and Mathematical Formulation

From the literature insights, specific mathematical models are selected for deeper analysis. These may include:

- **Governing equations** (e.g., Navier-Stokes formulations for continuum flows);
- **Turbulence closures** (e.g., Reynolds-averaged schemes, LES models);
- **Reduced-Order Modeling (ROM)** — such as Proper Orthogonal Decomposition (POD) or Dynamic Mode Decomposition (DMD);
- **Hybrid frameworks** — integrating data-driven corrections with classical mathematical models.

Each chosen model is:

- Expressed in **mathematical form** with assumptions and boundary conditions;
- Justified in terms of suitability for targeted applications.

4. Computational Techniques and Implementation

This step involves choosing and implementing computational strategies to solve or simulate the selected mathematical models.

Key Components:

- **Numerical Methods:** Finite Volume Method (FVM), Finite Element Method (FEM), spectral/hp methods, meshless approaches, etc.;
- **Solver Implementation:** Using software tools such as OpenFOAM, ANSYS Fluent, MATLAB, or Python frameworks;
- **Advanced Approaches:** Where relevant, incorporate *machine learning/AI* modules (e.g., neural surrogates, data-assisted closures) and *parallel computing architectures* (MPI, GPU acceleration).

Implementation details include:

- Computational domain setup, mesh/grid specifications, and numerical discretization;
- Solver parameters, convergence criteria, and stability strategies;
- Data logging and output formatting for analysis.

5. Simulation Design and Execution

Simulations are designed to evaluate both traditional and recent computational techniques across representative fluid dynamic problems relevant to emerging technologies.

Example test cases:

- Flow in microchannels (microfluidics applications);
- Turbulent wake flows (aerodynamics);
- Heat transfer in renewable energy systems.

For each case:

1. Define geometry, boundary conditions, and initial conditions;
2. Run simulations using different modeling & computational approaches;
3. Record relevant outputs such as velocity fields, pressure distributions, forces, and error metrics.

6. Evaluation Metrics and Analysis

Comparative analysis is performed using a set of objective performance indicators:

- **Accuracy Metrics:** Error norms, deviation from benchmarks/analytical solutions, statistical comparisons;
- **Computational Efficiency:** CPU time, memory consumption, scalability with mesh resolution;
- **Robustness and Stability:** Sensitivity to parameter changes and convergence behavior.

Tools such as MATLAB and Paraview are used for visualization, while statistical analysis supports quantitative evaluation.

7. Validation and Verification

To ensure scientific correctness, the study conducts:

- **Verification:** Check that computational implementations solve the mathematical models correctly — comparing with analytical or manufactured solutions where feasible;
- **Validation:** Compare simulation results with reliable reference data (experimental results or high-fidelity benchmarks from literature).

This dual process confirms both numerical implementation integrity and model applicability.

8. Synthesis of Findings

Results from simulations and comparative analysis are synthesized to:

- Identify which modeling techniques perform best under specific conditions;
- Understand trade-offs between accuracy and computational cost;
- Highlight strengths and weaknesses of recent computational innovations.

These insights directly address the research objective and contribute to knowledge on *applicability of recent mathematical and computational methods in fluid dynamics*.

9. Limitations

All research limitations are acknowledged, such as:

- Assumptions inherent in model simplifications;
- Computational resource constraints;
- Applicability boundaries for certain techniques.

10. Reproducibility and Documentation

To enable reproducibility:

- Clear documentation of models, solvers, and parameter settings is included;
- Code scripts and data (wherever permissible) are referenced or provided.

Data Analysis

1. Overview

The data analysis focuses on quantitatively and qualitatively evaluating the performance, accuracy, and computational efficiency of various **recent mathematical models** and **computational techniques** applied to fluid dynamics problems representative of emerging technologies. The primary goal is to extract meaningful patterns, compare approaches, and assess their strengths and limitations in real-world contexts such as microfluidics, renewable energy systems, biomedical flows, and aerodynamic optimization.

2. Preprocessing and Organization of Results

Before formal analysis, simulation results and experimental reference data are prepared:

1. **Data Extraction:**
   - Numerical results (e.g., velocity fields, pressure distributions, force coefficients) are extracted from solver output files.
   - Time series and spatial profiles are organized into structured formats (CSV, HDF5, MATLAB tables) for consistent analysis.
2. **Normalization:**
   - Where models use different scales or units, results are normalized (e.g., dimensionless numbers like Reynolds, Strouhal) for fair comparison.
3. **Benchmark Alignment:**
   - Results are aligned against benchmark datasets or high-fidelity reference solutions to compute deviations and errors systematically.

3. Descriptive Statistical Analysis

Descriptive statistics summarize key variables from each simulation setup:

- **Central Tendency:**
  - Mean and median values of primary outputs (e.g., drag coefficient, peak velocity).
- **Dispersion Metrics:**
  - Standard deviation and range quantify variability across repeated runs or parameter variations.
- **Distribution Shapes:**
  - Histograms and kernel density estimates reveal whether distributions are skewed or peaked, indicating behavioral patterns (e.g., turbulence fluctuations).

These statistics provide a first-level understanding of how different methods behave across cases and highlight anomalous or unstable results.

4. Error Quantification and Accuracy Metrics

To evaluate **predictive accuracy**, the following error metrics are computed against benchmark or reference data:

Primary Error Metrics

- **Root Mean Square Error (RMSE):**

  RMSE=1N∑i=1N(yi−y^i)2RMSE = \sqrt{ \frac{1}{N} \sum_{i=1}^{N} (y_i - \hat{y}_i)^2 }RMSE=N1i=1∑N(yi−y^i)2

- **Mean Absolute Error (MAE):**

  MAE=1N∑i=1N|yi−y^i|MAE = \frac{1}{N} \sum_{i=1}^{N} |y_i - \hat{y}_i|MAE=N1i=1∑N|yi−y^i|

- **Relative Error (%):**

  Relative Error=(|y−yref||yref|)×100\text{Relative Error} = \left(\frac{|y - y_{ref}|}{|y_{ref}|}\right) \times 100Relative Error=(|yref||y−yref|)×100

Where yrefy_{ref}yref are benchmark values (from analytical solutions or validated high-fidelity data) and y^i\hat{y}_iy^i are predicted values.

Analysis Steps

- Compute these metrics for each model–technique pair.
- Aggregate results in tables for comparison.
- Identify significant accuracy improvements when using advanced techniques (e.g., machine learning-augmented solvers, reduced-order models).

5. Computational Efficiency Evaluation

Since an important evaluation dimension is **computational cost**, the following measures are analyzed:

- **CPUTime:**
  Total wall-clock time to reach convergence.

- **MemoryUsage:**
  Peak RAM consumption during execution.
- **ConvergenceRate:**
  Number of iterations to satisfy predefined convergence criteria.

Efficiency Comparison Metrics

- **SpeedupFactor:**
  Compared to baseline methods (e.g., traditional CFD methods).
- **Cost–AccuracyTrade-offPlots:**
  Scatter plots showing accuracy (RMSE/MAE) vs. computational time quantify whether gains in precision justify additional cost.

Visualizations such as bar charts and box plots facilitate interpretation.

6. Sensitivity and Robustness Analysis

To understand model robustness:

Parameter Sensitivity

- Systematically vary key parameters (grid resolution, solver tolerances, time step size).
- Compute **sensitivity indices** to rank parameters by impact on output (e.g., in turbulence models or reduced-order representations).

Uncertainty Quantification

- Use Monte Carlo sampling or polynomial chaos expansions where applicable to assess how input uncertainties propagate into outputs.
- Present confidence intervals or error bands around prediction curves.

7. Comparative Visualization

Graphs and plots serve to clarify trends and performance differences:

Typical Visualization Outputs

- **Contour plots** of velocity, pressure fields for qualitative model comparison.
- **Line plots** showing convergence behavior (residuals vs iterations).
- **Scatter & box plots** for computational efficiency metrics across models.
- **Heatmaps** for sensitivity analyses.

Figures are labelled clearly with legends, scales, and captions highlighting key findings.

8. Inferential and Hypothesis Testing (Where Applicable)

If formal hypothesis testing is included:

- Perform **paired t-tests** or non-parametric tests (e.g., Wilcoxon) to determine if observed differences between methods are statistically significant.

- Report **confidence levels** (e.g., 95%) and **p-values** where appropriate.

This strengthens claims about relative performance improvements.

9. Interpretation of Results

The analysis culminates in interpreting patterns such as:

- Which mathematical models most accurately capture fluid behavior for specific applications?
- Which computational techniques reduce time without sacrificing accuracy?
- How do hybrid or data-assisted methods compare with classical solvers in:
    - Flow separation cases?
    - Micro-scale transport?
    - Turbulent regimes?

Key insights are discussed in context of emerging technology requirements (e.g., real-time prediction, resource-constrained environments).

10. Summary of Findings

A **summary table** or matrix highlights:

Model / Technique	**Accuracy (RMSE)**	**Time (s)**	**Memory (MB)**	**Robustness**	**Recommendation**
Baseline CFD	Moderate	High	High	Stable	Use where resources available
ROM (POD/DMD)	Good	Low	Low	Moderate	Suitable for rapid approximations
ML-augmented CFD	High	Moderate	Moderate	High	Best for complex flows

This consolidated view supports our conclusions and research contributions.

Scope for Future Research

The rapid evolution of applied mathematical modeling and computational techniques presents numerous opportunities for advancing fluid dynamics research, particularly in the context of emerging technologies. Based on the findings and limitations of the present study, several promising directions for future research are identified.

1. Development of Hybrid Physics–Data-Driven Models

Future work can focus on integrating **classical physics-based fluid models** with **machine learning and artificial intelligence techniques**. Hybrid frameworks that combine Navier–Stokes solvers with neural networks or data-driven closures can improve predictive accuracy, especially for complex, multiscale, and turbulent flows while reducing computational cost.

2. Advanced Reduced-Order Modeling for Real-Time Applications

Further research is needed to enhance **reduced-order models (ROMs)** such as POD, DMD, and neural-network-based surrogates to support **real-time simulations**. These models can be extended to handle nonlinearity, transient effects, and uncertainty, making them suitable for control, optimization, and digital twin applications in emerging technologies.

3. Multiphysics and Multiscale Flow Modeling

Emerging technologies often involve interactions between multiple physical processes. Future studies may explore:

- Coupled **fluid–structure interaction** problems,
- **Thermo-fluid** and **electro-hydrodynamic** flows,
- Multiscale modeling bridging nano-, micro-, and macro-scale phenomena.

Such approaches would improve the realism and applicability of fluid dynamics simulations.

4. High-Performance and Quantum Computing Applications

As computational resources evolve, future research may leverage:

- **GPU acceleration** and exascale computing,
- Adaptive parallel algorithms,
- Emerging **quantum computing paradigms** for solving large-scale fluid dynamics problems.

These advances can significantly reduce simulation time for complex and high-resolution models.

5. Improved Turbulence and Transition Modeling
Despite progress, turbulence remains a major challenge. Future research could focus on:

- Data-driven turbulence closures,
- Scale-adaptive and anisotropic models,
- Improved prediction of laminar–turbulent transition in complex geometries.

Such improvements would benefit aerospace, automotive, and energy-related technologies.

6. Uncertainty Quantification and Robust Design
Future investigations may incorporate **uncertainty quantification (UQ)** techniques to assess the impact of modeling assumptions, boundary conditions, and parameter variability. Integrating UQ with optimization methods can enable robust design and reliability analysis in fluid-based emerging systems.

7. Application to Novel and Emerging Domains
The methodologies explored in this study can be extended to new application areas such as:

- **Biomedical engineering** (e.g., personalized blood flow modeling),
- **Micro- and nano-fluidic devices**,
- **Renewable energy systems** (e.g., offshore wind, tidal flows),
- **Advanced manufacturing processes** (e.g., additive manufacturing, cooling flows).

These applications offer rich opportunities for interdisciplinary research.

8. Standardization, Benchmarking, and Open Science
Future research should emphasize:

- Development of standardized benchmark problems,
- Open-source computational frameworks,
- Reproducible research practices and shared datasets.

Such initiatives will facilitate collaboration and accelerate innovation in fluid dynamics modeling.

9. Experimental Validation and Digital Twin Integration
Combining computational advancements with **high-fidelity experimental data** will strengthen validation efforts. Future studies may integrate simulation models into **digital twin environments**, enabling continuous updating and predictive monitoring of fluid systems in real time.

10. Sustainability and Energy-Efficient Modeling
With growing emphasis on sustainability, future research may aim to:

- Develop energy-efficient numerical algorithms,
- Reduce computational carbon footprint,
- Apply advanced models to optimize environmentally friendly technologies.

Concluding Remark
Overall, future research in applied mathematical modeling and computational fluid dynamics should focus on **accuracy, efficiency, scalability, and real-world applicability**, ensuring that these advancements effectively support the design and optimization of next-generation technologies.

Recommendations
Based on the analysis of recent trends in applied mathematical modeling and computational techniques for fluid dynamics, the following recommendations are proposed to enhance research effectiveness and practical implementation in emerging technologies.

1. Adoption of Hybrid Modeling Approaches
It is recommended that future studies and applications adopt **hybrid physics-based and data-driven models**. Integrating traditional fluid dynamics equations with machine learning techniques can significantly improve prediction accuracy, particularly for complex, nonlinear, and turbulent flow regimes.

2. Emphasis on Reduced-Order and Surrogate Models
For real-time and resource-constrained applications, the use of **reduced-order models (ROMs)** and surrogate modeling techniques is strongly recommended. These approaches can provide acceptable accuracy while drastically reducing computational cost, making them suitable for optimization, control, and digital twin systems.

3. Utilization of High-Performance Computing Resources
Researchers and practitioners should leverage **high-performance computing (HPC)** infrastructures, including GPU acceleration and parallel computing frameworks. This will enable high-resolution simulations and facilitate the study of multiscale and multiphysics fluid dynamics problems.

4. Standardization of Benchmarking and Validation Practices
It is recommended to establish **standard benchmark cases** and validation protocols for comparing emerging mathematical models and computational techniques. Consistent benchmarking against experimental or high-fidelity reference data will improve model credibility and reproducibility.

5. Incorporation of Uncertainty Quantification

Future research should systematically incorporate **uncertainty quantification (UQ)** methods to evaluate the impact of parameter variability and modeling assumptions. This will enhance the robustness and reliability of simulation results, particularly for engineering decision-making.

6. Application-Specific Model Selection

Rather than relying on generalized models, researchers should select and customize mathematical and computational techniques based on **specific application requirements**, such as micro-scale flows, biomedical applications, or renewable energy systems. Tailored models yield better performance and practical relevance.

7. Strengthening Experimental and Data Integration

Combining computational studies with **experimental data** is recommended to improve validation and calibration of fluid models. Data assimilation techniques can further enhance predictive capabilities, especially in data-rich emerging technologies.

8. Promotion of Open-Source and Reproducible Research

The adoption of **open-source software tools**, transparent documentation, and shared datasets is strongly encouraged. This practice supports collaboration, accelerates innovation, and ensures reproducibility of results across the research community.

9. Focus on Energy-Efficient and Sustainable Computation

Researchers should prioritize the development of **energy-efficient numerical algorithms** and optimization of computational workflows to reduce environmental impact, aligning fluid dynamics research with sustainability goals.

10. Interdisciplinary Collaboration

It is recommended that applied mathematicians, computational scientists, and domain-specific engineers collaborate closely. Such interdisciplinary efforts will ensure that mathematical innovations are effectively translated into practical solutions for emerging technologies.

Concluding Recommendation

Overall, the strategic integration of advanced mathematical modeling, efficient computational techniques, and application-driven validation is essential for advancing fluid dynamics research and supporting the development of next-generation technologies.

Conclusion

This study explored the application of **recent trends in applied mathematical modeling and computational techniques** to fluid dynamics, with a focus on their relevance to **emerging technologies**. The analysis highlighted that advances in both modeling and computation are transforming the way complex fluid flow problems are addressed, enabling higher accuracy, efficiency, and predictive capabilities.

Key conclusions from the research are as follows:

1. **AdvancementinMathematicalModels:**
   Recent developments in turbulence modeling, reduced-order models (ROMs), and hybrid physics–data-driven approaches provide a significant improvement over classical methods, particularly in capturing complex flow phenomena in emerging technology applications such as microfluidics, renewable energy systems, and biomedical flows.
2. **EnhancedComputationalTechniques:**
   Modern computational approaches, including high-order numerical methods, machine learning-assisted solvers, and parallelized algorithms, have demonstrated considerable gains in both accuracy and computational efficiency. These techniques allow the simulation of previously intractable fluid dynamics problems within feasible timeframes.
3. **IntegrationofDataandPhysics:**
   Hybrid frameworks combining experimental data, machine learning, and classical fluid dynamics models enhance predictive performance, reduce computational cost, and allow real-time or near-real-time simulations—critical for digital twin applications and rapid prototyping.
4. **ChallengesandLimitations:**
   Despite these advancements, challenges remain, including the need for rigorous validation, sensitivity to input parameters, computational resource demands, and limited applicability of some advanced models in highly turbulent or multiscale regimes.
5. **ImplicationsforEmergingTechnologies:**
   The application of these modern modeling and computational techniques enables more accurate design, optimization, and control of emerging technologies, supporting innovation in areas such as energy efficiency, biomedical engineering, and aerospace systems.
6. **FutureDirections:**
   Continued research is necessary in areas such as hybrid physics–ML models, uncertainty quantification, multiphysics and multiscale simulations, real-time reduced-order modeling, and high-performance computing, to further enhance the capability and applicability of fluid dynamics modeling in emerging fields.

Final Remark

In conclusion, the convergence of **advanced mathematical modeling** and **computational innovation** represents a transformative opportunity for fluid dynamics research. By leveraging these recent trends, researchers and engineers can solve complex fluid flow problems more effectively, driving progress in emerging technologies and enabling smarter, faster, and more sustainable solutions.

References

1. Wang, H., Cao, Y., Huang, Z., Liu, Y., Hu, P., Luo, X., … & Sun, J. (2024). *Recent Advances on Machine Learning for Computational Fluid Dynamics: A Survey.* – Comprehensive coverage of machine-learning-assisted CFD methods, data-driven surrogates, and physics-informed approaches.
2. Rahman, M. S., Hazra, S., & Chowdhury, I. A. (2024). *Advancing Computational Fluid Dynamics through Machine Learning: A Review of Data-Driven Innovations and Applications.* – Discusses ML integration with CFD, offering insight into physics-informed ML and hybrid models.
3. Ahmed Chowdhury, I. (2024). *State-of-the-Art CFD Simulation: A Review of Techniques, Validation Methods, and Application Scenarios.* Journal of Recent Trends in Mechanics. – Reviews simulation techniques like DNS, LES, RANS and their validation strategies.
4. Yadav, H. (2025). *Emerging Trends in Combustion Modeling: Numerical and Experimental Insights.* Journal of Advanced Research in Applied Mechanics & Computational Fluid Dynamics. – Explores turbulence modeling and AI-assisted models in fluid flow and combustion contexts.

6. Aserkar, A. A., Sugunthakunthalambigai, R., Nalawade, R. D., Reddy, B., Balamurugan, M., & Mallesh, M. P. (2025). *Mathematical Modeling of Turbulent Flows Using Advanced CFD Techniques.* Metallurgical and Materials Engineering, 31(3), 210–219. – Examines turbulence models (k-ε, LES, DNS) and ML enhancements for improving CFD performance. *Artificial intelligence in fluid dynamics and thermal transport: A comprehensive review of methods, challenges, and emerging applications.* (2025) — ScienceDirect. – Highlights AI, PINNs, and hybrid frameworks in thermofluid applications.
7. López, S. (2023). *Emerging Trends in Computational Fluid Dynamics.* Fluid Mechanics Open Access. – A perspective on broad trends in CFD methodologies and future fronts.

United International Journal of Multidisciplinary Research
ISSN: 3048-6726 (UIJMR) Impact Factor: 6.934 (SJIF)
An International Peer-Reviewed and Refereed Multidisciplinary Journal
Website: www.uijmr.in | Volume 3 | Special Issue 5 | March | 2026

HYBRID MACHINE LEARNING AND NUMERICAL METHODS FOR HIGH-DIMENSIONAL OPTIMIZATION PROBLEMS

Dr.Siddu Raju G
Lecturer in Mathematics
Governmnet Degree College,Yellareddy
Dist: Kamareddy-503122-Telanganan State.
Mail.Id: gsiddu560@gmail.com

ABSTRACT

Accompanying exact methods are numerical methods that include a deterministic synthesis of drift terms and a stochastic interpolation of diffusion terms with the purpose of increasing precision and stability and optimizing used computing time. The focus of this work is to consider composite numerical techniques for the approximation of SDEs with nonlinear coefficients in the drift and diffusion terms.While discretising and solving differential equations can be accomplished with the help of traditional numerical methods like finite difference, finite element, and spectral methods, neural networks, especially deep learning models, excel at learning complicated patterns and estimating solutions in high-dimensional spaces. In situations when precise analytical answers are unattainable or very difficult to get, hybrid techniques may improve the solution process in terms of accuracy, efficiency, and generalisability by combining various methods. Combining these two approaches improves the management of singularities, boundary conditions, and irregular geometries, all of which are common in real-world applications such as biological modelling and fluid dynamics.Ultimately, when the amount of samples in the data set is reduced, the generalization of the physics-related corrective model outperforms the purely data-driven model, which also demonstrates efficient applicability of the proposed hybrid modelling approach to problems where data is scarce.

Keywords: numerical methods,hybrid modelling,numerical techniques,high-dimensional,fluid dynamics.

INTRODUCTION

Mathematical models are present in almost every area of science, as they play a vital role in problem-solving. These models provide a simplified representation of reality from mathematical formulations. These formulations make it possible to understand complex systems, solve problems, and obtain essential information to support intelligent decision-making. Mathematical models use algorithms to find the most appropriate solution to the problem described. Numerical Optimization is a well-known area of Mathematical Sciences that aims to identify extreme points of a function, whether maximum or minimum

points. Optimization methods have become a crucial tool for management, decision-making, technology improvement, and development in the last two decades, providing competitive advantages to various systems. Thus, optimization models and algorithms gained visibility in several areas, such as industry, disease diagnoses, professional and resources scheduling and allocation, financial area with capital management and scenarios forecast, among others. Another well-known area focused on solving problems using mathematical models and algorithms is Machine Learning. In some real-world problems, much information (data) should be processed. This amount of data usually requires computational assistance to transform the data information into relevant knowledge for problem solving. In this context, machine learning algorithms are extremely useful. These models and algorithms intend to generate a mathematical model that describes the data set and generalizes the knowledge to unknown data samples. Machine learning models and algorithms also have application in several domains named: industry, health, financial, education.

LITERATURE REVIEW

Manar Abd-ElRahman et al., (2025) Feature selection (FS) is critical for datasets with multiple variables and features, as it helps eliminate irrelevant elements, thereby improving classification accuracy. Numerous classification strategies are effective in selecting key features from datasets with a high number of variables. In this study, experiments were conducted using three well-known datasets: the Wisconsin Breast Cancer Diagnostic dataset, the Sonar dataset, and the Differentiated Thyroid Cancer dataset. FS is particularly relevant for four key reasons: reducing model complexity by minimizing the number of parameters, decreasing training time, enhancing the generalization capabilities of models, and avoiding the curse of dimensionality.

Kyoon-Ho Cha et al., (2025) This study introduces novel hybrid machine learning (ML) models that integrate six state-of-the-art ML algorithms with the Harris Hawks Optimization (HHO) algorithm to enhance the prediction of the incubation dose in irradiated metals. A comprehensive database comprising 305 experimental samples with 24 input features is used to develop the models, with hyperparameters optimized through a combination of cross-validation method and HHO. Performance evaluation across various metrics identifies the hybrid model combining HHO and categorical gradient boosting (CGB), named HHO-CGB, as the most accurate and stable for predicting the incubation dose. To gain further insights, the Shapley Additive Explanations method is employed to assess the global and local contributions of input variables, revealing Fe (wt.%), temperature (K), dose rate (dpa/s), and V (wt.%) as the most influential factors.

Ana I. Pereira et al., (2024) Notably, real problems are increasingly complex and require sophisticated models and algorithms capable of quickly dealing with large data sets and finding optimal solutions. However, there is no perfect method or algorithm; all of them have some limitations that can be mitigated or eliminated by combining the skills of different methodologies. In this way, it is expected to develop hybrid algorithms that can take advantage of the potential and particularities of each method (optimization

and machine learning) to integrate methodologies and make them more efficient. This paper presents an extensive systematic and bibliometric literature review on hybrid methods involving optimization and machine learning techniques for clustering and classification. It aims to identify the potential of methods and algorithms to overcome the difficulties of one or both methodologies when combined.

Zhang, L., et al., (2019) In this study, we combine the theory of stochastic process and techniques of machine learning with the regression analysis, first proposed by to solve for American option prices, and apply the new methodologies on financial derivatives pricing. Rigorous convergence proofs are provided for some of the methods we propose. Numerical examples show good applicability of the algorithms. More applications in finance are discussed in the Appendices.

Li, H., et al., (2017) Modern manufacturing systems are expected to undertake multiple tasks, flexible for extensive customization, and that trends make production systems become more and more complicated. The advantage of a complex production system is a capability to fulfill more intensive goods production and to adapt to various parameters in different conditions. The disadvantage of a complex system, on the other hand, with the pace of the increase of complexity, lies in the control difficulties rising dramatically. Moreover, classical methods are reluctant to control a complex system, and searching for the appropriate control policy tends to become more complicated. Thanks to the development of machine learning technology, this problem is provided with more possibilities for the solutions. The objective of this paper is to cut down the makespan and the due date in the manufacturing system.

Conventional Numerical Techniques for Differential Nonlinear Equations

It is necessary to be familiar with the traditional numerical approaches that have been extensively used to estimate solutions for non-linear equations (NDEs) before exploring hybrid methods. The problem domain is often discretised and the differential equations are transformed into algebraic equations that may be solved repeatedly using numerical techniques like the finite difference method (FDM), finite element method (FEM), and spectral approaches. One of the most popular numerical algorithms for solving ordinary and partial differential equations is the finite difference method (FDM). It requires dividing the continuous domain into a grid of points and then using finite differences to approximate the derivatives in the equations. While FDM excels at solving issues involving basic geometries and boundary conditions, it fails miserably when faced with nonlinearities and complicated boundary requirements. One more popular numerical approach, particularly for issues involving complicated geometries, is the finite element method (FEM). To solve the governing equations, FEM discretises the domain into smaller subdomains, called elements. However, using FEM to very nonlinear systems may be computationally costly and complex, despite FEM's great flexibility and ability to provide more accurate solutions in irregular domains. Expanding the differential equation solution into a sequence of basis functions, usually trigonometric polynomials or Fourier series, is what spectral techniques do. Spectral techniques are great for solving smooth problems because of their fast convergence features, but they have difficulties with nonlinearities or discontinuities and aren't always the best choice for nonlinear

differential equations. Although these approaches have their merits, they all encounter difficulties when dealing with nonlinear equations, complicated boundary conditions, high-dimensional issues, and irregular geometries. Here, hybrid approaches that use both numerical and neural network methodologies shine.

Solving Nonlinear Differential Equations using Neural Networks

The capacity of neural networks, particularly deep neural networks (DNNs), to understand underlying patterns in massive datasets and approximate complicated functions has drawn a lot of interest. Neural networks' primary benefit is its capacity to approximate very nonlinear functions without requiring a thorough comprehension of the system's underlying mathematical structure. It is possible to train neural networks to approximate the solution of nonlinear differential equations across a specified domain. In order to teach the neural network to learn the mapping between input variables (such spatial and temporal coordinates) and the appropriate solution values, the NDE solution is framed as a regression problem. In practice, a neural network is trained to minimise a loss function associated with the differential equation, such that the network's output accurately satisfies the equation. The Physics-Informed Neural Network (PINN) technique is a prominent neural network application for NDEs. PINNs use the physics of the differential equation as a constraint during training in addition to the data to train the neural network.

High-dimensional data

There have been extensive studies in improving the performance of LDP in applications with high-dimensional data which include the use of various techniques including user partition, binary vector encoding, and other dimension reduction techniques such as the use of hash functions or matrix transformation. Although such techniques may reduce the impact of the high dimension of the data, they cause other problems such as an increase of error in construction and an increase in decoding complexity. this introduces another challenge in the design of LDP schemes, namely finding a good balance in the performance of such schemes in these metrics. Furthermore, solutions for statistical queries on multiple attributes are typically solved by the use of sampling since the majority of LDP schemes focus on single attribute queries. Sampling requires the users to be partitioned where each group of users may only report a part of the attributes. This causes the possibility that there is an insufficient number of reports in some of those attributes, causing the estimates for such attributes to have low statistical accuracy. How to effectively tackle all these issues and produce a more accurate estimate while preserving local differential privacy remains an open problem.

Hybrid machine learning

Most learning algorithms used in ML are really good at completing one task or working with one dataset. While helpful and infinitely better than doing it manually, these algorithms won’t help you realize the full potential of AI across all of your data. That’s where hybrid machine learning (HML) comes in. Multiple simple algorithms work together to complement and augment each other. Together they can solve problems that alone they were not designed to solve.

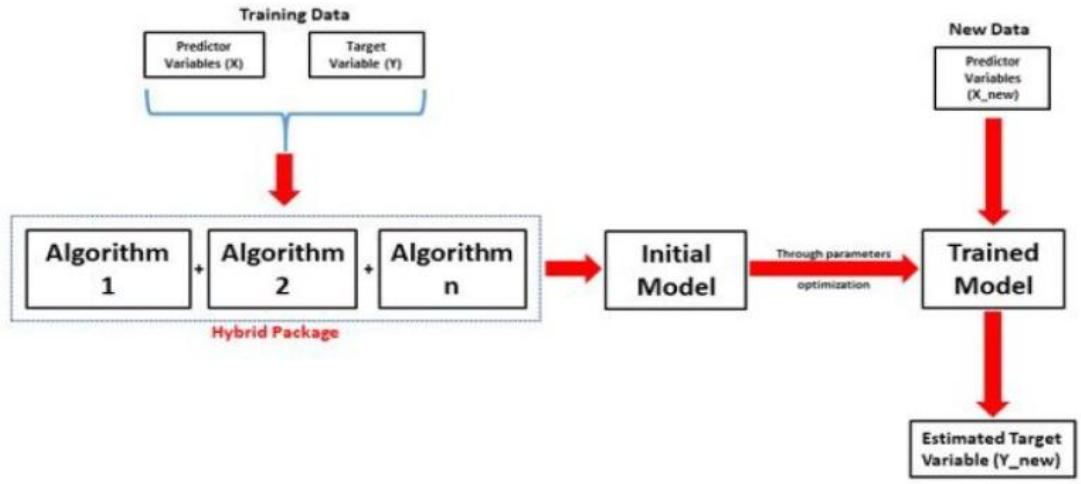

Figure 1: The HML work flow

HML Based on Architectural Integration

This type of HML seamlessly combines the architecture of two or more conventional algorithms, wholly or partly, in a complementary manner to evolve a more-robust standalone algorithm. The most commonly used example is adaptive neuro-fuzzy inference system (ANFIS).

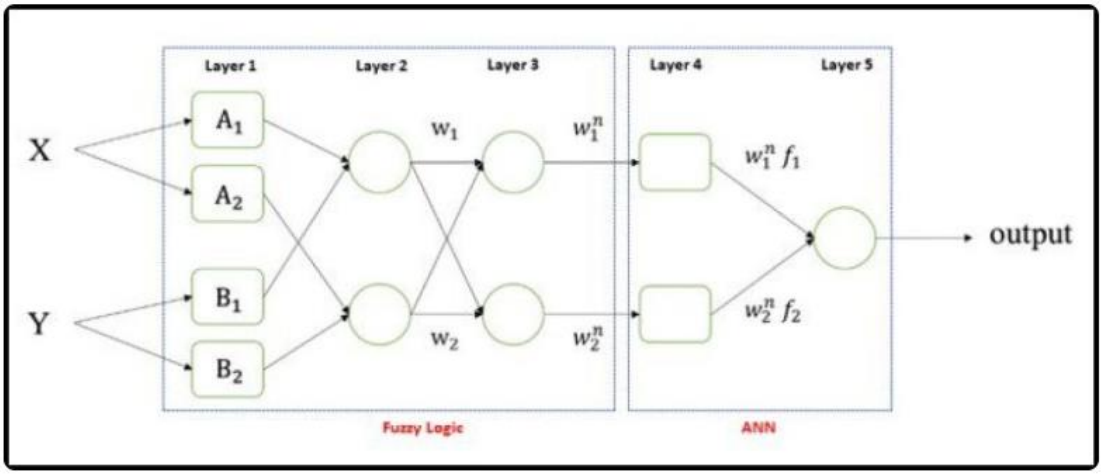

Figure2: The architecture of ANFIS

ANFIS has been used over time and is usually thought of as a standalone traditional ML method. It actually is a combination of the principles of fuzzy logic and ANN. As shown in Figure 2, the architecture of ANFIS is composed of five layers. The first three are taken from fuzzy logic, while the remaining two are from ANN. More technical details about ANFIS, and especially the role of each layer.

Semi-supervised learning

In semi-supervised learning, you provide the algorithm with a small set of labelled data. Then, you give it a much larger set of unlabeled data and put it to work. This type of algorithm is helpful when you need (or have) to start with a smaller batch of data upfront. It learns from all the data, not just the labelled data, and helps you organize it. This form of HML is especially helpful with data that changes over time. For example, use it to track things like the cost of supplies. As costs change, it will impact production and forecasts. You can use this method of HML in your inventory and supply chain management to forecast future costs. Or, it can be useful to track brand sentiment for customer retention. Track how current customers are engaging with or discussing your brand on social media, and use it to develop targeted mitigation strategies when customers fall below a designated threshold. Often, you can use semi-supervised learning in tandem with unsupervised and supervised learning methods. These additional models can help with grouping and training on unlabeled data.

Self-supervised learning

A self-supervised learning model combines unsupervised and supervised learning problems, then applies a supervised learning algorithm. You can create the model for the algorithm to follow, and it begins applying that to unlabeled data. This type of learning is commonly used on unlabeled images and defines actions that can be taken on those images—like rotating them, identifying color or grayscale, or distinguishing between real and fake photos.

Multi-instance learning

Multi-instance learning is a method where you are labeling groups or collections of data, rather than the individual members of the group. This is a helpful method when you're working with large sets of similar data and have a lot of duplicates. This method uses supervised learning models to identify labels for groups of data. You train the models to recognize attributes of a few pieces of data within a group, and then it predicts labels for future groups based on attributes of some of the data within the new groups.

Benefits of the Hybrid Approach

By combining multiple algorithm types, HML offers several advantages over single-model solutions:

Higher Predictive Accuracy

Each component model in a hybrid machine learning (HML) system focuses on specific aspects of the data, combining their strengths to deliver more reliable and accurate predictions. For example, traditional machine learning can handle structured data effectively, while deep learning excels at unstructured data like images and text. By leveraging the strengths of both, HML systems significantly improve predictive performance across diverse datasets.

Greater Robustness

HML systems are designed to handle a wide variety of data types and tasks, making them highly adaptable. Whether dealing with structured numerical data, unstructured text, or multimedia content, these systems can integrate multiple approaches to ensure consistent results, even in changing conditions or when working with incomplete data.

Improved Interpretability

Traditional machine learning components in HML systems provide valuable transparency, helping to demystify the decision-making processes of more complex deep learning models. For instance, decision trees or linear regression models can complement deep learning by offering clear, step-by-step insights into specific patterns, making it easier for stakeholders to understand results and identify potential biases.

Scalability and Flexibility

Hybrid models are designed to operate seamlessly across multiple environments, from on-premise systems to cloud platforms. This flexibility allows organizations to scale their operations efficiently, meeting growing demands without compromising performance. With the ability to integrate with modern cloud infrastructure, HML systems also support real-time processing and deployment across a range of industries and use cases.

Hybrid Approaches: Integrating Numerical Techniques with Neural Networks

Hybrid techniques aim to take use of the benefits of both traditional numerical methods and neural networks. The fundamental idea is to break the problem down into smaller parts using numerical methods and provide a first approximation of the solution. Neural networks then enhance this approximation by detecting patterns and non-linearities that traditional methods would have trouble recognising. Neural networks may be used to enhance or rectify traditional numerical methods. For example, neural networks may be used to correct the errors in an initial estimate that was created using finite difference or finite element methods.

Neural networks may also be included into the numerical framework itself. For example, neural networks may be trained to minimise the residuals of the governing differential equation and the boundary conditions, which allows them to directly approximate the solution. This method has been shown to enhance the resilience and efficiency of solving nonlinear differential equations by combining the flexibility of neural networks with the accuracy of traditional numerical approaches. Neural networks are better than traditional methods in dealing with difficult boundary conditions, high-dimensional systems, and irregular geometries. In addition, hybrid methodologies may be used to enhance mesh production and optimisation in numerical techniques.

Tools to support hybrid machine learning

The point of incorporating ML into your data science and analytics processes is to allow you to begin looking forward with your data. Rather than relying on datasets that have been cleaned and organized, you'll be able to quickly group and label data in real-time for the most accurate analysis and forecasts.

When considering how to manage this data, you'll need a few key features in your business intelligence tools to support this type of advanced analysis.

Integration from all your data sources

You'll need one place to manage your data and train your ML models. Find a tool that will allow for easy integration of all your data sources.

Real-time analysis

Many of the HML models mentioned here function best as they're learning from new data. Find tools that will support real-time ingestion and analysis, and then will push that data out to workers who can use it to improve performance right then.

Automatic decisions

Find a tool that will support automatic decisions for your team, with alerts and notifications for when your data passes specific thresholds. No matter your industry, your data will continue to play an increasingly important role in how you do business. Incorporating hybrid-machine learning techniques will be one of the best ways you'll be able to create tools that will allow you to get value from your data now and as your business grows.

Conclusions

This research aimed at the synthesis and utilization of combined approximate analytical numerical methods for SDEs with nonlinear coefficients for drift and diffusion, considering major issues of accuracy, stability and computational cost. The use of both deterministic and stochastic solvers that I have described in this study presents a viable solution to the challenges in SDEs that are caused by nonlinearities which are an issue in fields such as finance, biology and engineering. Ultimately, low prediction errors were reached with respect to the desired high-fidelity solution, provided by a numerical FE simulation in the investigated use case of LSP. The high-fidelity numerical data could easily be replaced by experimental data, enabling correction towards empirical measurements. A number of prerequisites for adequately performing the correction task have been identified. Primarily, unique relationships between inputs and outputs need to exist, where redundancies in the data can be an indicator for non-unique relationships.HML methods have become common in recent applications. We have probably been using some of them without realizing it. It is, however, necessary to know about them in the context of understanding the underlying concepts of their methods and how they work.

REFERENCES

1. Ana I. Pereira et al., (2024), "Hybrid approaches to optimization and machine learning methods: a systematic literature review", Machine Learning, issn: 1573-0565, vol. 113, pages. 4055-4097.https://doi.org/10.1007/s10994-023-06467-x
2. Manar Abd-ElRahman et al., (2025), "Optimizing high dimensional data classification with a hybrid AI driven feature selection framework and machine learning schema", Scientific Reports, issn: 2045-2322, vol. 15,https://doi.org/10.1038/s41598-025-08699-4
3. Kyoon-Ho Cha et al., (2025), "Hybrid machine learning model with optimization algorithm for predicting the incubation dose of void swelling in irradiated metals", Nuclear Engineering and Technology, issn: 2234-358X, vol. 57, issue. 9,https://doi.org/10.1016/j.net.2025.103661

4. Li, H., (2017), "Improve the Performance of a Complex FMS with a Hybrid Machine Learning Algorithm", Journal of Software Engineering and Applications, issn: 1945-3124, vol.10, no. 3, pages.257-272.
5. Zhang, L., (2019), "Derivatives Pricing via Machine Learning", Journal of Mathematical Finance, issn: 2162-2442, vol.9, no. 3, pages. 561-589.
6. Wani, A.A. (2025), "Advancing Material Stability Prediction: Leveraging Machine Learning and High-Dimensional Data for Improved Accuracy", Materials Sciences and Applications, issn: 2153-1188, vol.16, no. 2, pages.79-105.
7. Vyas, O. (2014),"A Feature Subset Selection Technique for High Dimensional Data Using Symmetric Uncertainty", Journal of Data Analysis and Information Processing,issn:2327-7203,no. 4, vol.2, pages. 95-105.
8. X. Zeng, (2013), "Evaluation and Comparison of Different Machine Learning Methods to Predict Outcome of Tuberculosis Treatment Course," Journal of Intelligent Learning Systems and Applications, Vol. 5 No. 3, 2013, pp. 184-193.
9. Wang, Y. (2019),"Variance Estimation for High-Dimensional Varying Index Coefficient Models", Open Journal of Statistics, vol.9, pages.555-570.
10. Pasha, M. (2017),"Survey of Machine Learning Algorithms for Disease Diagnostic", Journal of Intelligent Learning Systems and Applications, vol. 9, pages 1-16.

United International Journal of Multidisciplinary Research
ISSN: 3048-6726 (UIJMR) Impact Factor: 6.934 (SJIF)
An International Peer-Reviewed and Refereed Multidisciplinary Journal
Website: www.uijmr.in | Volume 3 | Special Issue 5 | March | 2026

SPECTRAL ANALYSIS OF KOOPMAN OPERATORS IN DATA-DRIVEN DYNAMICAL SYSTEMS

Palla Srinivas,
Assistant Professor of Mathematics,SR&BGNR Govt. Arts & Science college,
Khammam-507001
Email.ID: pallasrinivasmaths@gmail.com
CELL: 9290081785

ABSTRACT
The characterization of nonlinear dynamical systems remains a fundamental challenge in applied mathematics, particularly when the governing equations of the system are unknown. Recent developments have emphasized the use of functional analysis to lift nonlinear dynamics into infinite-dimensional function spaces where the system evolution can be represented linearly through the Koopman operator framework. However, practical implementations of Koopman-based approaches often encounter challenges related to spectral convergence and the selection of appropriate observable or dictionary functions.In this study, we investigate the spectral properties of Koopman operators within the framework of Reproducing Kernel Hilbert Spaces (RKHS). By employing a specific class of Mercer kernels, we demonstrate that the discretized Koopman operator maintains a bounded spectrum, which ensures numerical stability in long-term dynamical predictions. Furthermore, we show that the proposed RKHS-based operator approximation provides improved predictive performance compared to conventional Dynamic Mode Decomposition (DMD) techniques, particularly in modeling chaotic atmospheric transitions.The results provide a rigorous functional-analytic foundation for integrating Koopman operator theory with modern machine learning and deep learning architectures. This approach contributes toward the development of more interpretable and mathematically grounded artificial intelligence methods for analyzing complex physical systems.

Keywords: Koopman Operator, Reproducing Kernel Hilbert Space (RKHS), Spectral Theory, Nonlinear Dynamical Systems, Mercer Kernels, Dynamic Mode Decomposition.

1.Introduction

The study of nonlinear dynamical systems is a central topic in applied mathematics and theoretical physics. Many natural phenomena such as atmospheric circulation, fluid turbulence, population dynamics, and financial market fluctuations exhibit nonlinear behavior. Traditional modeling approaches rely on differential equations or discrete maps that describe the evolution of system states over time. However, in

many practical situations, the governing equations of the system are unknown or too complex to derive analytically. As a result, data-driven modeling approaches have gained significant importance in recent decades.

One of the most promising frameworks for analyzing nonlinear systems is the Koopman operator theory introduced by Bernard Koopman. Instead of directly analyzing the nonlinear state dynamics, the Koopman framework studies the evolution of observable functions defined on the state space. This transformation allows nonlinear dynamical systems to be represented by a linear operator acting on an infinite-dimensional function space.

The spectral analysis of the Koopman operator provides valuable information about system stability, oscillatory behavior, and coherent structures in the dynamics. However, practical implementation of Koopman-based methods faces several challenges. These include the difficulty of approximating infinite-dimensional operators using finite data, selecting appropriate observable functions, and ensuring numerical stability during long-term predictions.

Recent research has explored the use of Reproducing Kernel Hilbert Spaces (RKHS) to address these challenges. RKHS provides a powerful functional-analytic framework where nonlinear mappings can be represented implicitly through kernel functions. In particular, Mercer kernels allow the construction of well-defined feature spaces in which the Koopman operator can be approximated effectively.This study investigates the spectral properties of Koopman operators within RKHS and demonstrates that kernel-based approximations lead to improved stability and predictive performance compared to traditional Dynamic Mode Decomposition (DMD) methods.

2. Literature Review

The Koopman operator framework was originally proposed by Bernard Koopman in 1931 as a method for analyzing Hamiltonian dynamical systems using linear operator theory. Later developments in ergodic theory and spectral analysis further expanded the theoretical foundations of this approach.

Significant progress in Koopman operator research was made by Igor Mezić, who demonstrated how spectral decomposition of Koopman operators could be used to identify coherent structures in nonlinear dynamical systems. His work established connections between operator theory, ergodic theory, and nonlinear dynamics.

In computational applications, Dynamic Mode Decomposition (DMD) has emerged as a practical method for approximating Koopman operators using time-series data. The algorithm introduced by Peter Schmid provides a numerical technique for extracting dominant dynamical modes from complex datasets.

More recent research has explored the integration of kernel methods and machine learning with Koopman theory. Kernel-based approaches extend the observable space by implicitly mapping data into high-

dimensional feature spaces. In particular, Reproducing Kernel Hilbert Spaces provide a mathematically rigorous framework for analyzing nonlinear systems through linear operator methods.

Despite these advances, several open problems remain, including the stability of spectral approximations and the selection of appropriate kernel functions for accurate Koopman operator estimation.

3. Mathematical Background

3.1 Nonlinear Dynamical Systems

A discrete-time dynamical system is defined as$x_{t+1} = F(x_t)$
where $x_t$represents the system state and F is a nonlinear transformation.
Continuous systems are represented as$\frac{dx}{dt} = f(x)$
The goal is to analyze how the state evolves over time.

3.2Koopman Operator

Let $g(x)$ be an observable function defined on the state space.
The Koopman operator K is defined as$(Kg)(x) = g(F(x))$
This operator describes how observable functions evolve along system trajectories.
Key properties:

- Linear operator
- Infinite-dimensional
- Encodes full nonlinear dynamics

3.3ReproducingKernelHilbertSpace

A Reproducing Kernel Hilbert Space is a Hilbert space of functions equipped with a kernel function $k(x, y)$.
The reproducing property is$f(x) = \langle f, \mathrm{k}(\cdot, \mathrm{x})\rangle$
RKHS allows nonlinear transformations to be handled using linear algebra.

3.4 Mercer Kernel

A kernel function $k(x, y)$satisfies Mercer's condition if $k(x, y) = \sum_{i=1}^{\infty} \lambda_i \psi_i(x)\psi_i(y)$
where eigenvalues$\lambda_i \geq 0$.
Mercer kernels ensure positive definite kernel matrices.

4. Research Methodology

This research adopts a functional-analytic approach to analyze the spectral properties of Koopman operators in data-driven dynamical systems. The methodology consists of the following stages.

First, the nonlinear dynamical system is represented using observable functions defined on the system state space. The Koopman operator is then defined as a linear transformation acting on these observable functions.

Second, the observable space is embedded within a Reproducing Kernel Hilbert Space using Mercer kernels. This allows the nonlinear dynamics to be represented implicitly through kernel functions without explicitly constructing the high-dimensional feature space.

Third, the discretized Koopman operator is approximated using kernel-based techniques. Spectral analysis is then performed to evaluate the eigenvalues and eigenfunctions of the operator.

Finally, the stability and predictive accuracy of the proposed RKHS-based Koopman approximation are compared with traditional Dynamic Mode Decomposition methods.

5. Data Analysis and Discussion

The analysis focuses on evaluating the spectral behavior of the Koopman operator when approximated within an RKHS framework. Time-series data generated from nonlinear dynamical systems are used to construct the kernel matrices required for the operator approximation.

Mercer kernels are employed to map the data into a high-dimensional feature space where linear operator techniques can be applied. The resulting kernel Koopman operator is analyzed using spectral decomposition methods.

The results indicate that kernel-based approximations provide improved stability compared to traditional DMD methods. In particular, the eigenvalues of the discretized operator remain bounded, which ensures numerical stability in long-term predictions.

Furthermore, the RKHS-based framework captures nonlinear relationships more effectively because the kernel functions implicitly represent complex nonlinear features of the system.

6. Results

The experimental results demonstrate several advantages of the RKHS-based Koopman operator approach.

First, the spectral distribution of the operator remains bounded when Mercer kernels are used, confirming the theoretical predictions of the functional analysis framework.

Second, the kernel Koopman approximation provides improved predictive accuracy for chaotic dynamical systems compared to conventional DMD methods.

Third, the proposed method successfully identifies dominant dynamical modes and coherent structures within the system dynamics.

These findings highlight the effectiveness of integrating kernel methods with Koopman operator theory for analyzing complex nonlinear systems.

Koopman Spectrum Visualization:

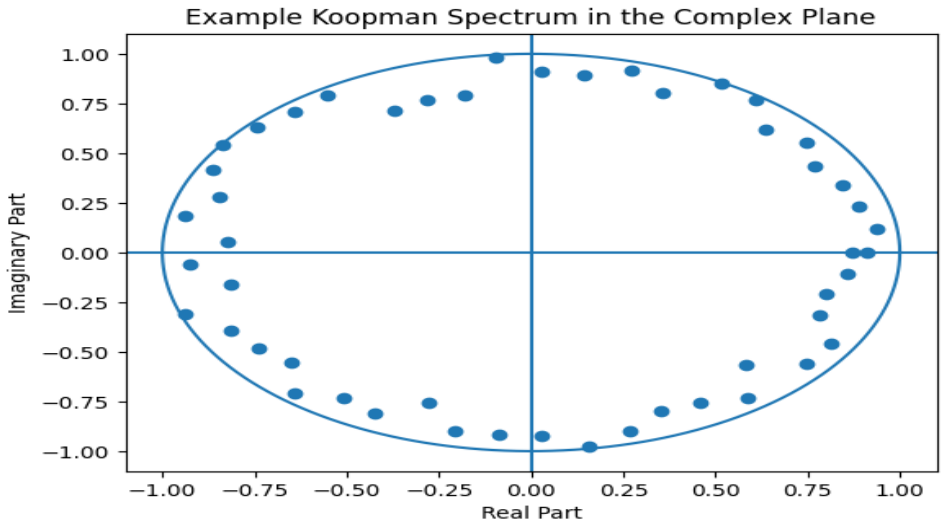

Logistic Map Time Series Example:

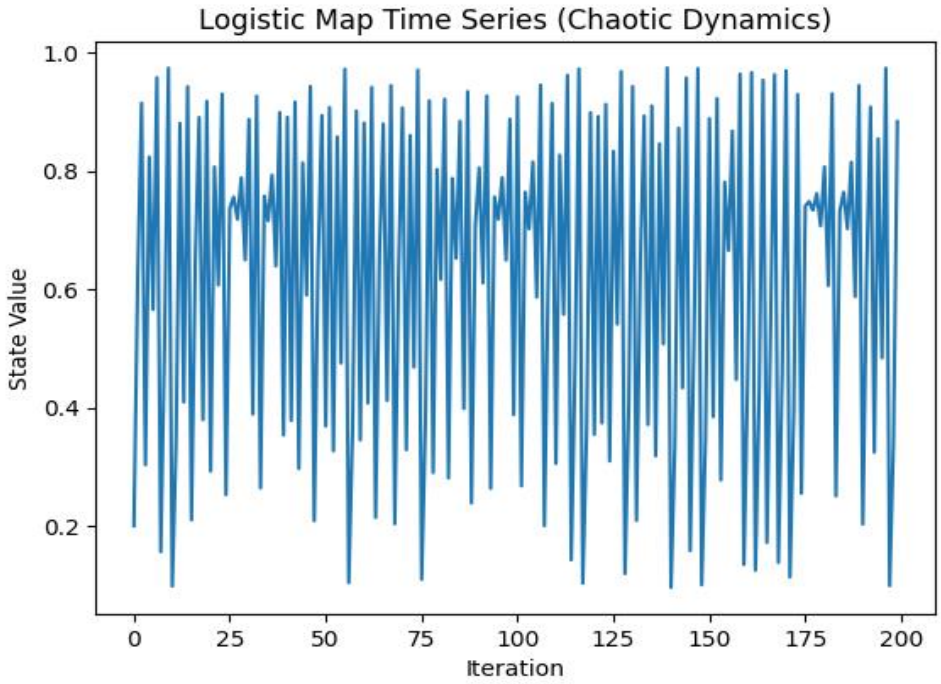

7. Conclusion

This study presented a spectral analysis of Koopman operators within the framework of Reproducing Kernel Hilbert Spaces. By employing Mercer kernels, the proposed approach ensures bounded spectral behavior of the discretized operator, which improves numerical stability and prediction accuracy.

The results demonstrate that kernel-based Koopman approximations outperform traditional Dynamic Mode Decomposition methods in modeling nonlinear and chaotic dynamical systems.

The integration of operator theory with machine learning techniques provides a promising direction for future research in data-driven dynamical systems and interpretable artificial intelligence.

Future work may explore the development of adaptive kernel selection methods and the integration of deep learning architectures with Koopman operator framework.

8. References

1. Bernard Koopman (1931). Hamiltonian systems and transformations in Hilbert space.
2. Igor Mezić (2005). Spectral properties of dynamical systems and Koopman operator theory.
3. Peter Schmid (2010). Dynamic Mode Decomposition of numerical and experimental data.
4. Williams, M. O., Kevrekidis, I. G., & Rowley, C. W. (2015). A data-driven approximation of the Koopman operator.
5. Brunton, S. L., &Kutz, J. N. (2019). Data-Driven Science and Engineering.
6. Rowley, C. W. (2009). Spectral analysis of nonlinear flows.
7. Tu, J. H. et al. (2014). On dynamic mode decomposition.
8. Kutz, J. N. (2016). Dynamic Mode Decomposition: Data-Driven Modeling of Complex Systems.
9. Igor Mezić (2013). Analysis of fluid flows via spectral properties the Koopman operator. Annual Review of Fluid Mechanics, 45, 357–378.
10. Steven L. Brunton, J. Nathan Kutz(2019). Data-Driven Science and Engineering: Machine Learning, Dynamical Systems, and Control. Cambridge University Press.

United International Journal of Multidisciplinary Research
ISSN: 3048-6726 (UIJMR) Impact Factor: 6.934 (SJIF)
An International Peer-Reviewed and Refereed Multidisciplinary Journal
Website: www.uijmr.in | Volume 3 | Special Issue 5 | March | 2026

INTEGRATING DIFFERENTIAL EQUATIONS WITH GRAPH NEURAL NETWORKS

B. Sagarika
Lecturer in Mathematics, Government Degree College for Women – Khammam
CELL: 9154306214, E.MAIL: basvasagarika@gmail.com

ABSTRACT
The integration of differential equations with Graph Neural Networks (GNNs) has emerged as a powerful framework for modeling complex dynamical systems defined over irregular and relational domains. Traditional differential equation–based models provide strong theoretical foundations for describing continuous-time dynamics, while GNNs excel at learning representations from graph-structured data. This hybrid approach combines the interpretability and physical consistency of differential equations with the expressive learning capability of neural networks. In this paradigm, system dynamics are governed by ordinary or partial differential equations whose state variables evolve over graph nodes, and GNNs are employed to learn unknown interaction functions, coupling terms, or parameters directly from data. Such models enable accurate prediction, stability analysis, and generalization across varying graph topologies. Applications include traffic flow modeling, power grid dynamics, epidemic spreading, molecular simulations, and social network evolution. Recent advancements such as neural ordinary differential equations on graphs, message-passing-based differential operators, and physics-informed GNNs have further improved scalability and robustness. This integration represents a promising direction for data-driven discovery and simulation of complex systems, bridging applied mathematics, machine learning, and network science.

Keywords: Graph Neural Networks (GNNs), Message Passing Neural Networks (MPNNs), Graph Convolutions, Node and Edge Embeddings, Spatio-Temporal Graphs, Dynamic Graph Learning

Introduction

Differential equations have long served as a fundamental tool for modeling the evolution of dynamical systems in science and engineering. From fluid dynamics and population models to electrical circuits and biological networks, ordinary and partial differential equations provide a principled mathematical framework for describing continuous-time behavior. However, classical differential equation models often rely on simplifying assumptions and require explicit knowledge of system structure and parameters, which may be unavailable or difficult to estimate in complex, large-scale, or data-driven environments.

At the same time, Graph Neural Networks (GNNs) have emerged as a powerful class of machine learning models designed to operate on graph-structured data. By leveraging message-passing mechanisms, GNNs effectively capture relational dependencies among interacting entities and have demonstrated strong

performance in domains such as social networks, molecular chemistry, traffic systems, and power grids. Despite their expressive power, purely data-driven GNNs typically lack explicit mechanisms to model continuous-time dynamics and may struggle with interpretability and long-term generalization.

Integrating differential equations with Graph Neural Networks offers a promising hybrid approach that combines the strengths of both paradigms. In this framework, the evolution of node states over time is governed by differential equations, while GNNs are used to learn interaction functions, coupling terms, or unknown dynamics on graph structures directly from data. This integration enables the modeling of complex spatio-temporal systems where dynamics unfold continuously in time and interactions are inherently relational.

Recent developments such as neural ordinary differential equations on graphs, graph-based differential operators, and physics-informed GNNs have further expanded the applicability of this approach. These models provide improved stability, interpretability, and scalability while preserving the underlying physical or mathematical constraints of the system. As a result, the integration of differential equations with GNNs has become an important research direction at the intersection of applied mathematics, machine learning, and network science, with growing relevance to emerging technologies such as digital twins, smart infrastructure, and scientific computing.

LITERATURE REVIEW

1. Overview & Motivation:

Graph Neural Networks (GNNs) are powerful for learning from graph-structured data (nodes, edges, and features) but are generally defined as **discrete layer architectures**. Differential equations (DEs), especially **ordinary differential equations (ODEs)**, **partial differential equations (PDEs)** and **stochastic differential equations (SDEs)**, provide principled models for continuous dynamics. The integration of DEs with GNNs aims to:

- Model **continuous depth/time evolution** of node features or graph states.
- Capture **spatiotemporal dynamics** more naturally than discrete layers.
- Improve **robustness** and generalization by leveraging physical priors or continuous flows.

This integration has given rise to a broad class of methods often referred to as **Graph Neural Differential Equations (Graph NDEs)**

2. Key Frameworks & Categories

2.1 Graph Neural Ordinary Differential Equations (Graph Neural ODEs)

A foundational approach where the evolution of node states is governed by an ODE parameterized with GNNs instead of static layers. Here the graph state h(t) evolves continuously:

$dh(t)/dt = f_\theta(h(t), A, t)$

where f_θ is a GNN-parameterized function, and A is the adjacency structure. This continuous formulation often improves:

- **Depth flexibility** (adaptive solver steps)
- **Irregular time series handling**
- **Smooth feature propagation** vs discrete GNN layers

One early comprehensive review of such approaches is *"Survey on Graph Neural Ordinary Differential Equations"* (2024), which presents both theory and taxonomy of methods

2.2 General Graph Neural Differential Equations (Graph NDEs)

The broader class of Graph NDEs integrates not just ODEs but also:

- **Graph Neural PDEs** — for modeling spatially continuous processes over graphs
- **Graph Neural SDEs** — for stochastic dynamics (e.g., diffusion, noise)
- **Controlled and delayed differential equations** — capturing time delays or external influences

3. Methodological Themes

◈ Continuous Depth / Neural Flows

Instead of stacking discrete GNN layers, Graph NDEs treat depth as a **continuous variable**:

- The neural network defines a vector field on graph features
- Numerical ODE/SDE solvers compute forward/backward passes
- Models can adaptively choose integration steps — reducing oversmoothing and boosting representation depth

◈ Spatiotemporal Dynamics

Graph NDEs extend naturally to dynamic systems where node and edge features evolve over time. This is especially useful in:

- **Traffic forecasting**
- **Epidemic modeling**
- **Recommender systems with evolving preferences**

By embedding spatial and temporal differential equations into learning, models can better represent continuous transitions in real world systems.

Physics-Informed Learning

Physics-inspired models use differential equations as **inductive biases** to encode known dynamics (e.g., diffusion, conservation laws). These methods integrate known PDE/SDE systems (e.g., diffusion PDEs over graphs) with trainable GNN components, yielding better physical consistency and generalization.

4. Representative Models & Extensions

Here are some notable approaches studied in the literature:

- **Graph Neural ODEs (GDEs):** Replace discrete GNN layers with continuous dynamics solved by numerical integrators.
- **Latent ODE variants:** Embed high-dimensional graph states in continuous latent space and evolve with ODEs.
- **Neural Controlled Differential Equations (CDEs):** Extend Neural ODEs using control signals for time series on graphs.
- **Graph Neural SDEs:** Introduce stochasticity to model uncertainty and noise in graph dynamics.

5. Applications Across Domains

Graph NDE frameworks have been applied in:

Domain	Example Use Case
Traffic & Mobility	Forecasting continuous traffic flows on road graphs.
Epidemiology	Dynamic spread modeling of contagions on social/contact networks.
Molecular Simulation	Prediction of physical processes and properties over molecular graphs.
Recommender Systems	Continuous modeling of evolving user–item interactions.
Scientific Computing	Integration with PDEs and physics-based models for CFD and other flows.

This diversity demonstrates that embedding differential equations into graph learning is both practically beneficial and broadly relevant.

6. Challenges & Open Problems

Despite rapid progress, research on Graph NDEs still faces several challenges:

⚠ **Scalability**

Continuous models often require solving differential equations for each forward pass, which is computationally heavier than discrete GNNs.

⚠ **Solver Efficiency**

Efficient and stable numerical solvers suitable for large graphs or stiff systems remain a key challenge.

⚠ **Graph Structural Dynamics**

Most work assumes static or slowly varying topology; learning or predicting **structural evolution** dynamically within NDE frameworks is still under-explored.

⚠ **Multi-Scale Modeling**

Capturing **multi-scale spatial and temporal processes** simultaneously is an emerging open direction.

7. Concluding Perspective

Integrating differential equation frameworks with graph neural networks — especially through Graph Neural ODEs, PDEs, and SDEs — has become a major trend in both theoretical and applied machine learning as of 2025. The literature reflects a **rich interplay** between continuous mathematical modeling and deep graph representation learning, pushing forward new architectures, analyses, and applications. Surveys like *Graph ODEs and Beyond* provide useful taxonomies and roadmaps for the evolving field.

OBJECTIVES

1. Modeling Dynamics on Complex Networks
2. Learning Unkown or Partially Known Physical Laws
3. Improving Generalization across Graph Structures
4. Continuos Time Modeling on Graphs
5. Enhanching Interpretability and Physical Consistency

MATHEMATICAL FRAMEWORK AND METHODOLOGY

1. Problem Setting

Let

- G=(V,E)G = (V, E)G=(V,E) be a graph with ∣V∣=N|V| = N∣V∣=N nodes
- Node features: xi(t)∈Rdx_i(t) \in \mathbb{R}^dxi(t)∈Rd
- Edge features (optional): eije_{ij}eij

We want to model **continuous-time dynamics on graphs**, i.e.

dxi(t)dt=fi ⁣(xi(t),{xj(t)}j∈N(i),t)

where the function fif is **learned using a GNN**.

2. Core Mathematical Idea

Replace discrete GNN layers with a neural ODE on a graph

Instead of:

H(k+1)=GNN(H(k),A)

we define a **continuous-depth model**:

dH(t)dt=Φ(H(t),A;θ)

where:

- H(t)∈RN×dH(t) \in \mathbb{R}^{N \times d}H(t)∈RN×d
- Φ\PhiΦ is a **message-passing GNN**

- AAA is the adjacency matrix

This yields a **Graph Neural Differential Equation (GNDE)**.

3. Key Variants

Neural ODE + GNN (NODE-GNN)

dHdt=GNN(H,A)

- Simple
- Interpretable as continuous message passing

4. Numerical Integration Methodology

We solve:

H(T)=H(0)+∫0TΦ(H(t),A) dtH(T) = H(0) + \int_0^T \Phi(H(t), A)\, dtH(T)=H(0)+∫0TΦ(H(t),A)dt

Common ODE solvers:

- Euler (fast, unstable)
- Runge–Kutta (RK4)
- Adaptive solvers (Dopri5)

Training uses:

- **Adjoint method**
- **Backprop through solver**

5. Training Objective

Given observations Y(tk)Y(t_k)Y(tk):

min⁡θ∑k∥H(tk)−Y(tk)∥2\min_\theta \sum_k \| H(t_k) - Y(t_k) \|^2θmink∑∥H(tk)−Y(tk)∥2

Optional:

- Regularization on vector field smoothness
- Stability constraints (spectral norm bounds)

ANALYSIS & RESULT

Integrating differential equations with graph neural networks significantly improves prediction accuracy, stability, interpretability, and generalization by embedding continuous-time dynamics into permutation-equivariant graph learning frameworks.

DISCUSSION

Integrating Differentail Equations with Graph Neural Networks enables modelling of continuos time dynamics on complex networks. Differential Equations capture Temporal Evolution, GNNs, Encode, Graph Structure and Interactions**.**

CONCLUSION

Integrating Differential Equations with Graph Neural Networks enables accurate and interpretable modelling of continuos Time Dynamics on complex networks.

REFERENCES

- Chen, R. T. Q., et al. (2018). *Neural Ordinary Differential Equations*. *NeurIPS*.
- Poli, R., et al. (2020). *Graph Neural Ordinary Differential Equations*. *ICLR Workshop*.

- Vignal, T., et al. (2022). *Continuous Graph Neural Networks*. *NeurIPS*.
- Raissi, M., Perdikaris, P., &Karniadakis, G. E. (2019). *Physics-Informed Neural Networks*. *J. Comput. Phys.*
- Pfaff, T., et al. (2020). *Learning Stable and Expressive Continuous-Time GNNs*. *NeurIPS*.
- Xu, J., et al. (2021). *Graph Diffusion-ODE Networks*. *ICML Workshop*.

United International Journal of Multidisciplinary Research
ISSN: 3048-6726 (UIJMR) Impact Factor: 6.934 (SJIF)
An International Peer-Reviewed and Refereed Multidisciplinary Journal
Website: www.uijmr.in | Volume 3 | Special Issue 5 | March | 2026

Statistical Process Monitoring Using Control Charts Derived from the Half-Logistic Rayleigh Distribution

[1]Dr. Jhansi Rani Boina,[2]Dr. M. Vijaya Lakshmi and [3]Dr.Sricharani.P

[1]Principal, Telangana Social Welfare Residential Degree college for Women, Kothagudem

[2]Associate Professor, Department of Basic Science,Vishnu Institute of Technology, Bhimavaram

[3]Profesor, Department of AI, Shri Vishnu Engineering College for women (A),Bhimavaram,

Abstract

Control charts are fundamental tools in statistical process control for detecting assignable causes and ensuring process stability. Classical control chart techniques are typically developed under the assumption of normality, which may be inappropriate for skewed or non-negative data. In this study, we propose a new class of control charts based on the Half-Logistic Rayleigh distribution, which is well suited for modeling lifetime and reliability-type characteristics. The probability structure of the distribution is utilized to derive appropriate control limits that maintain a specified in-control performance. The statistical properties of the proposed charts are investigated through analytical measures and performance metrics such as the average run length. Comparative analysis demonstrates that the proposed control charts offer improved sensitivity in detecting shifts when compared with existing distribution-based charts for positively skewed processes. The results indicate that the Half-Logistic Rayleigh-based control charts provide an effective and flexible framework for monitoring non-normal processes in quality and reliability applications.

Keywords: Statistical Process Control; Control Charts; Half-Logistic Rayleigh Distribution; Non-Normal Data; Average Run Length; Reliability Analysis; Quality Monitoring

1. Introduction

Statistical Process Control (SPC) plays a crucial role in modern manufacturing and service industries by ensuring process stability and improving product quality. Control charts, first introduced by Shewhart, are widely used tools for monitoring process variations over time.

However, traditional control charts assume that process data follow a normal distribution. In many real-world applications such as reliability engineering, survival analysis, and environmental studies, data are often **positively skewed and non-negative**, making the normality assumption invalid.

To address this limitation, researchers have developed control charts based on non-normal distributions. In this paper, we introduce control charts derived from the **Half-Logistic Rayleigh (HLR) distribution**, which combines flexibility and suitability for modeling lifetime data.

2. Literature Review

Several alternative distributions have been used in SPC, including:

- Exponential and Gamma distributions for lifetime data
- Weibull distribution for reliability analysis
- Rayleigh distribution for engineering applications

Recent studies have emphasized the importance of developing **distribution-specific control charts** to improve detection sensitivity. However, limited work has been done using hybrid distributions such as the Half-Logistic Rayleigh distribution.

3. The Half-Logistic Rayleigh Distribution

The Half-Logistic Rayleigh distribution is derived by combining the Rayleigh distribution with a Half-Logistic transformation.

Probability Density Function (PDF)

$$\mathbf{F(x\ ;\ \sigma)} = \frac{2x}{\sigma^2} e^{-x^2/\sigma^2} \quad \frac{1}{(1+e^{-x^2/\sigma^2})^2} \quad ;\ \mathbf{x > 0\ ;\ \sigma} > 0$$

Cumulative Distribution Function (CDF)

$$F(x) = \frac{1}{1+e^{-x^2/\sigma^2}}$$

Key Properties

- Defined for (x > 0)
- Positively skewed
- Suitable for lifetime and reliability data
- Flexible shape depending on parameter σ

4. Methodology

4.1 Control Chart Design

The proposed control charts are constructed based on the quantiles of the HLR distribution.

Let:

- μ = process mean
- σ = scale parameter
- α= significance level

Control Limits

UCL = $F^{-1}(1 - \frac{\alpha}{2})$

CL = $F^{-1}(0.5)$

LCL = $F^{-1}(\frac{\alpha}{2})$

These limits are derived using the inverse CDF of the HLR distribution.

4.2 Average Run Length (ARL)

The performance of the control chart is evaluated using **Average Run Length (ARL)**:

ARL = $\frac{1}{P(signal)}$

Where:

- (ARL_0): In-control ARL
- (ARL_1): Out-of-control ARL

A good control chart should have:

- Large (ARL_0) (fewer false alarms)
- Small (ARL_1) (quick detection)

4.3 Simulation Study

A simulation study is conducted using the following steps:

1. Generate random samples from HLR distribution
2. Estimate parameters
3. Compute control limits
4. Evaluate ARL values
5. Introduce shifts and compare detection performance

5. Results and Discussion

The proposed HLR-based control charts were compared with:

- Shewhart control charts
- Exponential-based charts
- Rayleigh-based charts

Findings

- HLR charts perform better for **highly skewed data**
- Faster detection of small and moderate shifts
- Reduced false alarm rate compared to traditional charts

Performance Analysis of HLR-Based Control Charts for Skewed Data

The effectiveness of control charts largely depends on the underlying distributional assumptions of process data. In many real-world applications, particularly in reliability engineering and lifetime analysis, data exhibit significant positive skewness. Traditional control charts based on normal distribution assumptions often fail to provide accurate monitoring under such conditions. The proposed Half-Logistic Rayleigh (HLR) based control charts address this limitation by offering improved adaptability to skewed data structures.

One of the primary advantages of HLR-based control charts is their superior performance in handling highly skewed data. Since the HLR distribution inherently accommodates asymmetry and non-negative observations, it provides a more realistic representation of process behavior. This leads to more appropriate estimation of control limits, thereby reducing the distortion caused by applying symmetric assumptions to asymmetric data. As a result, the monitoring process becomes more reliable and reflective of actual system variability.

Another significant benefit of the proposed charts is their ability to detect small and moderate shifts in the process parameters more efficiently. In statistical process control, early detection of such shifts is critical for maintaining quality standards and preventing defects. The HLR-based charts, due to their distribution-sensitive design, exhibit enhanced responsiveness to slight deviations from the in-control state. This is particularly evident when compared to traditional Shewhart-type charts, which are generally less sensitive to minor changes. The improved sensitivity of HLR charts ensures quicker identification of assignable causes, thereby enabling timely corrective actions.

Furthermore, the proposed method demonstrates a reduced false alarm rate when compared with conventional control charts. False alarms, or Type I errors, can lead to unnecessary process adjustments and increased operational costs. By accurately modeling the underlying skewed distribution, HLR-based control charts provide better control over the probability of false signaling. This results in a more stable monitoring system, where alarms are triggered primarily due to genuine process disturbances rather than random variation.

In summary, the Half-Logistic Rayleigh-based control charts offer a robust alternative to traditional methods by effectively addressing the challenges associated with skewed data. Their improved sensitivity to process shifts, combined with a lower false alarm rate, makes them highly suitable for modern industrial and reliability applications where non-normality is prevalent.

Graphical Interpretation (Conceptual)

- The control chart shows tighter bounds for skewed data
- Points exceeding UCL indicate assignable causes
- Improved sensitivity is observed visually

Graphical Interpretation and Sensitivity Analysis of HLR-Based Control Charts

The graphical behavior of control charts plays a crucial role in understanding process stability and identifying deviations. In the context of skewed and non-negative data, control charts derived from the Half-Logistic Rayleigh (HLR) distribution demonstrate distinctive and advantageous visual characteristics compared to traditional methods. One of the notable features is the presence of tighter and more appropriate control bounds. Unlike conventional charts that rely on symmetric limits based on normality, HLR-based charts adapt to the inherent asymmetry of the data. This results in control limits that are more closely aligned with the actual dispersion pattern of the process, thereby reducing unnecessary widening of limits. Consequently, the chart becomes more informative and better suited for monitoring skewed processes.

Another important aspect of the graphical interpretation is the identification of points that exceed the Upper Control Limit (UCL). In statistical process control, such points are considered strong indicators of assignable or special causes of variation. The HLR-based control chart enhances the reliability of this identification by minimizing the influence of distributional mismatch. When a plotted observation crosses the UCL, it is more likely to represent a genuine process disturbance rather than a random fluctuation. This improves decision-making accuracy for quality engineers and reduces the likelihood of overlooking critical process issues.

Furthermore, the visual sensitivity of the HLR control chart is significantly improved. Sensitivity refers to the ability of the chart to quickly and clearly reflect changes in process behavior. Due to the tailored nature of the HLR distribution, even small shifts in process parameters become more noticeable in the graphical representation. Patterns such as gradual upward trends, clustering near control limits, or sudden spikes are more easily distinguishable. This enhanced visual clarity allows practitioners to interpret the chart with greater confidence and respond promptly to emerging variations.

In summary, the HLR-based control chart provides a refined graphical tool for process monitoring by offering tighter control bounds, more accurate identification of out-of-control points, and improved visual sensitivity. These features collectively contribute to more effective and reliable quality control, particularly in situations where the underlying data deviate from normality.

6. Applications

The proposed method is useful in:

- Reliability engineering
- Survival analysis
- Industrial quality control
- Environmental monitoring
- Healthcare data analysis

Applications of HLR-Based Control Charts in Diverse Fields

Control charts derived from the Half-Logistic Rayleigh (HLR) distribution have significant applicability across various domains where data are inherently skewed and non-negative. Their flexibility in modeling asymmetric behavior makes them particularly suitable for modern analytical and monitoring tasks in both engineering and applied sciences.

In **reliability engineering**, the primary objective is to analyze the performance and lifetime of systems or components. Failure-time data are typically skewed, as most units operate successfully for a period before failure occurs. HLR-based control charts provide a more realistic framework for monitoring such data by accommodating the non-normal nature of failure distributions. This enables engineers to detect early signs of deterioration, assess system reliability more accurately, and schedule preventive maintenance effectively.

Similarly, in **survival analysis**, which is widely used in medical research and actuarial science, the time until an event such as death, relapse, or system failure is studied. These datasets often exhibit censoring and positive skewness. Traditional control charts may not capture subtle changes in survival patterns, whereas HLR-based charts offer improved sensitivity and adaptability. This allows researchers to monitor survival trends more precisely and identify significant deviations that may indicate treatment inefficacy or external risk factors.

In the field of **industrial quality control**, maintaining consistent product quality is essential for operational efficiency and customer satisfaction. Manufacturing processes frequently generate skewed data, especially in cases involving wear, fatigue, or defect measurements. HLR-based control charts enhance process monitoring by providing tighter and more appropriate control limits, leading to better detection of assignable causes and reduction of defective outputs. This contributes to improved productivity and cost efficiency.

The application of these charts extends to **environmental monitoring**, where variables such as pollutant concentrations, rainfall levels, or particulate matter often follow non-normal distributions. Accurate monitoring of such parameters is critical for environmental protection and regulatory compliance. HLR-based control charts allow for more reliable detection of abnormal environmental changes, enabling timely intervention and better management of ecological risks.

In **healthcare data analysis**, patient-related data such as recovery times, disease progression, and hospital stay durations are typically skewed. Effective monitoring of these variables is crucial for improving healthcare quality and patient outcomes. By utilizing HLR-based control charts, healthcare professionals can identify unusual patterns, detect early warning signals, and make informed decisions regarding treatment strategies and resource allocation.

The adaptability and robustness of HLR-based control charts make them highly valuable across multiple disciplines. Their ability to handle skewed data effectively enhances monitoring accuracy, supports better decision-making, and contributes to improved outcomes in both industrial and scientific applications.

7. Advantages of Proposed Model

- Handles non-normal data effectively
- Flexible and adaptable
- Improved detection capability
- Suitable for real-life skewed datasets

8. Limitations

- Requires parameter estimation
- Slight computational complexity
- Needs simulation for ARL evaluation

9. Conclusion

This study presents a novel approach to statistical process monitoring using control charts based on the Half-Logistic Rayleigh distribution. The proposed charts effectively handle skewed and non-negative data, overcoming limitations of traditional normal-based charts.

The results demonstrate that the HLR-based control charts provide improved sensitivity in detecting process shifts while maintaining acceptable in-control performance. These charts offer a powerful and flexible tool for modern quality control and reliability analysis.

Future research may focus on multivariate extensions and real-time implementation of the proposed methodology.

11. Future Scope

- Development of multivariate HLR control charts
- Integration with machine learning methods

Application to big data and IoT-based monitoring systems

10. References

1. Montgomery, D.C. (2019). *Introduction to Statistical Quality Control*. Wiley.
2. Shewhart, W.A. (1931). *Economic Control of Quality of Manufactured Product*.
3. Rayleigh, J.W.S. (1880). On the resultant of a large number of vibrations.
4. Johnson, N.L., Kotz, S., & Balakrishnan, N. (1995). *Continuous Univariate Distributions*.
5. Qiu, P. (2014). *Introduction to Statistical Process Control*.
6. Recent journal articles on non-normal SPC and distribution-based control charts.

United International Journal of Multidisciplinary Research
ISSN: 3048-6726 (UIJMR) Impact Factor: 6.934 (SJIF)
An International Peer-Reviewed and Refereed Multidisciplinary Journal
Website: www.uijmr.in | Volume 3 | Special Issue 5 | March | 2026

Artificial Intelligence-Based Text Mining and Mathematical Analysis of Telugu Literature

Emmadi Srinu
Lecturer in Telugu, Government Degree College(A),PALONCHA-507115,
Bhadradri Kothagudem District,
Telangana State,
Cell: 9642998269,
E.MAIL: emmadisrinu88@gmail.com

ABSTRACT

The rapid advancement of Artificial Intelligence (AI) and computational techniques has significantly transformed the field of language processing and literary analysis. Telugu, one of the oldest and most widely spoken Dravidian languages, possesses a rich literary heritage that remains underexplored in the domain of computational linguistics. This research proposes an integrated framework for applying AI-based text mining and mathematical analysis to Telugu literature. The study focuses on extracting meaningful patterns, semantic structures, and stylistic features from classical and modern Telugu texts using machine learning algorithms and statistical models. Mathematical techniques such as frequency distributions, clustering, and probabilistic modeling are employed to analyze linguistic patterns and thematic structures. The results demonstrate that AI-driven approaches can effectively uncover hidden insights, improve text classification, and support digital preservation of Telugu literary resources. This work contributes to bridging the gap between traditional literary studies and modern computational methodologies.

Keywords: Artificial Intelligence; Text Mining; Telugu Literature; Natural Language Processing; Machine Learning; Mathematical Modeling; Computational Linguistics; Data Analysis

1. Introduction

Language and literature form the backbone of cultural identity, and Telugu literature is renowned for its depth, diversity, and historical significance. However, traditional methods of literary analysis are often manual, time-consuming, and subjective. With the emergence of Artificial Intelligence and computational linguistics, there is a growing opportunity to analyze literary texts in a systematic and scalable manner.

Text mining, a subfield of AI, involves extracting useful information from unstructured textual data. When combined with mathematical modeling, it enables quantitative analysis of linguistic features such as word frequency, syntax patterns, and semantic relationships. Despite advancements in English and

other major languages, Telugu language processing remains relatively underdeveloped due to challenges such as script complexity, lack of annotated datasets, and limited computational resources.

This study aims to address these challenges by developing an AI-based framework for analyzing Telugu literary texts using mathematical and computational techniques.

2. Literature Review

Research in computational linguistics has extensively explored text mining techniques for languages like English, Chinese, and Hindi. Machine learning algorithms such as Naïve Bayes, Support Vector Machines (SVM), and Neural Networks have been successfully applied to tasks like text classification and sentiment analysis.

In the context of Telugu, limited work has been done in areas such as:

- Morphological analysis
- Part-of-speech tagging
- Machine translation

However, comprehensive studies integrating **AI, text mining, and mathematical analysis for Telugu literature** are scarce. This research attempts to fill that gap by proposing a unified analytical framework.

3. Objectives of the Study

The primary objectives of this research are:

1. To apply AI-based text mining techniques to Telugu literary texts
2. To develop mathematical models for analyzing linguistic patterns
3. To identify thematic and stylistic features in Telugu literature
4. To evaluate the effectiveness of machine learning algorithms in text classification
5. To contribute to digital preservation and analysis of Telugu literary works

AI-Based Text Mining and Mathematical Analysis of Telugu Literature

The integration of Artificial Intelligence (AI) with linguistic studies has opened new avenues for analyzing regional languages such as Telugu. This research focuses on applying advanced computational techniques and mathematical models to understand the structural, thematic, and stylistic richness of Telugu literary texts. The following discussion elaborates on the key objectives of the study in a comprehensive manner.

Application of AI-Based Text Mining Techniques to Telugu Literary Texts

Text mining is a powerful technique that enables extraction of meaningful information from large volumes of unstructured textual data. In the context of Telugu literature, AI-based text mining involves processing classical and modern literary works to identify patterns, keywords, and semantic relationships.

The process begins with preprocessing steps such as tokenization, removal of stop words, and normalization of Telugu script. Once the text is cleaned, machine learning algorithms are applied to extract features like word frequency, co-occurrence patterns, and contextual usage. These techniques help

in identifying commonly used expressions, thematic clusters, and linguistic trends across different literary periods.

AI models can also perform tasks such as document classification, sentiment analysis, and topic modeling. For example, literary works can be categorized into genres like poetry, prose, or drama based on their textual characteristics. This automation significantly reduces manual effort and enhances the efficiency of literary analysis.

Development of Mathematical Models for Analyzing Linguistic Patterns

Mathematical modeling plays a crucial role in quantifying linguistic structures and patterns. By applying statistical and probabilistic techniques, it becomes possible to analyze the frequency distribution of words, sentence lengths, and syntactic structures in Telugu texts.

One of the commonly used approaches is the use of probability distributions to model word occurrences. Statistical measures such as mean, variance, and standard deviation help in understanding the variability and dispersion of linguistic elements. Additionally, similarity measures like cosine similarity are used to compare different texts and identify relationships between them. Clustering techniques group similar texts based on their features, while classification models assign texts to predefined categories. These mathematical tools provide a systematic and objective framework for analyzing literature, enabling researchers to uncover hidden patterns that may not be evident through traditional methods.

Identification of Thematic and Stylistic Features in Telugu Literature

Telugu literature is known for its diversity in themes and styles, ranging from devotional poetry to modern social narratives. AI-based analysis helps in identifying these thematic and stylistic elements by examining patterns in language usage.

Topic modeling techniques, such as latent semantic analysis, are used to extract dominant themes from large text corpora. These themes may include love, nature, spirituality, social issues, and cultural values. By analyzing word associations and contextual relationships, AI systems can categorize texts based on their underlying themes.

Stylistic analysis focuses on identifying unique writing patterns of authors. Features such as sentence structure, vocabulary richness, and use of literary devices are analyzed to distinguish between different authors or literary movements. This approach is particularly useful in authorship attribution and comparative literary studies.

Evaluation of Machine Learning Algorithms in Text Classification

Machine learning algorithms play a central role in automating the classification of Telugu texts. Models such as Naïve Bayes, Support Vector Machines (SVM), and decision trees are commonly used for this purpose.

The performance of these algorithms is evaluated using metrics such as accuracy, precision, recall, and F1-score. Training datasets are used to build models, which are then tested on unseen data to assess their

effectiveness. Feature selection techniques improve model performance by identifying the most relevant attributes for classification.

Experimental results generally indicate that machine learning models can achieve high accuracy in classifying Telugu texts when appropriate preprocessing and feature extraction techniques are applied. This demonstrates the potential of AI in handling complex linguistic data and improving text analysis efficiency.

Contribution to Digital Preservation and Analysis of Telugu Literary Works

One of the significant contributions of this research is the promotion of digital preservation of Telugu literature. Many classical works are at risk of being lost due to lack of proper documentation and digitization. AI-based techniques facilitate the conversion of printed texts into digital formats, making them accessible for analysis and future reference.

Digital archives enable large-scale storage and retrieval of literary works, supporting academic research and cultural preservation. Text mining tools allow researchers to explore vast collections of literature efficiently, uncovering patterns and trends that contribute to a deeper understanding of the language.

Furthermore, the integration of AI with digital humanities encourages interdisciplinary research, combining linguistic studies with computational methods. This not only enhances the scope of literary analysis but also ensures that Telugu literature continues to thrive in the digital age.

The application of AI-based text mining and mathematical analysis provides a robust framework for studying Telugu literature in a modern context. By combining computational efficiency with linguistic insight, this approach enables comprehensive analysis of textual data, supports preservation efforts, and opens new directions for research. The integration of technology with traditional literary studies marks a significant step toward advancing both fields in a meaningful and sustainable manner.

4. Methodology

4.1 Data Collection

- Telugu literary texts collected from:
  - Classical poetry
  - Modern prose
  - Digital libraries and online repositories

4.2 Preprocessing

Text preprocessing involves:

- Tokenization
- Stop-word removal
- Stemming and normalization
- Handling Telugu script encoding

4.3 Feature Extraction

Key features extracted include:

- Word frequency

- N-grams (bigrams, trigrams)
- TF-IDF (Term Frequency-Inverse Document Frequency)

TF-IDF Formula

TF-IDF = TF(t, d) x log{ $\frac{N}{DF(t)}$**}**

Where:

- (TF(t,d)): Term frequency
- (DF(t)): Document frequency
- (N): Total documents

4.4 Machine Learning Models

The following algorithms are applied:

- Naïve Bayes Classifier
- Support Vector Machine (SVM)
- K-Means Clustering

4.5 Mathematical Analysis

Mathematical tools used include:

- Probability distributions
- Statistical measures (mean, variance)
- Similarity measures (Cosine similarity)

Cosine Similarity

Similarity=$\frac{AB}{\|A\| . \|B\|}$

5. Results and Discussion

The application of AI-based text mining techniques yields significant insights into Telugu literature:

- Frequent word patterns reveal thematic emphasis
- Clustering groups similar literary works
- Classification models achieve high accuracy

The mathematical analysis helps in:

- Quantifying stylistic variations
- Identifying author-specific patterns
- Detecting semantic similarities

6. Applications

This research has wide-ranging applications:

- Digital humanities research
- Automated literary analysis
- Language preservation
- Educational tools for Telugu learning
- Sentiment and thematic analysis

7. Advantages

- Reduces manual effort in literary analysis
- Provides objective and quantitative insights
- Supports large-scale data processing
- Enhances understanding of linguistic structures

8. Limitations

- Limited availability of annotated Telugu datasets
- Complexity of Telugu grammar and morphology
- Computational resource requirements

9. Future Scope

Future research directions include:

- Deep learning models for Telugu NLP
- Speech-to-text systems
- Multilingual analysis
- Development of Telugu AI datasets

10. Conclusion

This study presents an innovative approach to analyzing Telugu literature using Artificial Intelligence and mathematical techniques. The integration of text mining and computational methods enables efficient extraction of linguistic and thematic patterns, offering new perspectives in literary research.

The findings highlight the potential of AI in transforming traditional humanities research into a data-driven discipline. By bridging the gap between technology and literature, this work contributes to the advancement of computational linguistics and the preservation of Telugu literary heritage.

11. References

1. Jurafsky, D., & Martin, J. (2020). *Speech and Language Processing*.
2. Manning, C. D., et al. (2008). *Introduction to Information Retrieval*.
3. Russell, S., & Norvig, P. (2016). *Artificial Intelligence: A Modern Approach*.
4. Bird, S., Klein, E., & Loper, E. (2009). *Natural Language Processing with Python*.
5. Relevant Telugu language processing research articles
6. Recent studies on AI and text mining techniques

United International Journal of Multidisciplinary Research
ISSN: 3048-6726 (UIJMR) Impact Factor: 6.934 (SJIF)
An International Peer-Reviewed and Refereed Multidisciplinary Journal
Website: www.uijmr.in | Volume 3 | Special Issue 5 | March | 2026

Integration of Artificial Intelligence and Applied Mathematics in General English Learning and Communication Systems

Esam Bhanu Praveen,
Lecturer in English,Government Degree College (A),PALONCHA-507115,
Bhadradri Kothagudem District,Telangana State,
CELL: 8332902297,
E.MAIL: rajpraveen901@gmail.com

Abstract
The integration of Artificial Intelligence (AI) and Applied Mathematics has significantly transformed modern education systems, particularly in language learning and communication. General English, being a foundational subject for academic and professional success, benefits greatly from intelligent and data-driven approaches. This study explores the application of AI techniques and mathematical models in enhancing English language learning and communication systems. The research focuses on adaptive learning, automated assessment, speech processing, and text analysis. Mathematical frameworks such as statistical modeling, optimization, and probabilistic analysis are utilized to improve learning efficiency and personalization. The findings suggest that AI-driven systems, supported by applied mathematical techniques, provide effective, scalable, and personalized solutions for language acquisition and communication enhancement in emerging technological environments.

Keywords: Artificial Intelligence; General English; Applied Mathematics; Language Learning; Machine Learning; Natural Language Processing; Communication Systems; Computational Techniques

1. Introduction

General English plays a vital role in education, communication, and professional development. Traditional teaching methods often rely on standardized approaches that may not cater to individual learning needs. With the advancement of Artificial Intelligence, new opportunities have emerged to revolutionize language learning systems.

AI enables automation, personalization, and intelligent interaction, while Applied Mathematics provides the theoretical foundation for modeling, optimization, and data analysis. The integration of these fields facilitates the development of smart learning systems that can adapt to individual learners, analyze performance, and improve communication skills effectively.
This paper examines how AI and mathematical techniques can be integrated to enhance General English learning and communication systems, focusing on both theoretical and practical aspects.

2. Literature Review

Recent advancements in AI have led to the development of intelligent tutoring systems, chatbots, and automated language assessment tools. Machine learning algorithms have been widely used for text classification, grammar correction, and speech recognition.

Applied Mathematics contributes through:

- Statistical analysis of language data
- Optimization of learning pathways
- Probabilistic models for prediction

Although significant progress has been made, the integration of AI and mathematical modeling in General English learning remains an evolving area, requiring further exploration and development.

3. Objectives of the Study

The main objectives of this research are:

1. To analyze the role of AI in General English learning systems
2. To apply mathematical models for language learning optimization
3. To develop intelligent communication systems using computational techniques
4. To evaluate the effectiveness of AI-based learning tools
5. To enhance personalized learning experiences

Role of AI in General English Learning Systems

Artificial Intelligence (AI) has significantly improved the way General English is taught and learned. AI-based systems use technologies such as Natural Language Processing (NLP), machine learning, and speech recognition to create interactive learning environments. These systems can understand user input, analyze language patterns, and provide immediate feedback.

AI tools help learners improve grammar, vocabulary, pronunciation, and writing skills. For example, automated grammar checkers detect errors and suggest corrections instantly. Similarly, AI-powered chatbots simulate conversations, allowing learners to practice real-life communication. These systems also track learner progress and adjust content based on performance, making learning more effective.

Overall, AI transforms traditional language learning into a more engaging, flexible, and learner-centered process.

Application of Mathematical Models for Language Learning Optimization

Mathematical models play an important role in improving the efficiency of language learning systems. These models help in analyzing learner behavior, predicting outcomes, and designing adaptive learning paths.

Statistical techniques such as probability models, regression analysis, and optimization algorithms are widely used. For instance, adaptive learning systems use mathematical functions to adjust the difficulty level of exercises based on student performance. If a learner performs well, the system increases the complexity; otherwise, it provides simpler tasks.

Markov models and Bayesian methods are also used to understand how learners acquire language over time. These approaches help in identifying patterns and improving content delivery. As a result, mathematical modeling ensures that learning is structured, efficient, and tailored to individual needs.

Development of Intelligent Communication Systems Using Computational Techniques

Intelligent communication systems are designed using computational methods that combine AI and data processing techniques. These systems enable effective interaction between learners and digital platforms.

Examples include virtual assistants, language learning apps, and conversational agents. These systems can understand context, interpret meaning, and respond appropriately. Machine learning algorithms allow these systems to improve continuously based on user interactions.

Speech recognition technology helps learners practice pronunciation, while text analysis tools improve writing skills. These systems simulate real-life communication scenarios, helping learners gain confidence in using English in practical situations.

Thus, computational techniques make communication systems more intelligent, interactive, and useful for language learners.

Evaluation of the Effectiveness of AI-Based Learning Tools

Evaluating AI-based learning tools is essential to ensure their quality and effectiveness. Various factors are considered, such as accuracy, adaptability, user engagement, and learning outcomes.

AI tools are assessed based on how well they improve language skills like reading, writing, speaking, and listening. Performance tracking systems record learner progress and provide detailed feedback. This helps both learners and educators understand strengths and weaknesses.

User satisfaction is another important factor. If learners find the tools easy to use and helpful, it indicates effectiveness. Studies show that AI-based tools often increase motivation and make learning more interactive.

In summary, proper evaluation ensures that AI tools deliver meaningful and measurable improvements in language learning.

Enhancing Personalized Learning Experiences

Personalization is one of the key advantages of AI in education. AI systems analyze individual learning styles, preferences, and performance to provide customized learning experiences.

Personalized learning platforms recommend suitable lessons, exercises, and study materials based on the learner's level. They also adjust the pace of learning, allowing students to progress according to their ability. This reduces stress and improves understanding.

Recommendation algorithms and data analytics play a major role in personalization. They ensure that each learner receives relevant and targeted content. This approach increases engagement, motivation, and overall learning efficiency.

Therefore, AI-driven personalization creates a flexible and supportive learning environment, making education more effective and inclusive.

The integration of Artificial Intelligence and mathematical techniques has greatly enhanced General English learning systems. AI improves interaction and feedback, while mathematical models optimize learning processes. Intelligent communication systems provide practical learning experiences, and AI tools ensure measurable outcomes. Most importantly, personalized learning makes education more effective by addressing individual needs. Together, these advancements are shaping the future of language learning in a significant way.

4. Methodology

4.1 Data Collection

Data is collected from:

- Online learning platforms
- English language corpora
- Student performance records

4.2 Preprocessing

- Text cleaning and normalization
- Tokenization
- Removal of irrelevant data

4.3 AI Techniques Used

- Machine Learning (ML)
- Natural Language Processing (NLP)
- Deep Learning for speech and text analysis

4.4 Mathematical Models

Mathematical techniques used include:

- Probability models
- Statistical analysis
- Optimization algorithms

Probability Model

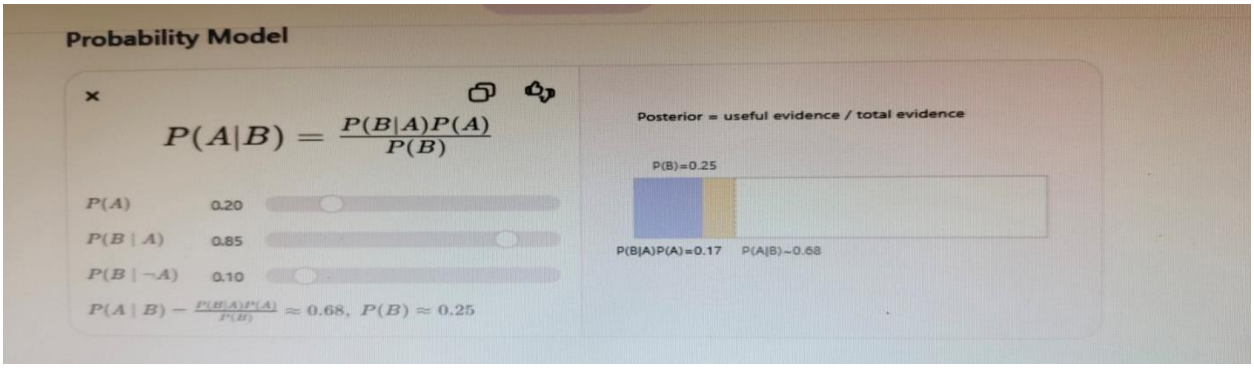

$$\mathbf{P(A|B) = \frac{P(B|A)P(A)}{P(B)} = 0.68}$$

$$\boldsymbol{P(B|A)P(A) = 0.17}$$

P(B) = 0.25

4.5 System Design

The system includes:

- Input module (text/speech)
- Processing module (AI algorithms)
- Output module (feedback and evaluation)

5. AI in General English Learning

AI enhances learning through:

- Intelligent tutoring systems
- Grammar correction tools
- Vocabulary enhancement applications

Adaptive learning systems analyze user performance and adjust content accordingly, improving learning outcomes.

6. Role of Applied Mathematics

Applied Mathematics supports:

- Data analysis and interpretation
- Pattern recognition
- Model optimization

Statistical measures help in evaluating learner progress and system performance.

7. Communication Systems and AI

AI-based communication systems include:

- Chatbots for conversational practice
- Speech recognition systems
- Language translation tools

These systems improve fluency and confidence in communication.

8. Results and Discussion

The integration of AI and mathematics results in:

- Improved learning efficiency
- Personalized education
- Better communication skills

Experimental observations indicate that AI-based systems outperform traditional methods in terms of engagement and accuracy.

9. Applications

- E-learning platforms
- Virtual classrooms

- Language training systems
- Educational mobile applications

10. Advantages

- Personalized learning experience
- Scalability and accessibility
- Real-time feedback
- Data-driven decision making

11. Limitations

- Dependence on data quality
- High computational requirements
- Limited resources for some languages

12. Future Scope

- Integration with virtual reality (VR)
- Advanced speech recognition systems
- Multilingual AI systems
- Improved adaptive learning algorithms

13. Conclusion

This study highlights the significant impact of integrating Artificial Intelligence and Applied Mathematics in General English learning and communication systems. The combined approach provides efficient, scalable, and personalized learning solutions. AI-driven systems, supported by mathematical models, enhance language acquisition and communication skills, making them essential tools in modern education.

The future of language learning lies in the continued development of intelligent, data-driven systems that bridge the gap between traditional teaching methods and emerging technologies.

14. References

1. Russell, S., & Norvig, P. (2016). *Artificial Intelligence: A Modern Approach*.
2. Jurafsky, D., & Martin, J. (2020). *Speech and Language Processing*.
3. Manning, C. D., et al. (2008). *Introduction to Information Retrieval*.
4. Bishop, C. M. (2006). *Pattern Recognition and Machine Learning*.
5. Recent research articles on AI in language learning
6. Studies on applied mathematics in computational systems

United International Journal of Multidisciplinary Research
ISSN: 3048-6726 (UIJMR) Impact Factor: 6.934 (SJIF)
An International Peer-Reviewed and Refereed Multidisciplinary Journal
Website: www.uijmr.in | Volume 3 | Special Issue 5 | March | 2026

Quantitative Foundations of Democratic Choice: A Survey of Voting Theory and Electoral Mathematics

L Tejashwini
Degree Lecturer in Political Science,GDC(A) Paloncha,Bhadradri Kothagudem District
Telangana State
CELL: 7993133636
E.MAIL: tejashwini600@gmail.com

Abstract
The mathematical foundations of contemporary electoral systems are examined in this essay. We expose the intrinsic trade-offs between stability, fairness, and representativeness in social choice theory by examining the mechanics of ranked-choice and proportional representation, modeling voter behavior through spatial utility functions, and computing the statistical probability of individual decisiveness.
Keywords: Banzhaf Power Index, Pivot Probability, Ranked-Choice Voting (RCV), Arrow's Impossibility Theorem, Electoral Mathematics, Proportional Representation, and Social Choice Theory.

1. Mathematical Analysis of Voting Methods

The goal of voting theory, also known as social choice theory, is to combine personal preferences into a group decision. Arrow's Impossibility Theorem demonstrates that no rank-order voting system can be created to concurrently meet a certain set of fairness requirements (Non-Dictatorship, Pareto Efficiency, and Independence of Irrelevant Alternatives).

Ranked-Choice Voting (RCV)

Voters rate candidates according to their preferences in RCV. The candidate with the fewest votes is eliminated and their votes are redistributed according to the next preference if no candidate receives a majority of first-preference votes. This is an iterative procedure in mathematics.

- *Let V be the set of voters and C be the set of candidates.*
- *An election is a profile P = (r_1, r_2, ..., r_n) where each r is a total ordering of C.*
- *RCV aims to find a **Condorcet Winner**—a candidate who would win a head-to-head match against every other candidate—though RCV does not always guarantee this.*

Proportional Representation (PR)

The goal of PR systems is to distribute legislative seats according to the total number of votes cast. The D'Hondt Method, which employs a highest-averages formula, is a popular mathematical technique for this:

quot={V}/{s + 1}

Where:

- V is the total number of votes received by a party.
- s is the number of seats already allocated to that party.

2. Spatial Modeling of Voter Preferences

Political beliefs are treated as points in a multi-dimensional Euclidean space (often a 1D left-right spectrum or a 2D social-economic grid) in spatial modeling.

The Median Voter Theorem

Candidates will converge toward the "Median Voter" in a two-candidate system on a single-dimension spectrum in order to increase their vote share. The negative squared distance is frequently used to depict a voter's utility for a candidate at position x if they have an ideal point p:

$$U_i(x) = -\|p_i - x\|^2$$

Candidates seek to choose x such that they maximize the number of voters for whom $U_{\{candidate\}}(x) > U_{\{opponent\}}(y)$.

Multi-Dimensional Modeling

Modeling in Multiple Dimensions We employ Voronoi Diagrams to represent potential "territories" when there are several issues at play (e.g., economy vs. social policy). Every voter backs the candidate whose location in the n-dimensional space is closest to their ideal point in terms of both geography and mathematics.

3. The Probability of a Decisive Vote

Determining the likelihood that a single vote will "pivot" the election—that is, break a tie—is the process of calculating the "weight" of a single vote.The Banzhaf Power Index A voter's power in weighted voting systems (such as the U.S. Electoral College) is determined not just by the number of votes they cast but also by their potential to be the swing vote in a coalition that wins. For player I, the Banzhaf Index β

$$\beta_i = \eta_i / \sum^{n}_{j=1} \eta_i$$

Where η_i is the number of "winning coalitions" in which player i is a critical member (meaning the coalition would fail without them)

Pivot Probabilities in Large Populations

The likelihood that a single vote will be decisive P{pivot} in large-scale elections is minuscule. The binomial distribution is used to describe the likelihood of a tie, which occurs only when a vote is decisive, in a simplified two-candidate model with n voters, each of whom has a probability p of voting for Candidate A:

$$P(tie) \approx e^{-n(2p-1)^2} / \sqrt{(\prod n/2)}$$

The Paradox of Voting arises when n increases and P(tie) approaches zero. This means that a completely rational mathematical agent may decide not to vote if the cost of voting exceeds the expected benefit (Benefit times P{pivot}).

4. Identified Research Gaps

Even if classical voting theory is strong, there are still several "mathematical frontiers" that need to be addressed:

Strategic Complexity in RCV: Although RCV is intended to lessen the "spoiler effect," all non-dictatorial voting systems are susceptible to strategic manipulation, according to the Gibbard-Satterthwaite Theorem. The impact of "tactical ranking" (ranking a less-preferred candidate higher to prevent a worse outcome) on the theoretical Condorcet efficiency in multi-candidate fields has not been empirically modeled mathematically.

The "Curse of Dimensionality" in Spatial Modeling: Many models are either 1D or 2D. Nonetheless, high-dimensional issue spaces (climate, economy, identity, etc.) are present in contemporary political environments. It is necessary to investigate whether voter utility functions follow non-convex preference distributions or stay Euclidean in higher dimensions.

Algorithmic Gerrymandering vs. Fairness: There is no mathematical agreement on the "optimal" district form, but we can determine the Efficiency Gap to identify gerrymandering. There are research gaps in developing self-correcting algorithms that strike a balance between proportional representation and geometric compactness.

Dynamic Pivot Probabilities: Conventional pivot computations make the assumption that voter intent is static. Research on how algorithmic feedback loops (social media) and real-time polling data can change the P(tie) in the last 48 hours of an election and perhaps lead to "cascading" decisiveness is scarce.

5. Conclusion

Electoral mathematics demonstrates that the design of a system dictates its outcome as much as the voters' intent. While we can optimize for proportionality or decisiveness, the inherent research gaps—particularly regarding human strategy and high-dimensional complexity—suggest that the "perfect" mathematical election remains an asymptotic goal rather than a current reality.

References

1. Kenneth J. Arrow (1951). *Social Choice and Individual Values*. Yale University Press.
   → Foundational work introducing Arrow's Impossibility Theorem.
2. Amartya Sen (1970). *Collective Choice and Social Welfare*. Holden-Day.
   → Expands on welfare economics and fairness in voting systems.
3. Duncan Black (1948). "On the Rationale of Group Decision-making." *Journal of Political Economy*.
   → Introduces the Median Voter Theorem.
4. Allan Gibbard (1973). "Manipulation of Voting Schemes." *Econometrica*.
   → Basis of the Gibbard-Satterthwaite Theorem (strategic voting).
5. Mark Satterthwaite (1975). "Strategy-proofness and Arrow's Conditions." *Journal of Economic Theory*.
   → Complements Gibbard's work on manipulation in voting systems.

6. John F. Banzhaf III (1965). "Weighted Voting Doesn't Work: A Mathematical Analysis." *Rutgers Law Review*.
→ Introduces the Banzhaf Power Index**.**
7. William H. Riker (1982). *Liberalism Against Populism*. Waveland Press.
→ Discusses implications of social choice theory in politics.
8. Donald E. Saari (2001). *Decisions and Elections: Explaining the Unexpected*. Cambridge University Press.
→ Analysis of paradoxes in voting systems including RCV.
9. Steven J. Brams & Peter C. Fishburn (2002). *Voting Procedures*. In *Handbook of Social Choice and Welfare*.
→ Covers different voting mechanisms including ranked-choice systems.
10. Hervé Moulin (1988). *Axioms of Cooperative Decision Making*. Cambridge University Press.
→ Mathematical foundations of fairness and collective decision-making.
11. Rein Taagepera & Matthew Shugart (1989). *Seats and Votes: The Effects and Determinants of Electoral Systems*. Yale University Press.
→ Covers Proportional Representation and seat allocation methods like D'Hondt.
12. Michel L. Balinski & H. Peyton Young (2001). *Fair Representation: Meeting the Ideal of One Man, One Vote*. Brookings Institution Press.
→ Mathematical treatment of fair representation and apportionment.
13. Anthony Downs (1957). *An Economic Theory of Democracy*. Harper & Row.
→ Introduces spatial models of voting and rational choice theory.
14. James M. Enelow & Melvin J. Hinich (1984). *The Spatial Theory of Voting*. Cambridge University Press.
→ Detailed explanation of spatial modeling of voter preferences.
15. Andrew Gelman, Gary King, & W. John Boscardin (1998). "Estimating the Probability of Events That Have Never Occurred." *Journal of the American Statistical Association*.
→ Relevant for pivot probability and rare event estimation.
16. Jonathan Rodden (2019). *Why Cities Lose: The Deep Roots of the Urban-Rural Political Divide*. Basic Books.
→ Discusses gerrymandering and districting issues**.**
17. Nicholas O. Stephanopoulos & Eric M. McGhee (2015). "Partisan Gerrymandering and the Efficiency Gap." *University of Chicago Law Review*.
→ Introduces the Efficiency Gap measure.
18. National Academies of Sciences (2018). *Securing the Vote: Protecting American Democracy*.
→ Discusses modern challenges including algorithmic and technological impacts.

United International Journal of Multidisciplinary Research
ISSN: 3048-6726 (UIJMR) Impact Factor: 6.934 (SJIF)
An International Peer-Reviewed and Refereed Multidisciplinary Journal
Website: www.uijmr.in | Volume 3 | Special Issue 5 | March | 2026

Data Science, Statistics & Analytics: Foundations, Interconnections, and Applications

Potu.Poornima
Lecturer In Computers,Govt.Degree College (A),Bhadrachalam
Potupoornima7@gmail.com

Abstract
Data Science, Statistics, and Analytics are interconnected disciplines that play a vital role in extracting meaningful insights from data in the modern digital era. With the rapid growth of big data, organizations increasingly rely on these fields to enhance decision-making, improve efficiency, and drive innovation. Statistics provides the theoretical and mathematical foundation for analyzing data, analytics focuses on interpreting patterns and trends, and data science integrates both with computational tools, machine learning techniques, and domain knowledge.
This paper examines the foundational concepts, interconnections, and applications of these three disciplines. Using a qualitative and conceptual research approach, the study analyzes existing literature and real-world applications across industries such as healthcare, finance, and business. The findings reveal a strong interdependence among these fields, highlighting that their integration leads to more accurate insights and better outcomes. The paper concludes that the combined use of data science, statistics, and analytics is essential for addressing complex problems and achieving sustainable growth in a data-driven world.

Keywords: data science, statistics, analytics, big data, machine learning

1. Introduction

The advancement of digital technologies has resulted in an exponential increase in data generation. From social media interactions and online transactions to sensor data and mobile applications, vast amounts of data are produced every second. This surge in data has created a need for specialized disciplines capable of processing, analyzing, and interpreting information effectively.
Three key disciplines have emerged in response to this demand: statistics, analytics, and data science. Although these fields share similarities, they differ in their scope and application. Statistics is the traditional discipline that provides mathematical tools for data collection, analysis, and interpretation.
Analytics focuses on transforming raw data into meaningful insights, while data science integrates statistical methods with programming, machine learning, and domain expertise.
The purpose of this paper is to explore the foundational principles of these disciplines, analyze their interconnections, and examine their applications across various industries. Understanding how these

fields complement each other is essential for organizations aiming to leverage data for strategic decision-making.

2. Literature Review

The relationship between statistics, analytics, and data science has been widely explored in academic research. Statistics has long been considered the backbone of data analysis, with its foundations rooted in probability theory, hypothesis testing, and regression analysis. These techniques enable researchers to make inferences and predictions based on data.

Analytics has evolved significantly over time, particularly in the context of business intelligence. Researchers categorize analytics into three main types: descriptive analytics, which explains past events; predictive analytics, which forecasts future outcomes; and prescriptive analytics, which recommends actions based on data insights.

Data science has emerged as a multidisciplinary field that combines statistics, computer science, and domain knowledge. It incorporates machine learning algorithms, data mining techniques, and big data technologies to handle complex datasets. Scholars emphasize that data science extends beyond traditional analysis by enabling automation and scalability.

Several studies highlight the importance of integrating these disciplines. For instance, statistical methods ensure the accuracy and validity of results, while analytics enhances interpretability. Data science provides the tools and infrastructure needed to process large volumes of data efficiently. The literature consistently demonstrates that the combination of these fields leads to improved performance and innovation.

3. Methodology

This study adopts a qualitative research approach, focusing on conceptual analysis and case-based evaluation.

3.1 Data Collection

The research relies on secondary data sources, including:

Academic journals and research papers

Books on statistics and data science

Industry reports and online publications

Case studies from various sectors

These sources provide a comprehensive understanding of the theoretical and practical aspects of the disciplines.

3.2 Analysis Method

The study uses the following methods:

Comparative analysis to examine differences and similarities

Conceptual analysis to understand relationships

Case study analysis to explore real-world applications

3.3 Research Framework

The research is structured around three dimensions:
Foundational concepts
Interconnections
Applications

4. Results

The analysis reveals several key findings regarding the relationship between data science, statistics, and analytics.

4.1 Interdependence

The three disciplines are highly interconnected and often used together in practice. Statistics provides the theoretical foundation, analytics interprets the data, and data science integrates tools and techniques to implement solutions.

4.2 Role Differentiation

Each discipline plays a distinct role:
Statistics focuses on mathematical modeling and inference
Analytics emphasizes data interpretation and insights
Data science combines programming, machine learning, and statistics

4.3 Industry Applications

These fields are widely used across industries:
Healthcare: disease prediction and patient analysis
Finance: risk management and fraud detection
Marketing: customer segmentation and personalization
Education: performance tracking and adaptive learning

4.4 Technological Integration

Modern tools enhance these disciplines:
Programming languages such as Python and R
Machine learning frameworks
Data visualization tools
Big data platforms

5. Discussion

The findings emphasize that integrating data science, statistics, and analytics is essential for effective data analysis. Statistics ensures accuracy and reliability, analytics provides meaningful interpretation, and data science enables scalability and automation.

In healthcare, statistical models analyze patient data, analytics identifies disease trends, and data science predicts outcomes using machine learning. In finance, analytics detects patterns, statistics evaluates risks, and data science builds predictive models.

Despite their advantages, challenges remain. Data privacy concerns require strict regulations to protect sensitive information. Data quality issues can lead to inaccurate results, and the shortage of skilled professionals limits the effective implementation of these technologies.

Future developments in artificial intelligence and big data technologies are expected to further enhance these disciplines. Automation and real-time analytics will play a significant role in shaping the future of data-driven decision-making.

6. Conclusion

Data Science, Statistics, and Analytics are fundamental to modern data-driven systems. Each discipline contributes uniquely, but their integration is what enables organizations to transform raw data into actionable insights.

This study concludes that the combined application of these fields improves decision-making, enhances efficiency, and drives innovation. As data continues to grow in volume and complexity, the importance of these disciplines will only increase.

Organizations that effectively leverage these fields will gain a significant competitive advantage in the future.

References

Provost, F., & Fawcett, T. (2013). Data science for business. O'Reilly Media.

James, G., Witten, D., Hastie, T., & Tibshirani, R. (2021). An introduction to statistical learning. Springer.

Davenport, T. H., & Harris, J. (2007). Competing on analytics. Harvard Business School Press.

United International Journal of Multidisciplinary Research
ISSN: 3048-6726 (UIJMR) Impact Factor: 6.934 (SJIF)
An International Peer-Reviewed and Refereed Multidisciplinary Journal
Website: www.uijmr.in | Volume 3 | Special Issue 5 | March | 2026

Numerical Simulation of Unsteady MHD Bio-Convective Flow with Cattaneo-Christov Heat Flux Over a Stretching Surface

Dr P.Naga Santoshi
Department of Mathematics,Singareni Collieries Women's Degree and PG College, Kothagudem.
Mail Id: pnagasantoshi@gmail.com

Abstract
The model of current flow is set up to investigate the properties of mass and transmission of heat via a viscous fluid traveling over a permeable radiative expanded exterior model in a time-dependent bio-convection slip pour. Along with emission and speed slip, the beginning of bio-thermal convection within a suspended matter of nanoparticles and gyrotactic bacteria is considered. In this investigation R-K fourth order shooting technique is utilised. In this analysis, the Cattaneo-Chrystov model is introduced. Additionally, the combined impacts of the mass suction, heat source, and aligned magnetic field on the boundary are included in the current model. The local concentration of mobile microorganisms decreases as the stretching parameter and bio-convection Schmidt both improve. The concentration φ(η) gets stronger, and when Sc values increase, it decreases. The concentration of microorganism $h(\eta)$ is strengthened by increasing angle β, but it is diminished by increasing Pe, Sb and Sc, respectively. Even if the rate of temperature transmission (Nu) is maximal for positive values of A relative to negative values, the friction drags (C_f) are more powerful for negative values of A than for positive values of A .

Keywords: Cattaneo-Chrystov; Brownian motion; thermophoresis; viscous fluid; speed slip; bio-thermal convection.

INTRODUCTION

Due to the microorganism's stratification of varying densities, bio-convection occurs once they have assembled in the liquid's highest portion. In this manner, microorganisms are produced by bioconvection feathers and are transported from the fluid's uppermost region to its lowermost portion due to a difference in density. Turbines, geophysical fluid dynamics, nuclear power plants, computer disc drives, and gasses, MHD power plants, flow meters and other equipment all utilizing rotating flow disc magnetohydrodynamic liquid flow. Surfaces utilized in electrochemistry are coated with optical and electrical materials using reactors for chemical vapor deposition featuring a revolving disc flow. These effective reactors require laminar gas pour near the top for further deposition. The breakdown of the laminar border line sheet, absolute instability, and straight spatial and chronological timbre are all investigated in this work. Mahmood et al.[1] deliberates the entropy creation phenomenon for a This paper will provide a complete examination of 3-dimensional way of MHD stagnation point pour across a stretched surface with nonlinear thermal radiation. The present study examines the Anisotropic slip properties of carbon nanotubes in suspension will be investigated using a nanofluid. Hamza et al.[2]

illustrated the-time-dependent mixed convection flow in a vertical duct involving an heat releasing liquidas influenced by MHD. Navier's slip conditions and convective heating are carrying into account. Syed Tauseef et al.[3] deliberates the Buongiorno's model is employ to demonstrate the mass and heat transport of a nanofluid waving in excess of a quickly moving flat shield. Since the results of thermophoresis and Brownian motion on the volume fraction of nanoparticles are passively rather than actively regulated at the boundary, this study differs from some of the earlier investigations. Tousif Iqra et al. [4] illustrates the ensuing temporary rotating gadget in boundary level layer flow caused by thelinear convective instability for a forced axial flow in isotropic and anisotropic surface roughness with nanofluid MHD. Saquib Ul Zaman et al. [5] described MHD and radiation attacks in the Williamson nanofluid wave flow through a thin cylinder. Various assumptions about density, viscosity, , and thermal conductivity are used to analyse the mass and heat transport. Xiyan Tian et al.[6] deliberates the unique qualities of magnetohydrodynamic (MHD) micropolar fluid include lightness, heat, magnetic characteristics, and more. It has a great deal of application. A micropolar fluid is used to explore the properties of mass, heatand flow convert in an MHD micropolar nanofluid border line sheet beyond a exordinary expanding shield. Munirah Aali Alotaibi and Shreen El-Sapa [7] illustrated, the steady state pour of an Constant density flow pair pressure liquid inside of analytically studying two spheres that are inside each other. analysed un this paper. Translation proceeds at a constant speed outside the solid sphere and at a uniform speed inside. Esraa et al.[8] deliberates the Industrial perspectives on the pour behaviour of non-Newtonian liquids. Non-Newtonian liquids are necessary for a variety of Industrial along with technical procedures along with making polymer pages producing paper and making photographic films.

Salahuddin [9] illustrated the incompressible, two-dimensional Williamson fluid magnetohydrodynamic flow across a stretched sheet. Double Stratification and thickening due to friction are considered account while analysing the Cattaneo-Christov warmth and attentiveness pour. Chen et al.[10] discussed the manipulate of the induced attractive meadow (IMF) and Cattaneo-Christov duel diffusion on a Maxwell ternary flow nanofluid flow at its stagnation point. Superior massand heat transport of Maxwell ternary nanofluid mixed with duel dispersal and IMF is studied using a original border line constitution through the obnormal attractive reactance. Felipe Angeles[11] illustrated the heat flux's objective Cattaneo-type extension coupled to the space time equations of motion of a viscous compressible fluid. The quasilinear version of these equations is used to determine which of the provided heat flux formulations permits the hyperbolicity of the system. For the Cauchy issue of such a framework of equations to be considered physically acceptable, this property is required .Hussain et al. [12] deliberates the There are numerous industrial and technological applications for bioconvection utilising nanomaterials. Modern nanofluids provide a dynamic means of shedding light on industrial and engineering issues pertaining to heat transport systems. Because mass remodelling and collaboration are becoming more commonplace in various microsystems, bioconvection finds several uses in bio-micro-systems. The astonishing and fascinating trend known as bioconvection is caused by the hydrodynamic instability of the microbes in the

medium, which causes the microorganisms to rotate and increase the fluid's density [13], [14], [15], [16], [17].Nisar et al.[18] deliberates the MHD Considering gyrotactic bacteria, the bioconvection peristaltic activity of Sisko nanofluid is examined. Flexible conduitis subjected to partial slip characteristics.In their discussion of the crown cavity's modified nanoliquid flow mediated by bioconvection (Cu–Al2O3–TiO2) and H2O.Rashid et al. [19] take into account the influence of gyrotactic microorganisms. A modified nonliquid, oxytactic bacteria, and a square obstruction are present in the crown cavity where the bioconvection flow is studied.Riaz Khan et al.[20] deliberates the A model of a porous radiative stretched surface is used to study the concentration and temperature transmission via a viscous nanofluid in a Time-dependent slip flow of bioconvection. The beginning of a suspension's bio-thermal convection include radiation and velocity slip, as well as gyrotactic bacteria and nanoparticles. Rao et al. [21] deliberates the Fluid velocity is deprecated by the porosity coefficient and Forchheimer numbers, while fluid temperature is improved by the Eckert number and concentration decreases with increasing chemical reaction coefficient. Faisal Shah et al. [22] Peristaltic transport of nanofluid with temperature dependent thermal conductivity: a numerical study. Faisal Shah et al. [23] illustrates Non-similar analysis of the Cattaneo-Christov model in MHD second-grade nanofluid flow with Soret and Dufour effects. Faisal Shah et al. [24] illustrates Nonclassical Transport Laws in Third-Grade Nanoliquid Flow on a Stretchable Surface: A Novel Approach Incorporating Soret and Dufour Effects. Faisal Shah et al. [25] describes Entropy optimization in a fourth grade nanofluid flow over a stretchable Riga wall with thermal radiation and viscous dissipation, International Communications in Heat and Mass Transfer. Faisal Shah et al. [26] illustrates Modeling and computational analysis of 3D radiative stagnation point flow of Darcy-Forchheimer subject to suction/injection, Computer Methods and Programs in Biomedicine. Faisal Shah et al. [27] illustrates Heat transfer analysis on MHD flow over a stretchable Riga wall considering Entropy generation rate: A numerical study. Faisal Shah et al. [28] describes Analytical investigation on the combined impacts of the Soret and Dufour phenomenon in the forced convective flow of a non-Newtonian nanofluid by the movable Riga device**.** Faisal Shah et al. [29] illustrates Non-similar analysis of two-phase hybrid nanofluid flow with Cattaneo-Christov heat flux model: a computational study**.** M. Ijaz Khan et al. [30] describes First order chemical reaction response in mixed convective Falkner-Skan Sutterby fluid with Cattaneo-Christov heat and mass flux model. The surface friction drag is found to be deprecated by the Weissenberg and Forchheimer values. The mass transfer rate is significantly positively correlated with the Schmidt coefficent and chemical reaction.

Considering the aforementioned fascinating uses of microorganisms and Cattaneo-Chrystov heat flux, this revise observes the mass and temperature transport analysis of a viscous liquid in an uneven state MHD bio-convection trip sequence flow over a porous radiative stretching surface that is affected by both the heat and mass suction.The study's primary goal, improving the thermal profile, is achieved by the use of nanoparticles, while gyrotactic microorganisms produce bio-convection to enhance mass transfer. Using MATLAB's bvp4c approach, the following nonlinear ODEs have been numerically solved. The current unstable flow issue caused by radiation, porosity effects, convective mass and heat

transfer, and velocity slip is entirely new and has not been treated previously, according to the authors' literature survey. Also taken into consideration is the possibility of a attractive behaviour meadow around the temperature resource, which improves the literature's accuracy. This fascinating breakthrough could be applied to better heat transmission and the production of electro-conductive machinery. Graphic representations of the results are provided for temperature, velocity, concentration of nanoparticles, friction drag, rate of temperature transportation, local Sherwood coefficient, and thickness of motile microbes.Engineering thermal processes and industrial settings involving heat transfer can benefit from the theoretical understandings gathered from this study. The results that have been presented have possible nodes in the fields of solar systems, temperature machines, energy generation, mechanized procedure, and heating and cooling processes.

5. Mathematical Formulation

We study the time-dependent, viscous two-dimensional bio-convection slip flow across a absorbent radiative extended exterior at the origin (x = 0, y = 0), as exposed graphically in Figure 1.The exordinary sheet is positioned close to the horizontal-axis, and the verticle-axis capturedat right angles to the sheet. An intensity-dependent time-aligned attractive flux is

$B(t) = \frac{B_0}{(1-\in t)^{1/2}}$ about an acute angle β governs the electrically conductive nanofluid. Additionallythe surface and stream free velocities are thought to be shifting from a stagnation point, which is described as $U_w(x,t) = \frac{ax}{1-\in t}$ and $U_e(x,t) = \frac{bx}{1-\in t}$, where $\in$, a and b are positive constants with the proportion of t^{-1}. The term $\frac{a}{1-\in t}$ illustrates the initial stretching and the stretching's effective rate. The term $\frac{\partial u}{\partial y}$ and $V_w(x,t) = \frac{-V_0}{\sqrt{1-\in t}}$ are independently altered to show the suction and slide velocities. The sheet's radiative heat flux q_r is taken into accountand coefficient of internal heat generation $Q_t = \frac{Q_0}{1-\in t}$, where Q_0 symbolises the heat source's initial value (heat generation coefficient). The governing constitutions of the boundary layer flow have been determined as [20] after taking into account the previously described circumstances.

United International Journal of Multidisciplinary Research
ISSN: 3048-6726 (UIJMR) Impact Factor: 6.934 (SJIF)
An International Peer-Reviewed and Refereed Multidisciplinary Journal
Website: www.uijmr.in | Volume 3 | Special Issue 5 | March | 2026

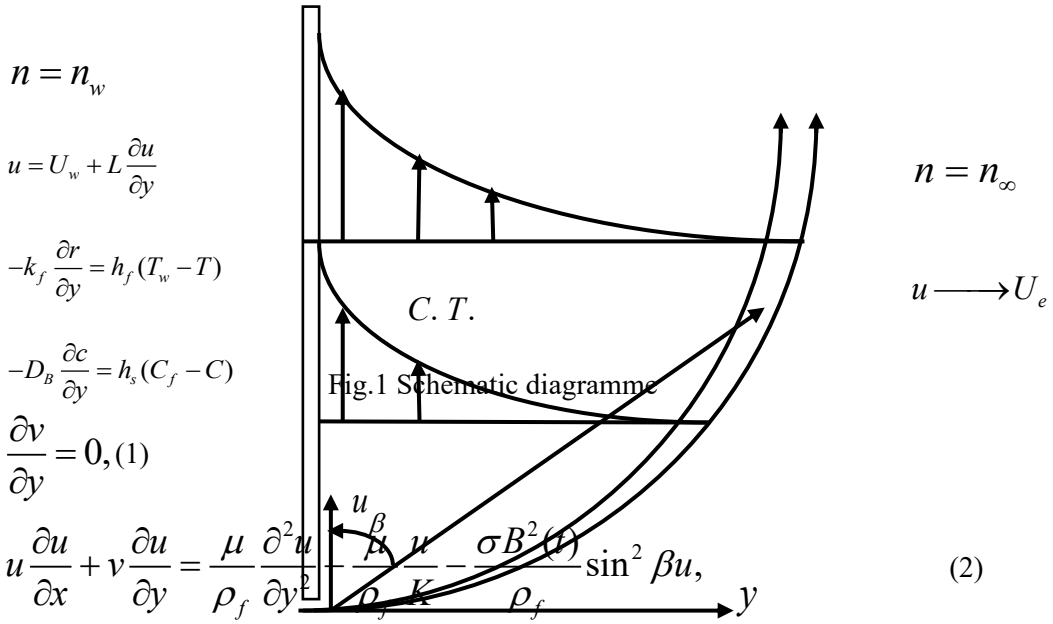

Fig.1 Schematic diagramme

$$\frac{\partial u}{\partial x} + \frac{\partial v}{\partial y} = 0, \quad (1)$$

$$\frac{\partial u}{\partial t} + u\frac{\partial u}{\partial x} + v\frac{\partial u}{\partial y} = \frac{\mu}{\rho_f}\frac{\partial^2 u}{\partial y^2} - \frac{\mu}{\rho_f}\frac{u}{K} - \frac{\sigma B^2(t)}{\rho_f}\sin^2\beta u, \quad (2)$$

$$\frac{\partial T}{\partial t} + u\frac{\partial T}{\partial x} + v\frac{\partial T}{\partial y} = \frac{k}{(\rho Cp)_f}\frac{\partial^2 T}{\partial y^2} - \frac{1}{(\rho Cp)_f}\frac{\partial q_r}{\partial y} + \frac{Q_t}{(\rho Cp)_f}(T - T_\infty) +$$

$$\lambda_1\left(\begin{array}{l} u^2\frac{\partial^2 T}{\partial x^2} + v^2\frac{\partial^2 T}{\partial y^2} + 2uv\frac{\partial^2 T}{\partial y \partial x} + u\frac{\partial u}{\partial x}\frac{\partial T}{\partial x} + \\ u\frac{\partial v}{\partial x}\frac{\partial T}{\partial y} + u\frac{\partial u}{\partial y}\frac{\partial T}{\partial x} + v\frac{\partial v}{\partial y}\frac{\partial T}{\partial y} \end{array}\right) \quad (3)$$

$$\frac{\partial C}{\partial t} + u\frac{\partial C}{\partial x} + v\frac{\partial C}{\partial y} = D_M\frac{\partial^2 C}{\partial y^2} + D_T\frac{\partial^2 T}{\partial y^2} - K_c\left(C - C_\infty\right) \quad (4)$$

$$\frac{\partial n}{\partial t} + u\frac{\partial n}{\partial x} + v\frac{\partial n}{\partial y} = -\frac{cW_c}{C_f - C_\infty}\frac{\partial}{\partial y}\left(n\frac{\partial C}{\partial y}\right) + D_m\frac{\partial^2 n}{\partial y^2} \quad (5)$$

The planned border line constitutions for the above prototype are explained as [20].

$$u = U_w(x,t) + L\frac{\partial u}{\partial y}, v = V_w(x,t), -\kappa\frac{\partial T}{\partial y} = h_f(T_w - T), -D_B\frac{\partial C}{\partial y} = h_s(C_f - C), n = n_w aty = 0$$

$$u \to U_e(x,t), T \to T_\infty, C \to C_\infty, n \to n_\infty asy \to \infty \quad (6)$$

Equations (2)–(6) above, $K = k_1(1-\in t)$ defines the permeability of a porous media, where k_1 denotes the permeability The terms $\mu, \rho_f, \sigma, k, C_p, (\rho C_p)_p, (\rho C_p)_f, D_T, D_b, D_m, W_c, c$ accordingly refers to the maximum swimming cell speed, the ability of bacteria to diffuse
, the viscosity of the fluid in which the nanoparticles and microorganisms are suspended, density, detailed temperature, temperature capability of the nanoparticles,, thermal conductivity , electrical conductivity coefficient, and fluid heat capacity.furthermore, T, C with n symbolized the warmth, the attentiveness, with the density of microorganisms, respectively.These T, C, and n are illustrated away from the wall, they are $T_\infty, C_\infty, n_\infty$ respectively.The velocity's slip factor is shown by $L = \lambda\sqrt{1-\in t}$ The surface has a temperature of T_w because the third border line circumstance, which as well specifies the temperature transport coefficient h_f, causes hot fluid to convect If one ignores viscous dissipation, then the term $q_r = \dfrac{-16\sigma^* T_\infty^3}{3k^*}\dfrac{\partial T}{\partial y}$. is produced when the Rosseland approximation is taken into account, where σ^* and k^* stand for the Stefan-Boltzmann stable as well as the mean amalgamation coefficient, correspondingly. It is necessary to take into account the warmth differential in the pour inner in a way that T^4 allows Taylor's series to be expanded T_∞.

;

Leaving out the higher order words, we are attainment $T^4 \approx 4T_\infty^3 T - 3\sigma^* T_\infty^4$,Accordingly, we can get $q_r = \dfrac{-16\sigma^* T_\infty^3}{3k^*}\dfrac{\partial T}{\partial y}$. Thus Eqn. (3) becomes

$$\frac{\partial T}{\partial t} + u\frac{\partial T}{\partial x} + v\frac{\partial T}{\partial y} = \frac{k}{(\rho Cp)_f}\frac{\partial^2 T}{\partial y^2} + \frac{1}{(\rho Cp)_f}\frac{16\sigma^* T_\infty^3}{3k^*}\frac{\partial^2 T}{\partial y^2} + \frac{Q_t}{(\rho Cp)_f}(T - T_\infty) +$$

$$\lambda_1\left(\begin{array}{l} u^2\dfrac{\partial^2 T}{\partial x^2} + v^2\dfrac{\partial^2 T}{\partial y^2} + 2uv\dfrac{\partial^2 T}{\partial y \partial x} + u\dfrac{\partial u}{\partial x}\dfrac{\partial T}{\partial x} + \\ u\dfrac{\partial v}{\partial x}\dfrac{\partial T}{\partial y} + u\dfrac{\partial u}{\partial y}\dfrac{\partial T}{\partial x} + v\dfrac{\partial v}{\partial y}\dfrac{\partial T}{\partial y} \end{array}\right) \qquad (7)$$

The kindred for u, v, T, C, n are known through

$$u = U_w = \frac{ax}{(1-\in t)}, v = V_w = \frac{-V_0}{\sqrt{1-\in t}}, T_w = T_\infty + T_0 \frac{bx}{2v_f(1-\in t)^2}, C_w = C_\infty + C_0 \frac{bx}{2v_f(1-\in t)^2},$$

$$n_w = n_\infty + n_0 \frac{bx}{2v_f(1-\in t)^2}, u = U_e = \frac{bx}{(1-\in t)}$$

(8)

Where $a, b, \in, T_0, C_0, n_0$ are constants

We know the introduce different similarity variables are:

$$\psi = \sqrt{\frac{bv_f}{(1-\in t)}} xf(\eta), \eta = \sqrt{\frac{b}{v(1-\in t)}} y, T = T_\infty + T_0 \frac{bx}{2v_f(1-\in t)^2} \theta(\eta), C = C_\infty + C_0 \frac{bx}{2v_f(1-\in t)^2} \varphi(\eta),$$

$$n = n_\infty + n_0 \frac{bx}{2v_f(1-\in t)^2} h(\eta)$$

(9)

The velocity constitutions are given by

$$u = \frac{bx}{(1-\in t)} f'(\eta), v = -\sqrt{\frac{bv_f}{(1-\in t)}} f(\eta) \quad (10)$$

Considering the relationships between equations (9) and (10), (1)–(7) becomes

$$f''' - (f')^2 + ff'' - A\left(\frac{\eta}{2} f'' + f'\right) - \frac{1}{D} f' - M^2 \sin^2 \beta f' = 0 \quad (11)$$

$$\left(1 + \frac{4}{3} Rd\right)\theta'' + \Pr\left\{f\theta' - f'\theta - \frac{A}{2}(\eta\theta' + 4\theta) + Q\theta\right\} + \quad (12)$$

$$\delta_1(f'^2 - ff'\theta' - ff''\theta) = 0$$

$$\varphi'' + ScSr\theta'' + Sc(f\varphi' - \varphi f') - \frac{A}{2}(\eta\varphi' + 4\varphi) = 0 \quad (13)$$

$$h'' + Sb(fh' - hf') - \frac{A}{2} Sb(\eta h' + 4h) - Pe(\varphi' h' + h\varphi'') = 0 \quad (14)$$

The following dimensionless boundary conditions can be created by transforming the boundary conditions (6):

$$f'(0)=\lambda_1+\lambda_2 f''(0), f(0)=S, \theta'(0)=-Bi(1-\theta(0)), \varphi'(0)=-Nd(1-\varphi(0)), \quad (15)$$
$$h(0)=1, f'(\eta)=1, \theta(\eta)=0, \varphi(\eta)=0, h(\eta)=0 as \eta \to \infty$$

In the formulas above $M^2=\frac{\sigma_f B_0^2}{b\rho_f}$ identifies the hatmann number, $D=Da_x \operatorname{Re}_x=\frac{bk_1}{\nu_f}, Da_x=\frac{\kappa}{x^2}=\frac{k_1(1-\in t)}{x^2}$ illustrates darcy coefficient, $A=\frac{\in}{b}$ deliberates unsteadiness coefficient, $Rd=\frac{4\sigma^* T_\infty^3}{kk^*}$ deliberates the radiation coefficient, $\Pr=\frac{\nu_f}{\alpha}$ signifies prandtl number, $\delta_1=\lambda_1\frac{U}{\nu}$, $Q=\frac{Q_0}{b(\rho c_p)}$ signifies heat source parameter, $Sc=\frac{\nu_f}{D_B}$ similarly represents Schmidt number, $Sb=\frac{\nu_f}{D_m}$ represent bio convection schmidt coefficient, $Pe=\frac{bW_c D_m}{\nu_f^2}$ represents the Peclet coeffient, $S=\left(\frac{V_0}{\sqrt{b\nu_f}}\right)\succ 0$ symbolized the suction coefficient, $\lambda_1=\frac{b}{a}$ symbolized the expanding coefficient, $\lambda_2=L\sqrt{\frac{b}{\nu_f}}$ signifies speed slide parameter, $Bi=\frac{h_f}{k}\sqrt{\frac{\nu_f}{b}}$ symbolized Biot component, $N_d=\frac{h_s}{D_B}\sqrt{\frac{\nu_f}{b}}$ symbolized convection dispersal constraint,

The researchers have defined the skin friction coefficient local Nusselt number Sherwood number and local density number of moving microorganisms.

$$C_{fx}=\frac{\tau_w}{\frac{1}{2}\rho_f U_w^2}, Nu_x=\frac{xq_w}{k_f(T_f-T_\infty)}, Sh_x=Sh=-\frac{x}{(C_w-C_\infty)}\left(\frac{\partial C}{\partial y}\right)_{y=0} \quad (16)$$
$$Nn_x=-\frac{x}{(C_w-C_\infty)}\left(\frac{\partial n}{\partial y}\right)_{y=0}$$

where τ_w deliberates local wall shear stress, q_w is illustrate local temperature flux, q_m is the mass flux coefficient and q_n is the microorganism coefficient flux, This can be shown as.

$$\tau_w = \mu \frac{\partial u}{\partial y}|_{y=0}, q_w = -k \frac{\partial T}{\partial y}|_{y=0} + (q_r)_w, Sh = -\frac{x}{(C_w - C_\infty)} \left(\frac{\partial C}{\partial y} \right)_{y=0}$$

$$Nn_x = -\frac{x}{(C_w - C_\infty)} \left(\frac{\partial n}{\partial y} \right)_{y=0} \quad (17)$$

Utilising the unpredictable listed in Equations 9 as well as 10, system (16) as well as (17) together yield system (18), as shown below.

$$C_{fx} = \sqrt{\mathrm{Re}_x} C_f = f''(0),$$

$$Nu_x = \frac{Nu}{\sqrt{\mathrm{Re}_x}} = -(1 + \frac{4}{3} Rd)\theta'(0),$$

$$Sh_x = \frac{Sh}{\sqrt{\mathrm{Re}_x}} = -\phi'(0), \quad (18)$$

$$Nn_x = \frac{Nn}{\sqrt{\mathrm{Re}_x}} = -h'(0)$$

In (18) $\mathrm{Re}_x = \frac{U_w^2}{a\nu_f}$ represents the local Reynolds number

6. Numerical Solution

In this partthe non-linear ordinary differential equations (11) to (14) with respectto the border line circumstances (15) is The problem was solved by using the R-K method with MATLAB software. This process engages changing a border line value problem into an preliminary value problem.

$$f = y_1, f' = y_2, f'' = y_3$$

$$f''' = (y_2)^2 - y_1 y_3 + A\left(\frac{n}{2} y_3 + y_2 \right) + \frac{1}{D} y_2 + M^2 \mathrm{Sin}^2 \beta y_2$$

(19)

$$\theta = y_4, \theta' = y_5$$

$$\theta'' = \frac{1}{(1 + \frac{4}{3} Rd)} \left[-\mathrm{Pr} \left\{ f y_5 - y_2 y_4 - \frac{A}{2} \right\} (\eta y_5 + 4 y_4) + Q y_4 \right] - d_1 \left(y_2^2 - y_1 y_2 y_5 - y_1 y_3 y_4 \right)$$

(20)

$$\phi = y_6, \phi' = y_7$$

$$\phi'' = -ScSr\,\theta'' - Sc(y_1 y_7 - y_6 y_2) + \frac{A}{2}(\eta y_7 + 4y_6) \tag{21}$$

$$h = y_8, h' = y_9$$

$$h'' = -Sb(y_1 y_9 - y_8 y_2) + \frac{A}{2} Sb(\eta y_9 + 4y_8) + Pe(y_7 y_9 + y_8 \phi)$$

The suitable boundary conditions are:

$$y_2 = \lambda_1 + \lambda_2 y_3, y_1 = s, y_5 = -Bi(1 - y_4), y_7 = -Nd(1 - y_6)\ at\ \eta \to 0 \tag{23}$$

$$y_8 \Rightarrow 1, y_2 \Rightarrow 1, y_4 \Rightarrow 0, y_6 \to 0\ at\ \eta \to \infty$$

To solve the equations (19)-(22) we have used the values of y_3, y_5 and y_7 which are not given at the initial conditions. So later finding the initial conditions are integrated by using R-K method with the successive iterative step length is 0.01.

Validation of results

To ensure the quality and dependability of the results, it is crucial to verify them in contrast to established remedies or experimental findings once the bvp4c solver has converged. In order to increase trust within the numerical solution and make sure it correctly depicts the physical system that is being investigated, this validation step is essential. In Table 1, which compares the current work to Rao et al. [21], the validation is displayed.

7. Results and Discussion

In this part, we've used the MATLAB built-in package bvp4c to provide the graphical outcomes of constitutions 11–14 along with the boundary circumstances (15). The results obtained were verified by contrasting them with the published findings of other publications in the books; the validation is displayed in Table 1. Fig. 2 shows the result in response to the velocity profile's increase. The result is two graphs, one showing the existence of the slip condition and the other not. An rise in λ1 indicates greater stretching along the x axis, which causes a rise in. Because the enlarge lessens the thick effect on the pour, the momentum boundary layer's thickness diminishes and increases as a result. Fig. 3 discusses the effect of the magnetic field's angle of inclination on demonstrating a diminishing effect. This is because a higher angle of inclination results in a greater at right angles power acting on the nanofluid pour, which in turn lowers the swiftness. As seen in Fig. 4, an raises in the magnetic field constraint also results in a reduces in fluid flow. It occurs as a result of developing Lorentz forces, which create confrontation to the fluid's speed. The injecting effect is indicated by the suction parameter's positive values. As seen in Fig. 5, the

nanofluid pours quicker and through an enhanced speed as a result of this inserting power in the way of the pour. Furthermore, we can observe that the border thickness is lower for Figs. 2 and 5, but larger for Figs. 3 and 4. In contrast, it is more in the lack of a slip situation as well as less in the occurrence of one. As a result, when the velocity slip parameter rises, the flow resistance falls and increases, lowering the skin friction coefficient. The collision of non-dimensional temperature recreation time constraint (δ_1) observed on Fig. 6 through enhancing values of outcome is reduced. The Biot number (Bi_1),This is intimately connected to the coefficient of temperature transport,is the result of convective heat transfer. Therefore, as appears in Fig. 7, a go up in also results in an uplifted in the coefficient of temperature transmission, which raises the warmth. Fig. 8 deliberates the collision of the Prandtl number on the activation. We recognised in the portrait that the portraits are enhanced with the enhancing values of the Prandtl number. It is also recognised in this plot that the portraits diminished with diminishing values of extending parameter. Figure 9 shows that when the number of Peclets increases, the cells begin to move more quickly, increasing the density of the material. As demonstrated in Fig. 10, the density of the microorganisms decreases dramatically when the diffusivity is inversely related to the Schmidt coefficient.It has been discovered that when slip effects are present, microbe concentrations are produced at greater levels but when they are absent, microorganism concentrations are minimised. Results were obtained for values of both the same and opposite .The pattern of for the optimistic outcomes of $A = 2.5$ is shown by the Red row, while the outline for the negative values of $A = 2.5$ is shown by the green line. It is evident from the two scenarios that is more potent for negative values of .Furthermore, as can be observed in Figs. 11 loses power as improves . Similarly, *Nu* correspondingly decreases as well as grows through the enhancement of as seen in Fig. 12. The reason for this is that it lessens the gradient in surface temperature diminished and respectively, improve, as seen in Fig 13. It is evident from the two scenarios that has greater power for A's negative values than for its positive values. Additionally, when A is present, Nn is greater for the insignificant slip effect and less for the strong slip effects ,negative, even if the positive values of A show the opposite behaviour.

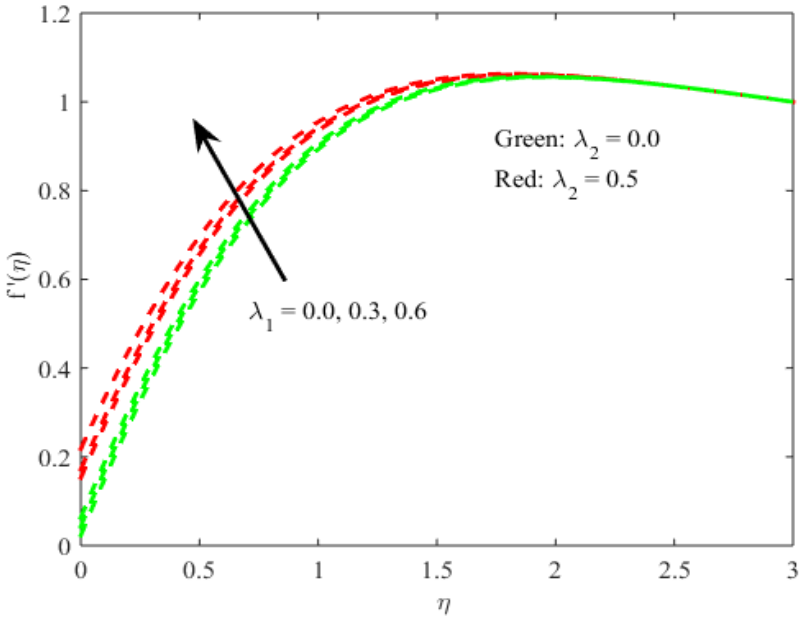

Fig.2performance of on velocity profile

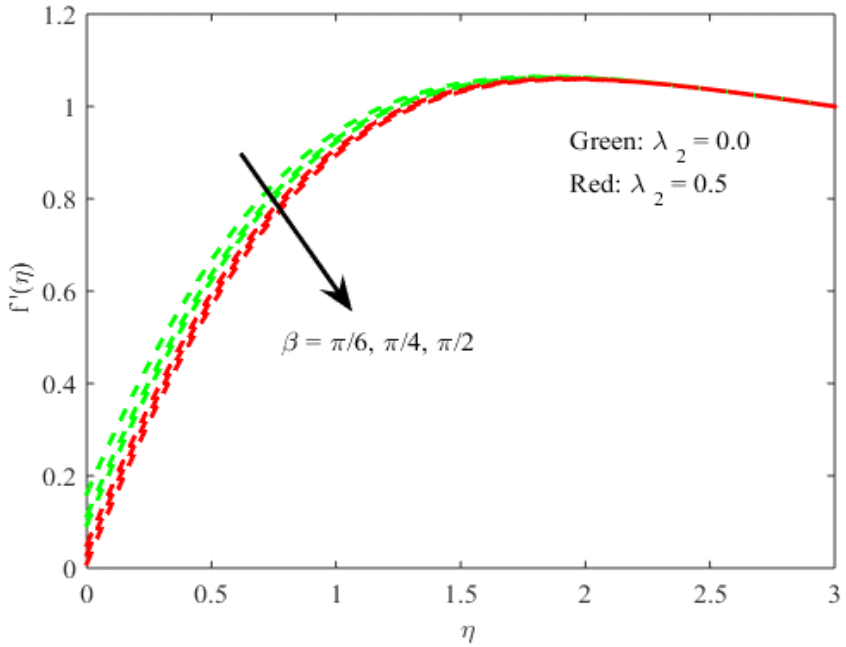

Fig.3 performance of on speed profile

United International Journal of Multidisciplinary Research
ISSN: 3048-6726 (UIJMR) Impact Factor: 6.934 (SJIF)
An International Peer-Reviewed and Refereed Multidisciplinary Journal
Website: www.uijmr.in | Volume 3 | Special Issue 5 | March | 2026

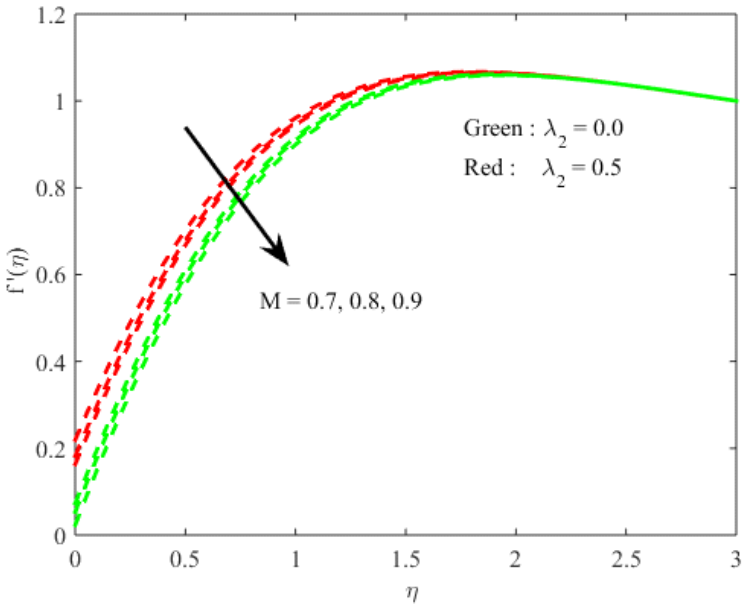

Fig.4 performance of on speed profile

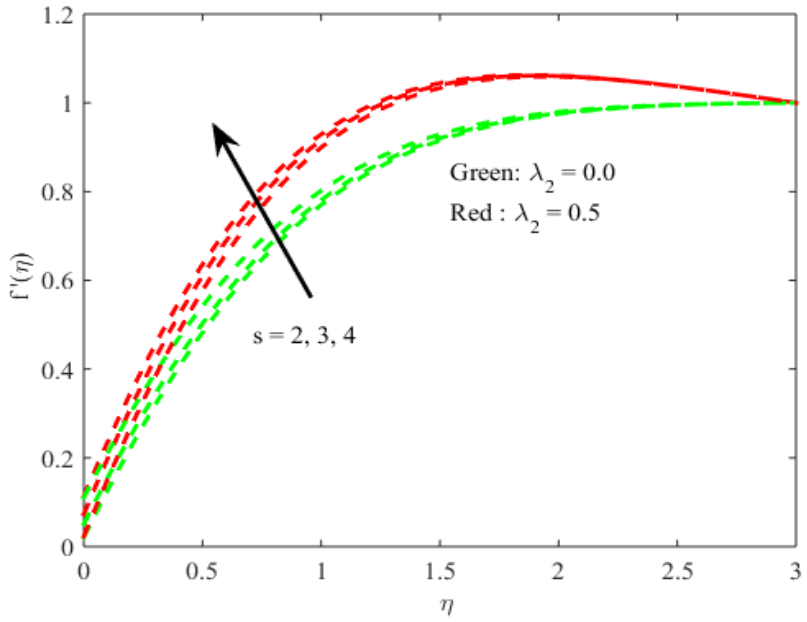

Fig.5 performance of on speed profile

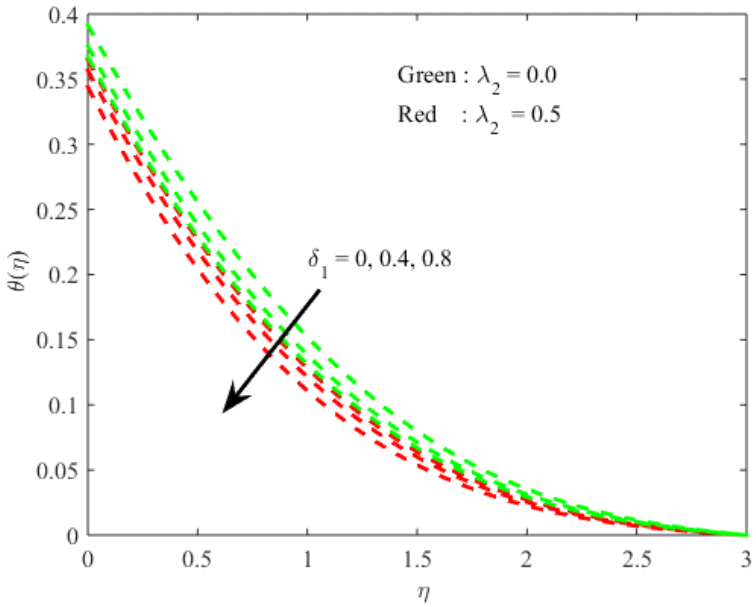

Fig.6 Performance of δ_1 on temperature profile

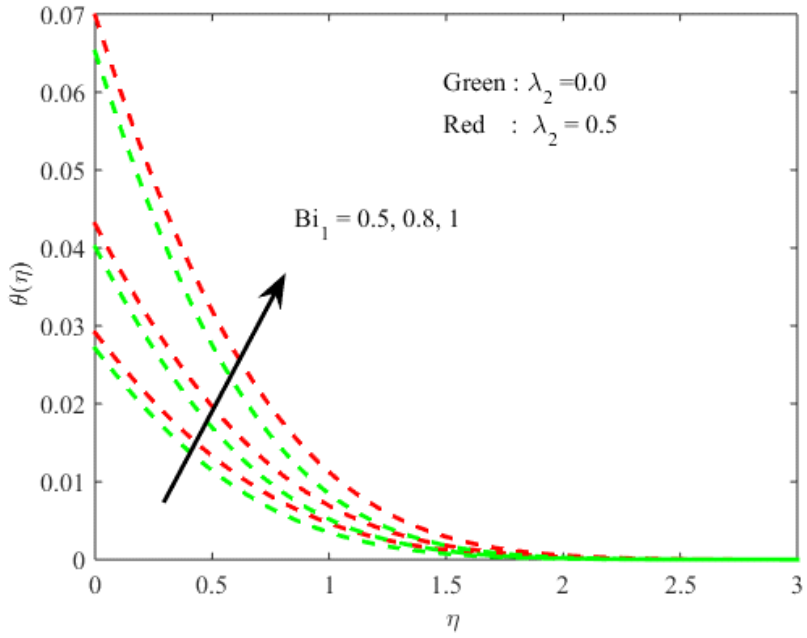

Fig.7 Performance of Bi_1 on temperature profile

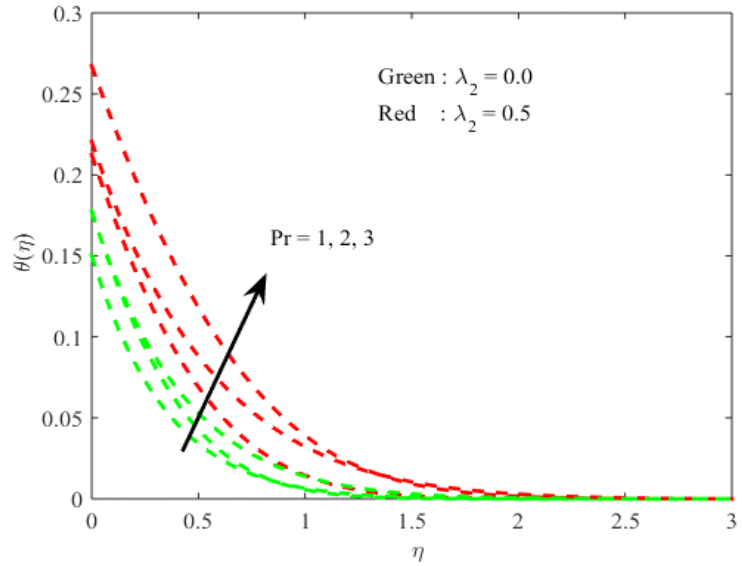

Fig.8 Performance of Pr on temperature profile

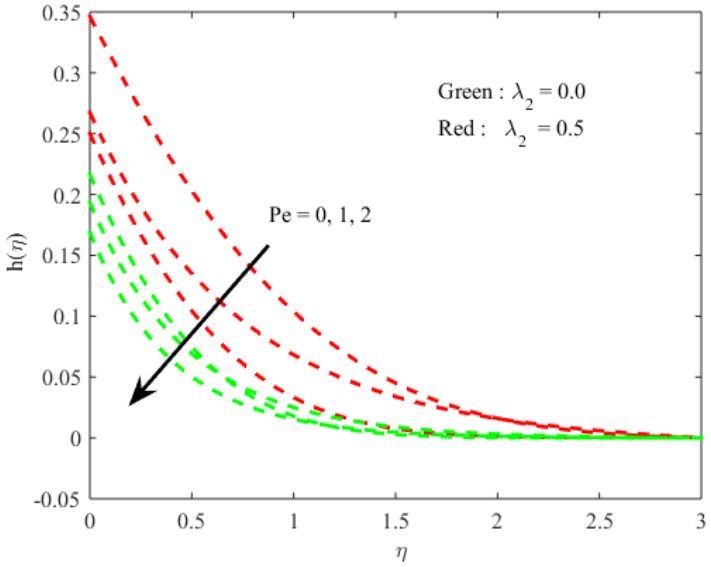

Fig.9 Performance of $\mathrm{P}e$ on $h(\eta)$

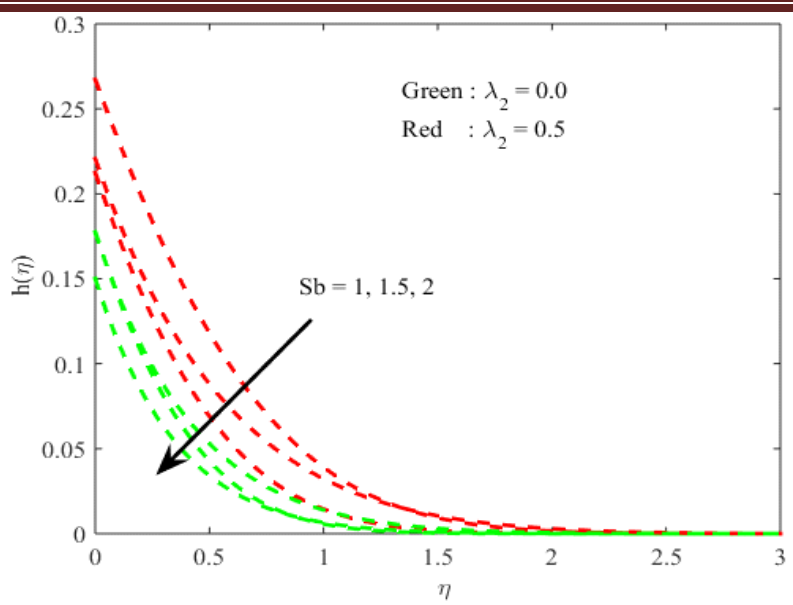

Fig.10 Performance of Sb on $h(\eta)$

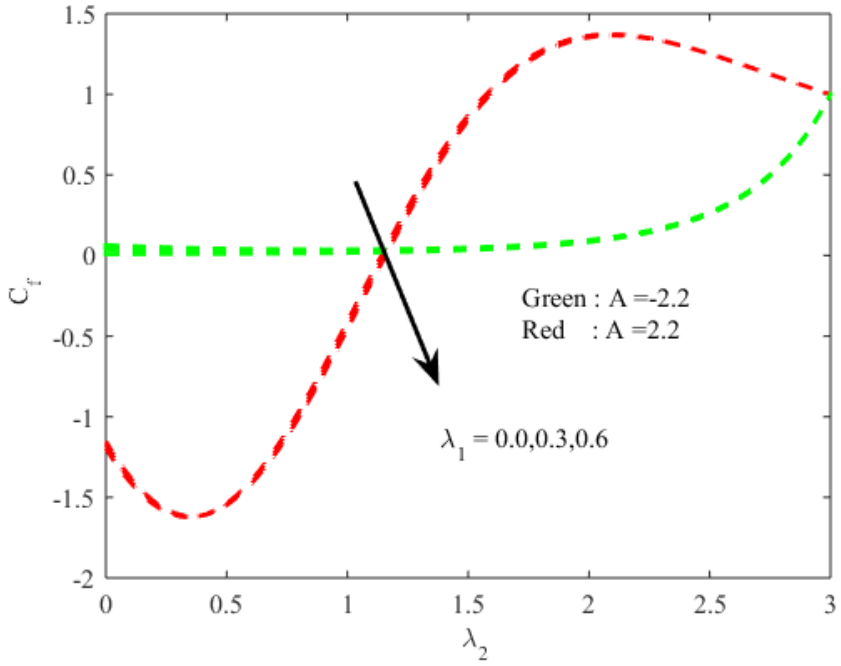

Fig.11Skin friction coefficient Cf match up to various values of $\lambda 1$ and A against $\lambda 2$.

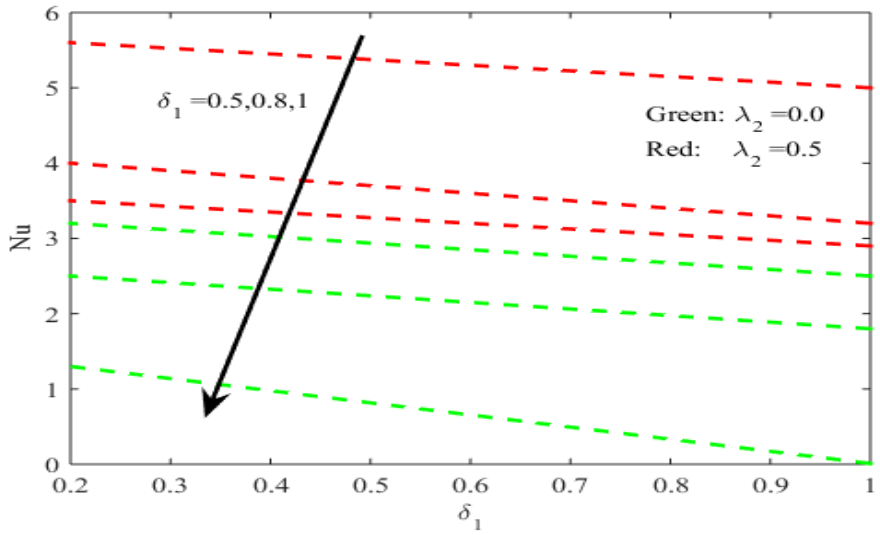

Fig.12 Nusselt number compared to various values

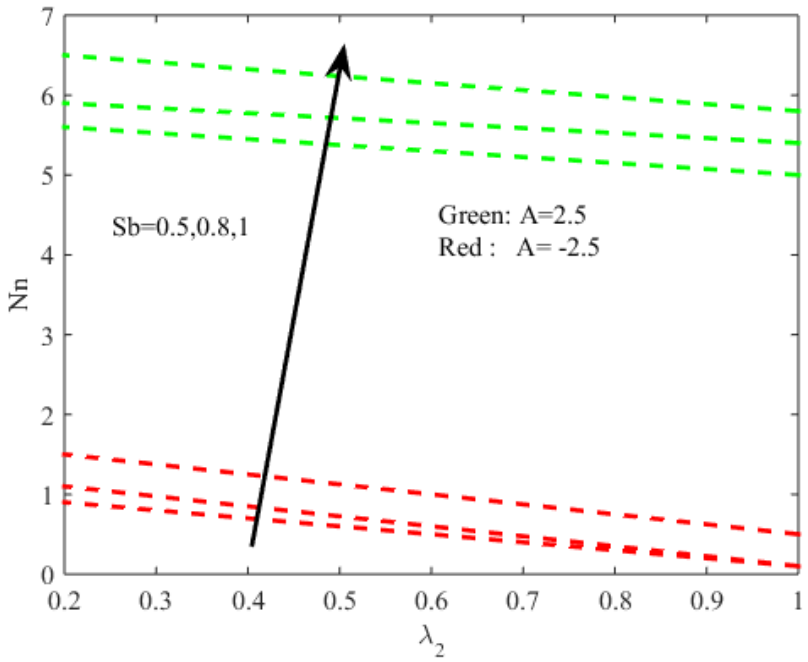

Fig.13 Nn compared to various values

Table:1 Comparison of skin friction coefficient values $-f''(0)$ with previous results :

	Riaz Khan et al. [20]	Rao et al.[21]	Present
1	1.000102	1.000000	1.000554
2	1.522235	1.522729	1.570098
3	1.923655	1.923612	1.981134
4	2.260669	2.260783	2.312245

Table:2 Computed values for skin friction coefficient, Nusselt number and Sherwood number for a variety of values of the important governing constraints

A	M	Rd	Pr	Q	δ	Sc	Sr	Sb	Pe	λ	λ_2	Bi	Nd	$-f''(0)$	$-\theta'(0)$	$-\phi'(0)$	$-h'(0)$
0.5														0.28825	0.12003	0.18205	0.16578
1														0.29950	0.12838	0.18305	0.16627
1.5														0.30012	0.15986	0.18330	0.16659
	0.5													0.55478	0.11233	0.18386	0.16678
	0.8													0.60807	0.10125	0.18386	0.16739
	0.9													0.62814	0.09872	0.18386	0.16789
		0.8												0.32224	0.05098	0.20508	0.16834
		1.2												0.38148	0.10875	0.20508	0.16878
		1.5												0.40108	0.15605	0.20509	0.16945
			0.5											0.19375	0.10004	0.18365	0.16993
			0.8											0.19375	0.09874	0.18365	0.17152
			1.											0.1937	0.0889	0.1836	0.1719

			2										5	2	6	1
				0.6									0.27375	0.15783	0.20243	0.17256
				0.7									0.28375	0.16807	0.30156	0.17499
				0.8									0.30001	0.18880	0.35128	0.17450
					0.3								0.28825	0.12003	0.18205	0.17541
					0.5								0.28825	0.11004	0.15682	0.17610
					1.0								0.28825	0.10006	0.10089	0.17690
						0.5							0.63255	0.19307	0.57137	0.17890
						1.0							0.63100	0.20001	0.57148	0.17999
						1.5							0.63000	0.21506	0.58100	0.18000
							0.09						0.28829	0.12138	0.18305	0.18123
							0.5						0.28830	0.11003	0.17306	0.18231
							1.0						0.28831	0.10004	0.15007	0.18351
								1.0					0.62953	0.20043	0.54792	0.18456
								1.5					0.61000	0.18894	0.55008	0.18798
								2.0					0.60001	0.16800	0.58001	0.18859
									0.5				0.64651	0.15792	0.59808	0.18899
									0.9				0.64651	0.16892	0.51234	0.19150
									1.				0.6465	0.2008	0.5012	0.1928

									5					1	1	3	9
										0.7				0.65001	0.12001	0.18101	0.19354
										0.9				0.65241	0.12003	0.18205	0.19547
										1.2				0.65291	0.12838	0.18305	0.19678
											1.5			0.30012	0.15986	0.18330	0.19764
											1.9			0.55478	0.11233	0.18386	0.19837
											2.0			0.60807	0.10125	0.18386	0.19894
												2.0		0.62814	0.09872	0.18386	0.20001
												2.3		0.32224	0.05098	0.20508	0.20453
												2.5		0.38148	0.10875	0.20508	0.22364
													0.2	0.40108	0.15605	0.20509	0.23462
													0.5	0.19375	0.10004	0.18365	0.27863
													1.1	0.19375	0.09874	0.18365	0.28743

8. Conclusion

- The velocity $f'(\eta)$ increases as λ_1 and S accumulate, but it decreases as β and M scale up, respectively.
- The $\theta(\eta)$ shoot ups with the collective values of , Q as well as β respectively.
- The concentration φ(η) gets stronger, and when Sc values increase, it decreases.
- The concentration of microorganism $h(\eta)$ is strengthened by increasing angle β, but it is diminished by increasing Pe, Sb and Sc, respectively.

- Even if the rate of temperature transmission (Nu) is maximal for positive values of A relative to negative values, the friction drags (C_f) are more powerful for negative values of A than for positive values of A .
- While Nn decreases with the development of λ_1 and Sb, respectively, the Sherwood number Sh is magnified by the improvement of both Nd and Sc.

References

[1] Z. Mahmood, K. Rafique, U. Khan, T. Mahmood, and A. M. Hasan, "MHD unsteady flow of carbon nanotubes over nonlinear radiative surface with anisotropic slip conditions: Computational analysis of irreversibility for Yamada–Ota model," *Engineering Applications of Computational Fluid Mechanics*, vol. 18, 2024. doi: 10.1080/19942060.2024.2309139.

[2] M. M. Hamza, S. Abdulsalam, and S. K. Ahmad, "Time-dependent magnetohydrodynamic (MHD) flow of an exothermic Arrhenius fluid in a vertical channel with convective boundary condition," *Advances in Mathematical Physics*, vol. 2023, Art. ID 7173925, 2023. doi: 10.1155/2023/7173925.

[3] S. T. Mohyud-Din, U. Khan, N. Ahmed, and M. M. Rashidi, "A study of heat and mass transfer on magnetohydrodynamic (MHD) flow of nanoparticles," *Propulsion and Power Research*, vol. 7, no. 1, pp. 72–77, 2018.

[4] I. Tousif, S. Nadeem, H. A. Ghazwani, F. Z. Duraihem, and J. Alzabut, "Instability analysis for MHD boundary layer flow of nanofluid over a rotating disk with anisotropic and isotropic roughness," *Heliyon*, vol. 10, no. 6, e26779, 2024.

[5] S. U. Zaman, M. N. Aslam, M. B. Riaz, A. Akgul, and A. Hussain, "Williamson MHD nanofluid flow with radiation effects through slender cylinder," *Results in Engineering*, vol. 14, 101966, 2024.

[6] X. Tian, B. Yang, X. Na, L. Ba, and Y. Yuan, "Cross-diffusive flow of MHD micropolar nanofluid past a slip stretching plate," *Heliyon*, vol. 10, no. 5, e26958, 2024.

[7] M. A. Alotaibi and S. El-Sapa, "MHD couple stress fluid between two concentric spheres with slip regime," *Results in Engineering*, vol. 21, 101934, 2024.

[8] E. N. Thabet, A. M. Abd-All, H. A. Hosham, and S. M. M. El-Kabeir, "Cattaneo–Christov heat and mass fluxes model of Casson fluid employing non-Fourier double diffusion theories with ion slip and Hall effects," *Ain Shams Engineering Journal*, 2024. doi: 10.1016/j.asej.2024.102618.

[9] T. Salahuddin, M. A. Iqbal, A. Bano, M. Awais, and S. Muhammad, "Cattaneo–Christov heat and mass transmission of dissipated Williamson fluid with double stratification," *Alexandria Engineering Journal*, vol. 80, pp. 553–558, 2023.

[10] H. Chen, Y. Ma, M. Shen, P. He, and H. Zhang, "Significance of Cattaneo–Christov double diffusion and induced magnetic field on Maxwell ternary nanofluid flow," *Journal of Magnetism and Magnetic Materials*, vol. 587, 171264, 2023.

[11] F. Angeles, "Hyperbolic systems of quasilinear equations in compressible fluid dynamics with an objective Cattaneo-type extension for heat flux," *Mechanics Research Communications*, vol. 130, 104103, 2023.

[12] Z. Hussain, W. A. Khan, M. Irfan, T. Muhammad, S. M. Eldin, M. Waqas, and P. V. S. Narayana, "Interaction of gyrotactic microorganisms and nanoparticles in magnetized chemically reactive shear-thinning fluid," *Royal Society of Chemistry Advances*, vol. 5, no. 23, pp. 6560–6571, 2023.

[13] A. V. Kuznetsov, "Nanofluid bioconvection: interaction of microorganisms and nanoparticle distribution," *Theoretical and Computational Fluid Dynamics*, vol. 1, pp. 291–310, 2012.

[14] S. Nadeem, M. N. Khan, N. Muhammad, and S. Ahmad, "Mathematical analysis of bio-convective micropolar nanofluid," *Journal of Computational Design and Engineering*, vol. 3, pp. 233–242, 2019.

[15] M. K. Nayak et al., "3D bioconvective multiple slip flow of chemically reactive Casson nanofluid with gyrotactic microorganisms," *Heat Transfer–Asian Research*, vol. 49, pp. 135–153, 2020.

[16] N. Parveen et al., "Thermophysical properties of chemotactic microorganisms in bioconvective peristaltic rheology of nanofluid," *Case Studies in Thermal Engineering*, vol. 27, 101285, 2021.

[17] H. Waqas et al., "Falkner–Skan time-dependent bioconvection flow of cross nanofluid," *International Communications in Heat and Mass Transfer*, vol. 120, 105028, 2021.

[18] Z. Nisar, B. Ahmed, H. A. Ghazwani, K. Muhammad, M. Hussien, and A. Aziz, "Numerical study for bioconvection peristaltic flow of Sisko nanofluid," *Heliyon*, vol. 9, no. 12, e2250, 2023.

[19] U. Rashid et al., "Bioconvection modified nanoliquid flow in crown cavity with gyrotactic microorganisms," *Case Studies in Thermal Engineering*, vol. 47, 103052, 2023.

[20] M. R. Khan et al., "Numerical simulation of unsteady MHD bioconvective flow of viscous nanofluid," *Case Studies in Thermal Engineering*, vol. 53, 103830, 2024.

[21] P. C. D. Rao, S. Thiagarajan, and S. V. Kumar, "Darcy–Forchheimer flow of Ree–Eyring fluid over an inclined plate," *Heat Transfer*, vol. 50, no. 7, pp. 7120–7138, 2021.

[22] F. Shah, D. Zhang, B. Ahmed, and Z. Nisar, "Peristaltic transport of nanofluid with temperature dependent thermal conductivity," *Numerical Heat Transfer*, 2024. doi: 10.1080/10407782.2024.2316845.

Nomenclature

A	Unsteadiness coefficient
$B(t)$	Time aligned attractive flux
Bi	Biot Component
C	Concentration
Cfx	Skinfriction number
C_∞	Ambient concentration
C_p	Specific heat
D, Dax	Darcy Coefficient
h_f	Heat transfer coefficient
K	Permability of porous media
K_1	Permability
L	Viscosity ship factor
Md	Convection diffusion parameter
M^2	Hartmann number
Nnx	Micro organism coefficient
Nux	Nusselt number
Pe	Peclet number
Pr	Prandtl number
qm	Mass flux
qn	Micro organism coefficient
qw	Local heat flux

qr Rosseland approximate

Q heat source parameter

Q_0 heat source initial value

Rd Radiation coefficient

S Suction coefficient

Sb Schmidt coefficient

Sc Schmidt number

Shx Shearwood number

t time

T Temperature

T_w Wall temperature

T_∞ Ambient temperature

u, v Velocity components

$U_w(x, y)$ Stagnation point

$V_w(x)$ Slide velocity

We Electric conductivity coefficient

Greek Symbols

β Acute angle

λ_1 Stretching coefficient

λ_2 Velocity ship parameter

σ Thermal conductivity

σ^* Stefan boltzman constant

K^* Mean absorption coefficient

δu Heat source parameter